5-19-2010

Improving Analytical Travel Time Estimation for Transportation Planning Models

Chenxi Lu
Florida Inernational University, luchenxi@hotmail.com

DOI: 10.25148/etd.FI10080410

FLORIDA INTERNATIONAL UNIVERSITY

Miami, Florida

IMPROVING ANALYTICAL TRAVEL TIME ESTIMATION FOR TRANSPORTATION PLANNING MODELS

A dissertation submitted in partial fulfillment of the

requirements for the degree of

DOCTOR OF PHILOSOPHY

in

CIVIL ENGINEERING

by

Chenxi Lu

2010

To: Dean Amir Mirmiran
College of Engineering and Computing

This dissertation, written by Chenxi Lu, and entitled Improving Analytical Travel Time Estimation for Transportation Planning Models, having been approved in respect to style and intellectual content, is referred to you for judgment.

We have read this dissertation and recommend that it be approved.

_____
Zhenmin Chen

_____
Albert Gan

_____
Mohammed Hadi, Co-Major Professor

_____
Fang Zhao, Co-Major Professor

Date of Defense: May 19, 2010

The dissertation of Chenxi Lu is approved.

_____
Dean Amir Mirmiran
College of Engineering and Computing

_____
Interim Dean Kevin O'Shea
University Graduate School

Florida International University, 2010

DEDICATION

I dedicate this dissertation to my parents, Qingyun Liu, Duoyu Lu, and my wife, Xiaoxia Zhang. Without their patience, understanding, support, and most of all love, the completion of this work would not have been possible.

Also, I dedicate this dissertation to my daughter, Jiongni Lu, whose birth has brought wonderful fun, great motivation, and inspiration into my life.

ACKNOWLEDGMENTS

First, I would like to thank Dr. Fang Zhao for her guidance in all aspects during the last few years. Her breadth of knowledge and hard work in the transportation field impressed me. Without her advice and support I would not be able to complete this degree.

I also would like to thank my committee members for their encouragement, support, and suggestions. Dr. Hadi, as my co-major professor, has advised me in signal timing optimization with TRANSYT-7F and travel time simulation with CORSIM and has kept pushing me toward the completion of this dissertation work. Dr. Gan provided very useful suggestions about simulation and experimental design. It is a great pleasure to have Dr. Chen on my committee. He is an expert on statistical analysis and always ready to steer me to the right direction of modeling. I would like to thank Dr. L. David Shen, who taught me about mass transit technology, planning, and operations, and gave me career advice.

I want to thank my colleagues for working together with me all these years at FIU, especially Dr. Lee-Fang Chow, Dr. Soon Chung, Dr. Xuemei Liu, Dr. Jing Qi, Hongbo Chi, Shanshan Yang, and Dr. Keqiang Xing. I am also grateful to Dr. Halit Ozen, Yan Xiao, and Patricio Alvarez. The discussion of technical issues with them always gave me new insights. Ms. Amy Diaz, Ms. Lilia Silverio, Ms. Laura Osorno, and Ms. Haydee Cadena provided services to all students in the college and department, who helped me a lot in my foreign study. I would like to thank Ms. Tiffany Farjardo, who edited this manuscript.

I would like to acknowledge financial support of the Department of Civil and Environmental Engineering. A Florida International University Dissertation Year Fellowship by the University Graduate School has made it possible for me to focus on my dissertation work in the last year of my study.

Finally, I would like to thank all of my friends who have helped me throughout the past years. Your support is appreciated!

ABSTRACT OF THE DISSERTATION

IMPROVING ANALYTICAL TRAVEL TIME ESTIMATION FOR TRANSPORTATION PLANNING MODELS

by

Chenxi Lu

Florida International University, 2010

Miami, Florida

Professor Mohammed Hadi, Co-Major Professor

Professor Fang Zhao, Co-Major Professor

This dissertation aimed to improve travel time estimation for the purpose of transportation planning by developing a travel time estimation method that incorporates the effects of signal timing plans, which were difficult to consider in planning models. For this purpose, an analytical model has been developed. The model parameters were calibrated based on data from CORSIM microscopic simulation, with signal timing plans optimized using the TRANSYT-7F software. Independent variables in the model are link length, free-flow speed, and traffic volumes from the competing turning movements.

The developed model has three advantages compared to traditional link-based or node-based models. First, the model considers the influence of signal timing plans for a variety of traffic volume combinations without requiring signal timing information as input. Second, the model describes the non-uniform spatial distribution of delay along a link, this being able to estimate the impacts of queues at different upstream locations of an intersection and attribute delays to a subject link and upstream link. Third, the model shows promise of improving the accuracy of travel time prediction. The mean absolute

percentage error (MAPE) of the model is 13% for a set of field data from Minnesota Department of Transportation (MDOT); this is close to the MAPE of uniform delay in the HCM 2000 method (11%). The HCM is the industrial accepted analytical model in the existing literature, but it requires signal timing information as input for calculating delays. The developed model also outperforms the HCM 2000 method for a set of Miami-Dade County data that represent congested traffic conditions, with a MAPE of 29%, compared to 31% of the HCM 2000 method.

The advantages of the proposed model make it feasible for application to a large network without the burden of signal timing input, while improving the accuracy of travel time estimation. An assignment model with the developed travel time estimation method has been implemented in a South Florida planning model, which improved assignment results.

TABLE OF CONTENTS

CHAPTER PAGE

1 INTRODUCTION 1
1.1 Background 1
1.2 Problem Statement 5
1.3 Research Goal and Objectives 6
1.4 Dissertation Organization 8

2 LITERATURE REVIEW 10
2.1 Travel Time Estimation in Current Planning Practices 10
2.1.1 Link-Based Volume Delay Function 10
2.1.2 Node-Based Delay Function 18
2.2 Technical Problems in Traffic Assignment 26
2.3 Travel Time Simulation 28
2.3.1 Simulation Models 28
2.3.2 Micro-simulation Software Packages 29
2.4 Potential Modeling Approaches 32
2.5 Summary 35

3 TRAVEL TIME ESTIMATION 36
3.1 Experiment Design 37
3.2 Evaluation of Optimization Strategies 40
3.2.1 Objective Functions and Simulation Engines 43
3.2.2 Random Seed Number 46
3.3 Simulation 47
3.4 Data Filtering 55
3.5 Summary of Simulation Data 57

4 STATISTICAL ANALYSIS 58
4.1 Degree of Congestion Defined by the Ratio of Volume to Capacity 60
4.2 Degree of Congestion Defined by the Ratio of Volume to Saturation Flow Rate 72
4.3 Unified Model 79
4.4 Effect of Speed 82
4.4.1 Degree of Congestion Defined by the Ratio of Volume to Capacity 82
4.4.2 Degree of Congestion Defined by the Ratio of Volume to Saturation Flow Rate 85
4.5 Summary of Model Development 87

5 MODEL EVALUATION 89
5.1 Evaluation Based on Minnesota Data 89
5.1.1 Capacity-Based Travel Time Models 91
5.1.2 Saturation-Based Travel Time Model 97

5.2 Evaluation Based on Miami-Dade County Data 101
5.2.1 Capacity-Based Model 102
5.2.2 Saturation-Based Travel Time Models 107
5.3 Summary of Evaluation 110

6 MODEL APPLICATION FOR TRAFFIC ASSIGNMENT 112
6.1 Technical Issues of Model Application 114
6.1.1 Preparing Intersection Topology Information 114
6.1.2 Updating Link Traffic Attributes 116
6.1.3 Method of Successive Average 118
6.1.4 Spillback Delay from Downstream to Upstream 119
6.2 Model Application for a Hypothetical Network 120
6.3 Model Application in the SERPM Model 126
6.4 Convergence of Assignment 134
6.5 Summary of Model Application in Assignment 140

7 CONCLUSIONS AND FUTURE WORK 141
7.1 Conclusions 141
7.2 Limitations and Future Work 143

REFERENCES 145

APPENDICES 151

VITA 196

LIST OF TABLES

TABLE		PAGE
Table 2.1	Functional form candidates for speed-flow curves (Dowling 2006).	17
Table 2.2	Comparison of micro-simulation software packages.	32
Table 3.1	Influential factors on travel time delay.	39
Table 3.2	Optimized signal plans for an intersection with subject volume of 200 vphpl and cross-street volume of 200 vphpl.	44
Table 3.3	Optimized signal plans for an intersection with subject volume of 750 vphpl and cross-street volume of 750 vphpl.	45
Table 3.4	Optimized signal plans for an intersection with subject volume of 1,400 vphpl and cross-street volume of 1,400 vphpl.	45
Table 3.5	Testing random seeds for the scenario that both traffic volumes from subject direction and cross-street direction are 200 vphpl.	47
Table 3.6	Comparison of delays between CORSIM simulation and existing models.	54
Table 3.7	Filtering of simulation data.	56
Table 4.1	Fitted parameters for developed model with degree of congestion defined by volume to reduced physical capacity.	61
Table 4.2	Percentage error between nine capacity-based models and simulated data.	71
Table 4.3	Fitted parameters for the delay model with saturation flow rate.	73
Table 4.4	Percentage error between nine saturation-based models and simulated data.	79
Table 4.5	Fitted parameters for capacity-based unified models.	80
Table 4.6	Fitted parameters for unified models with saturation flow rate.	80
Table 4.7	Percentage error between unified models and simulated data.	81
Table 4.8	Fitted parameters for capacity-based models for different free flow speeds.	83

Table 4.9 Percentage error between the capacity-based models and simulated data for different speeds. ····· 85

Table 4.10 Fitted parameters for saturation-based models for different free flow speeds. ····· 85

Table 4.11 Percentage error between the saturation-based models and simulated data for different speeds. ····· 87

Table 5.1 Field collected data from MDOT (Davis 2007). ····· 90

Table 5.2 Travel time calculated by different planning models for the MDOT data. ····· 92

Table 5.3 Mean absolute percentage error for different planning models in comparison with MDOT data. ····· 94

Table 5.4 Correlations between paired samples by the models and from MDOT field data. ····· 96

Table 5.5 Statistical test for the paired difference based on MDOT field data. ····· 97

Table 5.6 Travel time by different models in comparison with the MDOT data. ····· 99

Table 5.7 Correlation between three travel time models based on MDOT data. ····· 99

Table 5.8 Statistical test for the paired differences under light traffic. ····· 101

Table 5.9 Operational parameters of 7 intersections along US-1 in Miami-Dade. ····· 102

Table 5.10 Travel time calculated by different planning models in comparison with US-1 data. ····· 103

Table 5.11 Mean absolute percentage error for different planning models in comparison with US 1 data. ····· 104

Table 5.12 Correlations between paired samples by the models and from US-1 data. ····· 105

Table 5.13 Comparison of travel time by two developed models with US-1 data. ····· 108

Table 5.14 Correlation between three travel time models based on MDOT data. ····· 108

Table 5.15 Statistical test for the paired differences for three models under congested traffic. ····· 109

Table 6.1 OD trip matrix for hypothesis test case. ····· 121

Table 6.2 MAPE of assigned traffic volumes for the developed model and SERPM model. ····· 133

Table 6.3 Paired samples correlations for developed model and SERPM model. ····· 133

Table 6.4 Paired samples test for developed model and SERPM. ····· 133

Table 6.5 Required iterations for convergence by network size. ····· 137

Table A.1 Optimized signal plans for an intersection with subject volume of 200 vphpl and cross-street volume of 200 vphpl. ····· 151

Table A.2 Optimized signal plans for an intersection with subject volume of 200 vphpl and cross-street volume of 750 vphpl. ····· 151

Table A.3 Optimized signal plans for an intersection with subject volume of 200 vphpl and cross-street volume of 1,400 vphpl. ····· 152

Table A.4 Optimized signal plans for an intersection with subject volume of 750 vphpl and cross-street volume of 200 vphpl. ····· 152

Table A.5 Optimized signal plans for an intersection with subject volume of 750 vphpl and cross-street volume of 750 vphpl. ····· 153

Table A.6 Optimized signal plans for an intersection with subject volume of 750 vphpl and cross-street volume of 1,400 vphpl. ····· 153

Table A.7 Optimized signal plans for an intersection with subject volume of 1,400 vphpl and cross-street volume of 200 vphpl. ····· 154

Table A.8 Optimized signal plans for an intersection with subject volume of 1,400 vphpl and cross-street volume of 750 vphpl. ····· 154

Table A.9 Optimized signal plans for an intersection with subject volume of 1,400 vphpl and cross-street volume of 1,400 vphpl. ····· 155

Table B.1 Testing random seeds for the scenario that both traffic volumes from subject direction and cross-street are 200 vphpl. ····· 156

Table B.2 Testing random seeds for the scenario that traffic volumes from subject direction and cross-street are 200 vphpl and 500 vphpl. ····· 156

Table B.3 Testing random seeds for the scenario that traffic volumes from subject direction and cross-street are 200 vphpl and 700 vphpl. ····· 156

Table B.4 Testing random seeds for the scenario that traffic volumes from subject direction and cross-street are 500 vphpl and 200 vphpl. ····· 157

Table B.5 Testing random seeds for the scenario that traffic volumes from subject direction and cross-street are 500 vphpl and 500 vphpl. ····· 157

Table B.6 Testing random seeds for the scenario that traffic volumes from subject direction and cross-street are 500 vphpl and 700 vphpl. ····· 157

Table B.7 Testing random seeds for the scenario that traffic volumes from subject direction and cross-street are 700 vphpl and 200 vphpl. ····· 158

Table B.8 Testing random seeds for the scenario that traffic volumes from subject direction and cross-street are 700 vphpl and 500 vphpl. ····· 158

Table B.9 Testing random seeds for the scenario that traffic volumes from subject direction and cross-street are 700 vphpl and 700 vphpl. ····· 158

LIST OF FIGURES

FIGURE		PAGE
Figure 2.1	Prototype of a multi-layer artificial neural network.	33
Figure 3.1	Simulated four-legged intersection.	38
Figure 3.2	Dummy nodes designed for the links attached to an intersection.	49
Figure 3.3	Spatial distribution of delay for different scenarios of subject traffic conditions.	50
Figure 3.4	Spatial distribution of delay for different scenarios of subject traffic conditions (first 1, 000 feet).	50
Figure 3.5	Delay-volume relations in subject direction for the different scenarios of cross-street traffic conditions for the first 200-foot segment.	51
Figure 3.6	Subject delay versus cross-street volume for the different scenarios of subject traffic conditions at the first 200-foot segment.	52
Figure 3.7	Delay spatial distribution for different subject left-turn ratios.	52
Figure 3.8	Delay spatial distribution for different cross-street left-turn ratios.	53
Figure 4.1	Predicted delay response to various link lengths.	62
Figure 4.2	Predicted delay versus degree of congestion in subject approach.	63
Figure 4.3	Predicted delay versus degree of congestion for cross-street.	64
Figure 4.4	Delay distribution along a link of Type 11 intersection. Volumes for both directions are 700 vphpl.	64
Figure 4.5	Predicted versus simulated delays for Type11 intersection by the capacity-based model.	66
Figure 4.6	Predicted versus simulated delays for Type12 intersection by the capacity-based model.	66
Figure 4.7	Predicted versus simulated delays for Type13 intersection by the capacity-based model.	67
Figure 4.8	Predicted versus simulated delays for Type21 intersection by the capacity-based model.	67

Figure 4.9 Predicted versus simulated delays for Type22 intersection by the capacity-based model. 68

Figure 4.10 Predicted versus simulated delays for Type23 intersection by the capacity-based model. 68

Figure 4.11 Predicted versus simulated delays for Type31 intersection by the capacity-based model. 69

Figure 4.12 Predicted versus simulated delays for Type32 intersection by the capacity-based model. 69

Figure 4.13 Predicted versus simulated delays for Type33 intersection by the capacity-based model. 70

Figure 4.14 Predicted versus simulated delays for Type11 intersection by the saturation-based model. 74

Figure 4.15 Predicted versus simulated delays for Type12 intersection by the saturation-based model. 75

Figure 4.16 Predicted versus simulated delays for Type13 intersection by the saturation-based model. 75

Figure 4.17 Predicted versus simulated delays for Type21 intersection by the saturation-based model. 76

Figure 4.18 Predicted versus simulated delays for Type22 intersection by the saturation-based model. 76

Figure 4.19 Predicted versus simulated delays for Type23 intersection by the saturation-based model. 77

Figure 4.20 Predicted versus simulated delays for Type31 intersection by the saturation-based model. 77

Figure 4.21 Predicted versus simulated delays for Type32 intersection by the saturation-based model. 78

Figure 4.22 Predicted versus simulated delays for Type33 intersection by the saturation-based model. 78

Figure 4.23 Predicted versus simulated delays for unified model. 81

Figure 4.24 Predicted versus simulated delays for Type22 intersection with free flow speed of 40 mph by the capacity-based model. 83

Figure 4.25 Predicted versus simulated delays for Type22 intersection with free flow speed of 30 mph by the capacity-based model. ····· 84

Figure 4.26 Predicted versus simulated delays for Type22 intersection with free flow speed of 40 mph by the saturation-based model. ····· 86

Figure 4.27 Predicted versus simulated delays for Type22 intersection with free flow speed of 30 mph by the saturation-based model. ····· 86

Figure 6.1 A flow chart of assignment process with new developed travel time model. ····· 113

Figure 6.2 Schematics drawing of four-leg intersection with approaches of subject1, subject2, cross1 and cross2. ····· 114

Figure 6.3 Turn attribute definition for ending node C. ····· 116

Figure 6.4 A hypothetical network. ····· 121

Figure 6.5 Assignment results based on the BPR equation. ····· 122

Figure 6.6 Assignment results based on the developed model. ····· 123

Figure 6.7 Loaded traffic on the link between Nodes 201 and 202. ····· 125

Figure 6.8 Loaded traffic on the link between Nodes 206 and 208. ····· 125

Figure 6.9 Network of Southeast Regional Planning Model. ····· 127

Figure 6.10 A script layer of assignment process with the developed model applied for the AM-peak period in SERPM. ····· 128

Figure 6.11 Turning volumes at junction node 15848. ····· 129

Figure 6.12 Turning volume definition for the link from Node 15846 to Node 15848. ····· 130

Figure 6.13 Network with 48 links. ····· 134

Figure 6.14 Network travel cost changes with assignment iterations for (a) network with 48 links; (b) network with 168 links. ····· 135

Figure 6.15 Network travel cost changes with assignment iterations for (a) network with 468 links; (b) network with 736 links. ····· 135

Figure 6.16 Network travel cost changes with assignment iterations for (a) network with 12,013 links; (b) network with 19,181 links. ····· 136

Figure 6.17 Network travel cost changes with assignment iterations for SERPM network with 47,898 links. ····· 136

Figure 6.18 Required iterations for convergence increase with network size. ····· 138

Figure 6.19 Assigned traffic volumes for links between Nodes 5404 and 10736, and 9514 and 9524. ····· 138

Figure 6.20 Assigned traffic volumes for links between Nodes 17546 and 17544, and 22420 and 23191. ····· 139

Figure 6.21 Assigned traffic volumes for links between Node 5158 and 7240, and 5228 and 10718. ····· 139

CHAPTER 1

INTRODUCTION

1.1 Background

Transportation planning is important in the development of a regional transportation system. A properly planned and designed transportation system improves the quality of life, promotes the sustainable development of communities, supports economic development, and protects the environment. Transportation planning may be long-range or short-term. Long-range planning involves the evaluation of investment strategies to help develop a systematic plan of transportation improvements within the timeframe of 20 or more years. Short-term planning focuses on site, corridor, and subarea level planning analysis with a short-term horizon of one to six years. Short-term planning strategies therefore maximize the use of the existing system with minimum new construction (Weiner 1997). Short-term planning results are documented as the Transportation Improvement Program (TIP), which is based on improvement projects identified in long-range planning. The TIP aims to allocate the limited transportation resources among the various capital and operating needs of the area, based on a clear set of short-term transportation priorities (FHWA and FTA 2007).

Long-range planning is often assisted by travel demand models. Today the most widely used model is the four-step trip-based model, which includes four major sequential steps: trip generation, trip distribution, modal split, and traffic assignment. The first step, trip generation, is a procedure for estimating the amount of travel in a given forecast horizon, typically 15 to 30 years into the future. The amount of travel may be measured in terms of the number of trips or journeys produced and attracted to different

locations, as a function of land use, demographics, and socioeconomic attributes of households, *etc*. Trip distribution then matches the trip productions and trip attractions to create origin-destination (O-D) tables. During the third step, modal split, the proportion of trips accomplished using each of the alternative travel modes between O-D pairs is estimated. Finally, traffic assignment finds routes for mode-specific trips and estimates the traffic flow for each link in a network. Among these four steps, trip distribution, modal split, and traffic assignment all depend on the estimation of travel cost, usually expressed as a generalized cost function that combines the time, distance, and monetary cost associated with the travel. Travel costs affect a traveler's choice of destination, as well as the choice of a travel mode that is less expensive and more convenient than all other possible alternatives. In traffic assignment, the traveler's choice of route is assumed to be based on the lowest generalized cost. Because travel cost is a key factor influencing travel behavior, inaccurate cost estimation will result in errors in all aspects of modeling, including inaccuracies in O-D tables, mode shares, and traffic volumes in a network.

Many Metropolitan Planning Organizations (MPOs) are considering replacing current four-step trip-based models with a tour-based or activity-based model (TRB 2007). Four-step models are limited in several aspects. For instance, the treatment of trips in isolation cannot model multi-stop trip chains. Lacking a time dimension, it is ineffective in the analysis of peak spreading and choice of departure time in general. A SHRP 2 Technical Expert Task Group for Project C10, appointed by the Transportation Research Board, is currently developing an integrated, advanced travel demand model with mode choice capability and fine-grained, time-sensitive networks (SHRP2 2010). Moreover, the trip-based model is insensitive to policy contexts, such as congestion

pricing (Bhat *et al*. 2004). Tour-based modeling introduces a spatial dimension and connects isolated trips. Activity-based modeling considers the scheduling of activities in both time and space dimensions, and constraints they impose on each other. The activity-based approach aims at predicting travel demand by modeling the decision-making process of individual travelers (RDC 1995). A traveler's route selection is constrained not only by available transportation modes, but also spatial, temporal, and inter-personal interdependence. AMOS (Activity-Mobility Simulator) is the first operational activity-based simulator prototype, which is intended to serve as a short-term transportation planning and policy analysis tool (RDC 1995). TRansportation ANalysis SIMulation System (TRANSIMS) was originally funded by the U.S. Congress to advance the state of travel forecasting. It integrates advanced modeling practices, such as population synthesis, activity-based modeling, and microscopic simulation. Currently, TRANSIMS has yet to be implemented by MPOs for their core travel forecasting activities (TRB 2007). Currently, three agencies in North America have implemented advanced activity-based models and eight others are designing and implementing activity-based models for deployment (VHB 2006). The majority of planning agencies are still using four-step trip-based models. However, many incremental improvements have been made by integrating advanced techniques of activity-based models into existing four-step models (VHB 2006). Population synthesizer is one such example.

Some activity-based models employ dynamic or micro-simulation traffic assignment. However, the computational cost of dynamic traffic assignment or micro-simulation is high. Generally speaking, these models still cannot be feasibly applied at the metropolitan level with a reasonable expenditure of computation time and resources

(TRB 2007). Contracted by a Committee of Determination of the State of the Practice in Metropolitan Area Travel Forecasting, Transportation Research Board, to determine the state of metropolitan planning, the consulting firm VHB, Inc. conducted a web-based survey of MPOs. The survey showed that 91% of the large MPOs participated in the survey used trip based models and the equilibrium assignment method, which accounts for delays and congestion when assigning traffic to specific routes (VHB 2006). The Bureau of Public Roads (BPR) equation (BPR 1964) has been used for many years to estimate delays and congestion. However, while it is viewed as having yielded good results for freeways, it is lacking in accuracy for arterial roadways where intersection delays and queuing contribute to a significant portion of total travel time. Some MPOs have been improving the estimation of arterial congestion by separately modeling delays for arterial roads and intersections (TRB 2007).

While travel cost may include monetary costs, such as tolls, and other less quantifiable values, such as safety and scenery, a major component of travel cost is travel time. Hence, it is critical to estimate travel time accurately. Having evolved over the last several decades, most travel time estimation models are now based on macro analytical formulas. These analytical formulas are usually derived from different theoretical perspectives with parameters calibrated based on field data. Thus, interpreting the results from such formulas is mainly dependent on the theoretical framework adopted. The results will not be valid if the constraints and assumptions of the theory do not apply for a given problem.

These formulas are limited in their ability to provide accurate travel time estimates due to the complexity of traffic flow and traffic control. The complexity of

traffic results from the diversity of the characteristics and personal traits of participants in traffic, such as drivers, vehicles, roadways, and traffic controls; the fact that aggressiveness, reaction time, vision, *etc.,* vary widely among drivers; and that roadways are varied with regard to their accessibility, mobility, geometry size, horizontal/vertical alignment, *etc*. Moreover, it should be noted that commonly used methods, such as BPR equation, have been developed for uninterrupted traffic flow, which is unsuited for interrupted flow with control device. Traffic control is highly involved due to the varying combinations of cycle length, phase split, phase sequence, and offsets. In particular, control delays at signalized intersections are not adequately modeled being that the effects of signal timing, such as changes in cycle length, phase split, and sequence, are not considered in the formula.

1.2 Problem Statement

This research seeks to address the shortcomings of existing travel time estimation methods for interrupted traffic flow on urban streets. For signalized intersections, intersection delays account for a significant amount of travel time. If not properly modeled, the quality of travel time estimation for urban streets is significantly negatively impacted.

The most widely used travel time functions in planning are the BPR equation (BPR 1964), canonical equation (Spiess 1990), and Akcelik equation (Akcelik 1991). The problems in the current travel time estimation methods are the following:

1) The mostly commonly used travel time estimation models, such as the BPR equation, is originally intended for uninterrupted flows, and is not suitable for interrupted flows with control devices.

2) The effect of signal timing plans is not adequately considered.
3) The BPR equation estimates delays based on the congestion level of a link. For signalized intersections, however, delay is dependent on the congestion level of not only a subject approach, but also competing approaches.
4) Delays due to the spillback of traffic from downstream of an intersection are usually not considered. However, the spillback of vehicle is commonly seen in a central business district (CBD) or a congested area, which causes additional delays for upstream links.

Zhao and Ding's work shed some light on the way to overcome the above constraints (Zhao and Ding 2006; Ding 2007; Ding *et al*. 2009). However, their models did not address link delay estimation separately from intersection delays. Moreover, ANN model is a black box approach that does not make planners and modelers comfortable because the logic of the models cannot be seen.

1.3 Research Goal and Objectives

The goal of this research is to improve travel time estimation on urban streets for static traffic assignment purposes by taking advantages of a microscopic simulation tool to develop analytical models of travel time for a link and for intersections separately. The research attempts to improve the estimations of both signalized intersection delays and link travel time by considering signal timing plans and competing traffic flows. The objectives of this study include the following:

1) Apply microscopic simulations to generate data for travel time estimation models. Microscopic simulation has been used widely in traffic operations and has proven to be powerful with regard to estimating travel time for a variety of

2) Improve existing travel time models used in travel demand forecast by considering influential factors that are otherwise overlooked in the current practice: signal plan at an intersection, queue delay on a link, and traffic flows from competing approaches. Travel time estimation, and thus travel demand modeling, may be improved by properly considering these factors.
3) Determine the feasibility of accounting for spillback effects in the proposed delay model. The spillback effect from a downstream link on an upstream link often occurs under congested conditions and when the link length is not long enough to accommodate all vehicles. Estimating the impacts of queues at different locations upstream of the signal allows the splitting of link delays between the controlled link and upstream links, based on the link length.
4) Demonstrate that the proposed travel time estimation models have the potential to be applied in practice by testing them in region planning model of a large network and the ability of the models to improve traffic assignment results.

1.4 Dissertation Organization

The dissertation is organized into seven chapters. Chapter 1 introduces the background of transportation planning, the problem of travel time estimation in current four-step trip-based models, and the goal and objectives to be achieved in this research.

Chapter 2 presents a literature review covering the travel time estimation in current planning practices, the technical problems in traffic assignment, travel time simulation, and statistical models. The purpose of this review is to understand the limitations of current travel time estimation methods and enlighten a way to improve the current models through travel time simulation and statistical models.

Chapter 3 describes the method for generating travel time data that is employed in this research, including signal optimization, travel time micro-simulation, and data filtering. The chapter also discusses the design of an experiment to obtain valid delay data for the model development in the next chapter.

Chapter 4 describes the model development. This chapter presents two types of models with degree of congestion defined by the ratio of volume to capacity, or by the ratio of volume to saturation flow rate. The sensitivity analysis on lane configuration and speed helps to understand whether and how these factors should be considered in the models.

Chapter 5 evaluates the developed models using the field data from the Minnesota Department of Transportation (MDOT), as well as the CORSIM simulation data for US-1 in Miami-Dade County, Florida. This chapter is to provide evidences whether a model developed based on simulation data performs well in the prediction of travel time.

Chapter 6 provides a case study of model application to traffic assignment. The chapter discusses whether the developed model is applicable in a large network, what the technical problems in application are, and how some of the problems are solved.

Chapter 7 concludes several advantages of the developed travel time model, indicates the limitations of the model, and recommends issues for future research.

CHAPTER 2

LITERATURE REVIEW

Travel time, as a major component of travel cost, is important for traffic assignment, as well as for traffic distribution and modal split in four-step trip-based models. Hence, an accurate and efficient estimation of travel time is important for long-range transportation planning. This chapter reviews the current practice and attempts to improve travel time estimation.

2.1 Travel Time Estimation in Current Planning Practices

In current practice, there are mainly two types of travel cost functions: link-based volume delay functions and node-based delay functions. Link-based volume delay functions describe how delays increase due to traffic congestion. When applied to urban streets, the link capacity of intersections is reduced to a "practical capacity" due to delays caused by at-grade traffic crossings. Many researchers have argued that a link-based delay function may not properly capture the impacts of intersection delays, which account for a significant amount of total travel time. Subsequently, node-based delay functions have been suggested to separately model delays on a link and at an intersection.

2.1.1 Link-Based Volume Delay Function

Historically in the U.S., the cost function used in most travel demand models is the Bureau of Public Roads (BPR) function (BPR 1964), which was originally developed for uninterrupted flow, such as freeway flow. This function, when applied to urban streets that have closely spaced intersections with control devices, considers the additional delays at intersections by reducing link capacity to a "practical capacity". It is assumed

that delay depends on the flow of the link itself (v) and is affected by link capacity (c). The equation is as follows:

$$t = t_0\left[1+\alpha\left(\frac{v}{c}\right)^{\beta}\right] \tag{2-1}$$

where

t = total travel time on the link (seconds per vehicle, or s/veh);

t_0 = free-flow travel time (s/veh);

v = traffic volume or demand (vehicles per hour, or vph);

c = practical capacity (vph);

α = model parameter, 0.15 in the standard BPR formula and can be calibrated for the different facility types and different regions; and

β = model parameter, 4.0 in the standard BPR formula and can be calibrated for the different facility types and different regions.

When applied to an urban street, the capacity is reduced to a practical value, for instance, 750 vehicles per hour per lane (vphpl) for a divided arterial, 592 vphpl for an undivided arterial, and 530 vphpl for a collector (FDOT 1997).

Dowling *et al.* (1997; 1998) and Skabardonis *et al.* (1997), however, found that the BPR equation tends to underestimate travel time near capacity (when volume over capacity ratio is larger than 0.80). To attend to this issue, they refitted the BPR equation to accommodate speed-flow data for freeways and signalized arterials using the 1994 Highway Capacity Manual (HCM). They modified the BPR equation by assigning a higher value, 10, to β; and the value of parameter α was suggested to be 0.05 for signalized arterials and 0.2 for other facilities. The capacity for signalized arterials is

reduced to reflect the splitting of green time. The equation for signalized arterials developed by Dowling *et al.* (1997; 1998) is below:

$$t = \left[t_0 + \frac{1}{2} N \times C \left(1 - \frac{g}{C} \right)^2 \times PF \right] \left[1 + 0.05 \left(\frac{v}{c} \right)^{10} \right] \tag{2-2}$$

where

t = predicted mean travel time on the link (s/veh);

t_0 = free flow travel time (s/veh);

N = number of signals on the link;

g = effective green time (seconds);

C = cycle length (seconds);

PF = progression adjustment factor;

v = traffic volume or demand (vph); and

c = capacity (adjusted by green time/cycle length ratio; vph).

The progression adjustment factor, PF, is in turn given by:

$$PF = \frac{(1 - P) f_{PA}}{1 - \frac{g}{C}} \tag{2-3}$$

where

PF = progression adjustment factor;

P = proportion of vehicles arriving on green;

f_{PA} = supplemental adjustment factor for platoon arriving during green;

g = effective green time (seconds); and

C = cycle length (seconds).

When *P* is unknown, NCHRP 387(Dowling 1997) recommends the following default values for *PF*:

PF = 0.9 for uncoordinated actuated signals;

PF = 1.0 for uncoordinated fixed time signals;

PF = 1.2 for coordinated signals with unfavorable progression;

PF = 0.9 for coordinated signals with favorable progression; and

PF = 0.6 for coordinated signals with highly favorable progression.

Spiess (1990) concluded that the BPR equation, particularly with a higher β, such as greater than 4, requires a large number of iterations to reach equilibrium in traffic assignment. Spiess defined a set of conical equations to replace the widely used BPR equation. His proposed equation is as follows:

$$t = t_0\left[2 + \sqrt{\alpha^2\left(1-\frac{v}{c}\right)^2 + \beta^2} - \alpha\left(1-\frac{v}{c}\right) - \beta\right] \tag{2-4}$$

where

t = travel time on the link (s/veh);

t_0 = free-flow travel time (s/veh);

v = traffic volume or demand (vph);

c = capacity (vph);

α = model parameter, usually assumed to be 4; and

β = $(2\alpha - 1) / (2\alpha - 2)$.

The parameter α, used in the conical equation, remains the same as the steepness, β, in the BPR equation. This makes the transition from the BPR equation to the conical equation smooth. The conical equation avoids the inherent drawbacks of the BPR

equation with a higher steepness, β; however, the weakness of accommodating proper intersection delay remains in conical equation as it does in BPR equation.

Alternatively, Akçelik (1991) proposed a time-dependent speed-flow function for back-of-queue modeling at signalized intersections. He modified his own time-dependent form (Akçelik 1981) to overcome both conceptual problems and calibration difficulties inherent in Davidson's travel time equations, in which the delay is not finite for flows near and above capacity (Davidson 1966; 1978). The alternative speed-flow function shows promise of addressing the slow convergence problem in equilibrium traffic assignment when the value of β in the BPR equation is higher than 4. It also provides more accurate results than the BPR function (Dowling *et al*. 1998). The equation is incorporated into the 2000 Highway Capacity Manual (HCM 2000). The equation is as follows:

$$t = t_0\left[1 + 0.25 r_f\left(z + \sqrt{z^2 + \frac{8J_A \times x}{c \times t_0 \times r_f}}\right)\right] \tag{2-5}$$

where

t = travel time per unit distance (s/veh/km);

t_0 = free-flow travel time per unit distance (s/veh/km);

J_A = delay parameter;

z = x - 1;

x = v/c, degree of saturation;

v = traffic volume or demand (vph);

c = capacity (vph); and

r_f = ratio of analysis period (seconds) to t_0.

The delay parameter, J_A, in the above equation represents quality of service provided by road section. This form accommodates delay estimation for an intersection with a constant parameter, which remain unchanged during the traffic assignment process. However, this value may not be available for new development. Furthermore, as suggested by the author, a better form of the travel time function would model separately both the free-flow travel time and the delays along a link and at an intersection (Akçelik 1991).

In South Florida, the volume delay function for the current Southeast Regional Planning Model (SERPM) 6.5 is a modified BPR equation, with average link speed adjusted based on the default green time (g) and cycle length (C) at intersection. Note that the model is applied on a roadway facility with an intersection or several intersections. The equation is as follows (Corradino 2008):

$$t = \left(\frac{L}{S_f}\right) \times \left[1 + \alpha\left(\frac{v}{c}\right)^{\beta}\right] \tag{2-6}$$

where

t = travel time on a facility (hours per vehicle or h/veh);

L = length of the facility (miles);

S_f = mean speed of an urban interrupted facility (miles per hour or mph);

v = traffic volume or demand (vph);

c = practical capacity (vph);

α = calibrated parameter, 0.35 when posted speed is less than 35 mph, otherwise 0.55;

β = calibrated parameter, 4.05 when posted speed is less than 35 mph, otherwise 5.05;

The mean speed of an urban interrupted facility, S_f, is given as follows:

$$S_f = \frac{L}{\frac{L}{S_{mb}} + \frac{N \times D}{3600}} \tag{2-7}$$

where

L = length of a facility (miles);

S_{mb} = mid-block free-flow speed (mph);

N = number of signals at the facility; and

D = average delay per signal (seconds).

Mid-block free-flow speed, S_{mb}, and average delay, D, are:

$$S_{mb} = 0.79 S_{post} + 12 \tag{2-8}$$

$$D = 0.5 PF \times C\left(1 - \frac{g}{C}\right)^2 \tag{2-9}$$

where

S_{post} = posted speed of the facility (mph);

PF = progression adjustment factor, defined in Equation (2-3);

g = effective green time (seconds); and

C = cycle length (seconds).

Link-based volume delay functions are still widely used in practice because of their advantages for planning applications, especially some of the functions with improved intersection delay estimation, such as the Dowling method and SERPM model.

These functions are monotonically increasing with volume, which satisfies the equilibrium requirement in assignment. Dowling and Skabardonis (2006) also investigated some functional forms that could potentially be used in travel demand models; however, it was found that only the BPR, Akcelik, and exponential forms in Table 2.1 have the traits required for equilibrium assignment. In contrast, the other functional forms in the table, such as linear, logarithmic, power, and polynomial forms, do not have the traits required.

Table 2.1 Functional form candidates for speed-flow curves (Dowling 2006).

Function Form	Functional Forms	Comments
Linear	$S = -a \cdot x + b$	Not acceptable. Reaches zero speed at high *v/c*.
Logarithmic	$S = -a \cdot \ln(x) + b$	Not acceptable. Has no value at $x = 0$ (the logarithm of "*x*" approaches negative infinity).
Exponential	$S = a \cdot S_0 \cdot \exp(-b \cdot x)$	Has all traits required for equilibrium assignment.
Power	$S = a / x^b$	Not acceptable. It goes to infinity at $v/c = x = 0$.
Polynomial	$S = -a \cdot x^2 - b \cdot x + c$	Not acceptable. It reaches zero speed at high *v/c*.
BPR	$S = S_0 /[1 + a(x)^b]$	Has all traits required for equilibrium assignment.
Akcelik	$S = \dfrac{L}{L / S_0 + 0.25\{(x-1) + [(x-1)^2 + a \cdot x]^{1/2}\}}$	Has all traits required for equilibrium assignment.

Note: S = predicted speed;
x = volume/capacity ratio;
a, b, c = global parameters for equation;
L = link length; and
S_0 = link free-flow speed.

2.1.2 Node-Based Delay Function

Although modelers favor link-based volume delay functions, it is thought that the accuracy of delay estimation may be improved by estimating delay separately on a link and at an intersection. On the whole, this would make travel time forecasting useful to other design and operation practices. The Highway Capacity Manual (HCM), as such, is an important reference for this purpose.

The HCM is a publication of the Transportation Research Board (TRB) in the U.S. It has been a reference for transportation engineers, scholars, and practitioners as the industry standards on planning, design, and operations. There have been four editions of the HCM from 1950 to 2000; the first edition in 1950, the second edition in 1965, the third edition in 1985, and the most recent edition in 2000. The 1985 edition, along with its 1994 and 1997 major updates, is the first near universally accepted document among traffic engineers and planners (HCM 2000). The original 1985 edition described widely recognized relationships for traffic delay and its 1994 update heavily revised the signalized intersection procedure. The HCM 2000 edition is the most current version, and features a complex intersection procedure. This edition incorporates research results from many studies and is compiled under the guidance of a TRB technical committee. The manual is intended to provide systematic and consistent methods for transportation practitioners and researchers. The intersection delay equation is as follows (HCM 2000):

$$d = d_1 \times PF + d_2 + d_3 \tag{2-10}$$

where

d = control delay per vehicle (s/veh);

d_1 = uniform delay assuming uniform arrivals (s/veh);

PF = progression adjustment factor;

d_2 = incremental delay to account for effect of random arrivals and oversaturation queues (s/veh); and

d_3 = initial queue delay (s/veh).

Uniform delay, d_1, and incremental delay, d_2, are given as follows:

$$d_1 = \frac{0.5C\left(1-\frac{g}{C}\right)^2}{1-\min(1,X)\times\left(\frac{g}{C}\right)} \tag{2-11}$$

$$d_2 = 900T\left[(X-1)+\sqrt{(X-1)^2+\frac{8k\times I\times X}{c\times T}}\right] \tag{2-12}$$

where

C = cycle length (seconds);

g = effective green time for lane group (seconds);

X = volume to capacity (v/c) ratio for the lane group (also termed degree of saturation);

v = volume of lane group (vph);

c = capacity of lane group (vph);

T = duration of analysis period (hours);

k = incremental delay adjustment for the actuated control; and

I = incremental delay adjustment for the filtering or metering by upstream signals.

The appendix of HCM (HCM 2000) provides a quick estimation method when only minimal data are available. The quick estimation method includes six steps:

assembly of the input data, determination of left-turn treatment, lane volume computations, estimation of signal timing plan, calculation of the critical v/c ratio, and calculation of average vehicle delay. The input data may be assumed or default values. The objective of using quick estimation method is to minimize the need for collection of detailed field data. The other steps include several sub-steps for determination and calculation.

While a great deal of research has been done on the applications of the HCM method for transportation planning (Horowitz 1991; 1992; 1997), incorporating the HCM procedures to an equilibrium assignment algorithm still faces obstacles. First, the HCM provides conventional guidelines for setting cycle lengths and lengths of green phases, but does not incorporate these principles into its delay procedures. Second, HCM delay equation is discontinuous, nonmonotonic, and nonintegratable. This may cause convergence problems for most of the equilibrium assignment methods (Horowitz 1991). For instance, a preferred equilibrium assignment method, Frank-Wolfe decomposition, cannot handle delay as a function of multiple approach volumes at an intersection. The convergence problem may, however, be solved by applying the method of successive averages (MSA). A test involving applying the 1985 edition HCM travel time model in traffic assignment (Horowitz 1992) indicated that, although multiple equilibrium assignment results are possible, the differences between these solutions are small and manageable. Horowitz (1997) concluded that the 1994 update of intersection delay is more complicated, but has a less dramatic effect on traffic assignment algorithms. Third, the time period of analysis for oversaturated flow has been set to 15 minutes in HCM (Akcelik 1991), but travel forecasting is typically done for a minimum time period of one

hour. The HCM does not indicate how the time period may be changed for the purposes of travel forecasting (Horowitz 1991). Horowitz concluded that a credible solution could still be delivered after solving these problems, but using HCM model complicates the modeling process.

In the NCHRP 3-79 report, Bonneson (2008) developed procedures to revise the HCM 2000 methodology to predict traffic speed on urban streets. Several factors that influence signal delay are considered, such as signal coordination (i.e., platoon dispersion), green interval timing (i.e., average phase duration), semi-actuated signal coordination (i.e., signal offset relationship), upstream signal metering, and queue spillback. The procedures also improve the running time method by considering the influence of segment length on free flow speed, delay due to vehicle turning, factors influencing free-flow speed (e.g., access point density, lane width, lateral clearance), delay due to proximity of other vehicles (i.e., effect of traffic density on speed), and delay due to parking maneuvers. These procedures will be included in the next version of the HCM, but will have little effect from point of view of traffic assignment modeling.

Aashtiani and Iravani (1999) proposed a method to estimate intersection delays that took into account the significant amount of intersection delay in a large network. They argued that, while traffic engineers have obtained reasonably accurate results for a small-sized network by including delays at intersections, the approach employed is not straightforward in modeling practices for large networks (Aashtiani 1999). Their method is based on Webster's delay equation and provides a simple way to estimate red time. It was then validated by comparing the results to data observed in the city of Tehran. The travel time is given as follows (Aashtiani 1999):

$$t = t_{link}(x) + d_{node}(x) \tag{2-13}$$

where

t = travel time (minutes per vehicle or m/veh);

x = traffic volume on entering link (vph, passenger car equivalent);

$t_{link}(x)$ = link travel time (m/veh); and

$d_{node}(x)$ = average delay at intersection (m/veh).

The link travel time, $t_{link}(x)$, is estimated using the modified BPR equation with consideration to cycle length and link width, as follows:

$$t_{link}(x) = L \times t_0 \left[1 + 0.15 \left(\frac{x}{c \times w} \right)^4 \right] \tag{2-14}$$

where

L = link distance (meters);

t_0 = link free flow travel time per unit distance (minutes per meter);

x = traffic volume on entering link (vph, passenger car equivalent);

c = capacity of each link per meter of the street width (vehicles per hour per meter);

w = width of the link (meters).

The intersection delay is given below:

$$d_{node}(x) = \frac{r^2}{2C\left(1 - \frac{x}{\mu \times w}\right)} \tag{2-15}$$

where

r = red time of the traffic light (minutes);

C = cycle length of the traffic light (minutes);

μ = exiting rate of traffic volume per meter of the street width (vehicles per hour per meter, passenger car equivalent); and

w = width of the link (meters).

In the model, street width is used instead of number of lanes; this is due to driving behavior in Tehran, where the number of lanes does not necessarily dictate the number of cars being accommodated across the width of a street (Aashtiani 1999). The significance of this model is that it provides a simple method to approximate cycle length and red time as follows:

$$C_j = 1 + \left(\sum_i \frac{w_{ij}}{8} \right) \left(\frac{s_j}{4} \right) \tag{2-16}$$

$$r_{ij} = 1.2 C_j \left(1 - \frac{w_{ij}}{\sum_i w_{ij}} \times \frac{s_j}{2} \right) \tag{2-17}$$

where

C_j = cycle length of the traffic light for intersection j (minutes);

r_{ij} = red time for link from node i to node j (minutes);

j = intersection ending with node j;

i = node with a link connecting to intersection j;

w_{ij} = cycle length weight for link from node i to node j (minutes); and

s_j = number of links ending at intersection j.

The value of w_{ij} is given below:

w_{ij} = 2 if the link is local or a collector;

w_{ij} = 3 if the link is a minor arterial;

w_{ij} = 4 if the link is a major arterial; and

w_{ij} = 5 if the link is an expressway.

However, the estimation of cycle length and red time for intersection delay is varied by function class level, irrespective of traffic flow details.

The Israel Institute of Transportation Planning and Research (Caliper 2002) has calibrated a logit-based volume delay function (VDF) for both travel link and intersection. The total delay on a link is the sum of the link delay, D_l, and intersection delay, D_n:

$$d = D_l + D_n \tag{2-18}$$

where

d = total delay on a link (s/veh);

D_l = link delay (s/veh); and

D_n = intersection delay (s/veh).

Link delay and intersection delay are separately expressed as follows:

$$D_l = \frac{t_0 \times b_1}{1 - \frac{b_2}{1 + \exp\left[b_3 - b_4 \times \left(\frac{v}{c} \right) \right]}} \tag{2-19}$$

$$D_n = \frac{d_0 \times p_1}{1 - \frac{p_2}{1 + \exp\left[p_3 - p_4 \times \left(\frac{v}{X} \right) \right]}} \tag{2-20}$$

where

t_0 = free-flow travel time on the link (s/veh);

v = volume or demand (vph);

c = link capacity (vph);

b_1, b_2, b_3, b_4 = parameters;

d_0 = free-flow travel time at the intersection (s/veh);

X = intersection capacity (vph); and

p_1, p_2, p_3, p_4 = model parameters.

In the above formula, intersection delays depend on the intersection capacity, which is calculated as a function of link capacity and expected green light percentage for a signalized intersection. Thus, analysts need calibrate eight parameters, b_1, b_2, b_3, b_4, p_1, p_2, p_3, and p_4, before applying them to a transportation model.

Zhao *et al*. (2006), Ding (2007) and Ding *et al*. (2009) proposed an artificial neural network (ANN) model to predict intersection delay based on traffic volumes from all movements of intersection. In their study, the authors assumed that signal timing plans are optimized in a future year and created simulated traffic data from TRANSYT-7F for which signal timing plans were optimized. The data were used to train artificial neural networks (ANN) to predict intersection delays. The delay model was applied to a network consisting of 20 nodes, and the results suggested that it is possible to reach convergent network equilibrium solutions using traffic volumes from multiple links of an intersection. The authors suggested link travel time estimation to be improved because intersection delays need to be separated from that estimated using the BPR equation, which already partially considered delays at intersections. Moreover, the authors admitted that a black box model approach is undesirable to planners and modelers because the logic of the models is invisible.

According to the literature review in this section, there are two kinds of travel time functions: link-based and node-based. Both of these functions have their advantages and disadvantages. Link-based methods are widely used because of their ability to satisfy the equilibrium assignment requirement. Alternatively, node-based methods are mainly aimed at improving the accuracy of delay estimation by incorporating realistic intersection delay, because intersection delay often compromises a large portion of total travel time, which is usually not taken into adequate consideration by link-based methods.

Although there are several node-based methods for estimating intersection delays for planning purposes, an obvious disadvantage is that they require, at a minimum, signal timing information. Unfortunately, this information is often not readily available for a base year and, especially, a future year. Given this limitation, the automated estimation of a realistic signal timing plan for an intersection becomes a challenge. On the other hand, coding signal plans for intersections is also a significant burden even if the information *is* available. Furthermore, there may be a large computational cost and convergence problem for a large network model when node-based delay estimation is involved. Consequently, node-based methods are not widely used, and the BPR equation is still the most popular for travel time estimation.

2.2 Technical Problems in Traffic Assignment

Information on traffic signal timing plans is important for the accurate estimation of intersection delay in node-based methods, as well as some link-based methods, which attempt to improve their delay estimation by introducing intersection delays. However, coding actual signal timing plans for a large scale network requires significant efforts.

Moreover, signal plans are continually optimized for better traffic operations, and signal plans for a forecast year are unavailable.

To address these issues, several researchers (Allsop, 1974, 1976; Gartner, 1976; Allsop and Charlesworth, 1977) have formulated a traffic-response signal control problem with a solution that does not require explicit relationship between optimal control settings and link flows for a given O-D matrix (Chiou, 2003).

In practice, there are two kinds of simulation methods to solve traffic-response signal control problems. Heydecker and Khoo (1990), Yang (1995), Yang and Yagar (1995), Wong (1995), Wong *et al*. (2001), and Chiou (1999, 2003) adopted a bi-level programming technique. The upper level deals with the traffic control problem and the lower level solves the traffic assignment problem. The combined traffic signal and assignment problem is solved iteratively between these two levels. This method is promising for dynamic traffic assignment problems. However, it cannot be applied to large networks, or to a static assignment problem (Hu *et al*., 2008).

Charlesworth (1977) discussed a method that deals with both the signal timing optimization problem and the traffic assignment problem independently, and then reiterates this process until convergence is reached. Smith and Vuren (1993) discussed the fundamentals of these problems and revealed that there may be many equilibrium solutions that do not converge. Gartner (1976), Gartner and Al-Malik (1996), and Lee and Machemehl (1999, 2005) investigated the convergence issue inherent in combined signal control and assignment problems; it was subsequently found that the equilibrium/incremental assignment method and the method of successive averages (MSA) (Sheffi, 1985), a transformation of the Frank-Wolfe algorithm, may be used for

resolving the aforesaid convergence discrepancies.

2.3 Travel Time Simulation

In this study, simulation software is employed to generate traffic data for the development of a travel time estimation model. There are a number of considerations in choosing a modeling approach, such as the context of decision-making, accuracy required, availability of data, the state of the art in modeling, resources available for the study, data processing requirements, and the skill level and training of the analysts (Ortuzar and Willumsen 2004). There are also non-technical limitations, such as social, political, and policy issues, available resources, and the training and skill level of modelers. The following sections review available simulation models and software packages.

2.3.1 Simulation Models

There are three types of simulation models, macroscopic simulation, mesoscopic simulation, and microscopic simulation. Macroscopic simulation models are based on the macro deterministic relationships of the flow, speed, and density of a traffic stream, as compared to the microscopic simulation that tracks individual vehicles. The computing requirements are low for macroscopic simulation models; however, they do not provide as much detail as microscopic models do. Some of the software packages for macroscopic simulation include TRANSYT-7F, PASSER, SATURN, KRONOS, and VISTA (Jeannotte *et al*., 2004a; 2004b).

Mesoscopic models simulate individual vehicles as in microscopic models. However, they are more similar to macroscopic simulations in that they consider vehicle movements over a link at an aggregate level. Several mesoscopic software packages are

available, such as CONTRAM (Continuous Traffic Assignment Model), DYNAMIT, DYNASMART, *etc*. (Jeannotte *et al*., 2004a; 2004b).

Microscopic simulation is recognized as a powerful tool for solving complex transportation problems, particularly when it is employed to capture the system impacts from queuing and oversaturation problems (Bloomberg and Dale 2000; Jones *et al.* 2004). In microscopic simulation, the movement of individual vehicles is tracked. Under oversaturation conditions, theories are complicated by uncontrollable variants, which need "a method whereby events on a road are reproduced in the laboratory by means of some machine which simulates behavior of traffic" (Webster 1958). The generic approach is not limited by the specific geometry of roadway, types of control, and traffic flow conditions. As such, it is generally agreed upon that microscopic simulation is capable of producing realistic results with proper model calibration and validation. For these reasons, more and more analysts are interested in applying microscopic simulation to transportation planning.

2.3.2 Micro-simulation Software Packages

There are a number of commercially available micro-simulation software packages, and the most popular ones include CORSIM, Paramics, VISSIM, AIMSUN, and SimTraffic (Jeannotte *et al*., 2004a; 2004b). Although some functions or implementations may differ, they all analyze both driver characteristics and the behavior of individual vehicles, and use car-following, lane-changing, and gap-acceptance algorithms. Jones *et al*. (2004) conducted a comprehensive comparison of simulation software, such as CORSIM, SimTraffic, and AIMSUN. Based on their experiments and a review of the key literature, they concluded that all three software packages can provide

reasonable results for typical simulation applications, although all three have individual strengths and weaknesses. CORSIM is a software package used throughout the U.S. and, consequently, has been extensively studied and well documented in the literature. CORSIM was developed by the Federal Highway Administration (FHWA) and has been in use for more than 30 years. As such, the driver behavior and vehicle performance models employed by CORSIM are widely accepted.

SimTraffic is a fully functional micro-simulation tool developed for the Synchro signal timing optimization program, originally intended with a focus on coordinated system timing plans. SimTraffic is thought to be the easiest for use and for network coding. However, SimTraffic is no better than CORSIM at modeling complex situations.

AIMSUN was developed in Spain and is primarily used in Europe. AIMSUN features the ability to model large urban and regional networks, and also possesses a dynamic assignment feature. These are unavailable in CORSIM and SimTraffic. AIMSUN also provides good three-dimension (3D) visualization.

The VISSIM software is developed by PTV AG of Karlsruhe, Germany and is part of the PTV-Vision suite of transportation planning and traffic engineering software programs. VISSIM is a multi-modal simulation software and is good for presentations to non-technical audiences due to its two or three-dimensional traffic flow modeling and video output. Bloomberg and Dale (2000) compared CORSIM and VISSIM in terms of not only the features provided but also performance. Based on their own experience, a literature review, and technical analysis, they concluded that CORSIM and VISSIM are more similar than different. At the intersection level, level of service (LOS) and throughput from the two models are similar, and both models are different from the HCM

calculations in some cases. For congested intersections with complex geometries, these models are more appropriate than the HCM method. The values of travel time from the VISSIM and CORSIM models are different due to their different car following and gap acceptance values, although the differences in their travel time estimations are consistent.

Paramics is a microscopic simulation software, developed in the UK during the 1990s. The complete edition of the Paramics suite includes eight modules: Modeller, Processor, Analyser, Monitor, Designer, OD-Estimator, Converter, and Programmer. In addition to the basic features that are similar to other simulation software, OD-Estimator, Converter, and Programmer are distinct modules that extend the capabilities of input, output, and simulation. Estimator is an O-D Matrix estimation tool designed to integrate seamlessly with the core Paramics modules. Programmer allows users to replace the core Paramics simulation with their own behavior models. Programmer can be used for ITS deployment, real-time connectivity and control, connectivity to real-world hardware and software systems, and advanced or customized model behaviors. Converter can work with data from various sources including Emme/2, Mapinfo, ESRI, Synchro, CORSIM, Cube/TP+/Viper, flat ASCII, and CSV. Converter can also be taught to read data with a format other than that mentioned above. A significant disadvantage of the Paramics model is the use of and reliance on O-D matrices to derive traffic volumes.

Table 2.2 summarizes the features of the micro-simulation software packages based on literature review.

Table 2.2 Comparison of micro-simulation software packages.

	CORSIM	SimTraffic	AIMSUN	VISSIM	Paramics
Coding time	Medium	Short	Long	Long	Long
Output	2D	3D	3D	3D	3D
Features	Main Features	Most Features	Full Feature	Full Feature	Full Feature
Travel time	Acceptable	Acceptable	Acceptable	Acceptable	Acceptable
Optimization Interface	TRANSYT-7F	Synchro	TRANSYT-7F/Synchro	Synchro	GENOSIM
Origin	US	US	Spain	Germany	UK
Cost	Low	Medium	High	High	High

2.4 Potential Modeling Approaches

With traffic data from simulation, the casual relationship between travel time (delay) and influential variables can be obtained by statistics analysis.

Ding (2007) employed artificial neural networks (ANNs) for determining intersection delays. ANNs are non-linear statistical data modeling tools. They mimic the learning process of the human brain and build the relationship between given input and output by repeated learning from given examples.

As stated by Hornik *et al*. (1989), the multitasking ability of the human brain is actually a result of the powerful neural architecture of connections or parallel distributed processing. A common type of ANN is a multi-layered, feed-forward neural network, which usually includes an input layer, an output layer, and one or more hidden layers (neurons). The neurons are connected through a transfer function, a weight matrix and a bias term. Figure 2.1 shows an artificial neuron network with one *n*-element input layer, one *p*-element hidden neuron layer and one *m*-element output layer. The neurons in the hidden layer, *a*, are output of transformation of input elements of *x*. *g* is a transfer function for the neurons in the hidden layer. The expression is as follows:

$$a = g(W_1 x + b_1) \tag{2-21}$$

where

W_1 = connection weight matrix between neurons and input;

b_1 = bias vector of hidden layer; and

x = input vectors.

Similarly, f is a transfer function for output and the output is expressed as follows:

$$y = f(W_2 a + b_2) \tag{2-22}$$

where

W_2 = connection weight matrix between neurons and output;

b_2 = bias vector of output layer; and

a = neurons in the hidden layers.

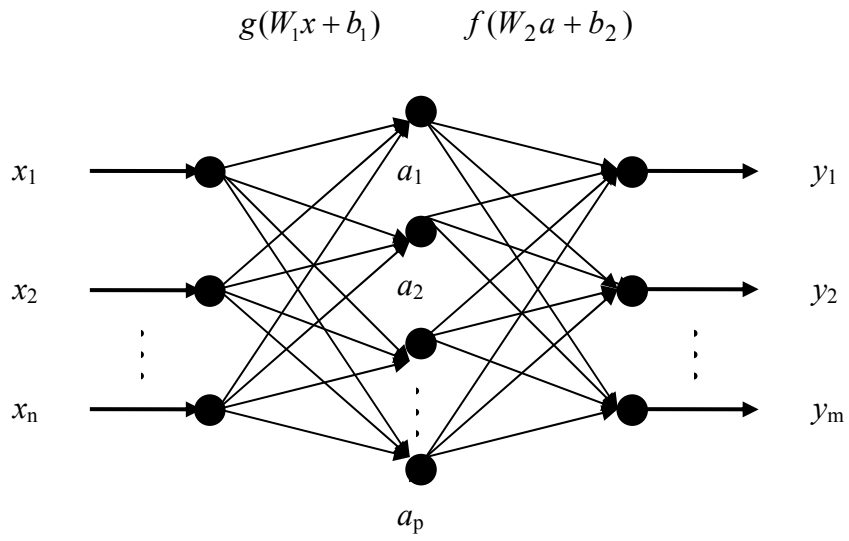

Figure 2.1 Prototype of a multi-layer artificial neural network.

An ANN model is an adaptive system that modifies its structure given the external and internal information that flows through the network during the learning process. The weight matrix and bias term are adjusted to minimize the error between the model output and the desired output during the training phase when a large number of samples are presented to the model. In the application phase, the well-trained parameters

of the model can predict the output based on the input. An ANN model is suitable for situations where the relationships are not well understood, highly involved, and non-linear.

Besides ANN model, statistical model may be an analytical function of independent variables. Independent variables could be factors that affect link travel time (delay) and, for practical purpose, should be readily available, such as link distance, speed, and traffic volumes at an intersection. A generalized model could be exemplified as follows:

$$t = f(L, x, z) + e \tag{2-23}$$

where

t = travel time or intersection delay;

L = distance from the intersection;

x = degree of congestion for subject traffic, subject traffic flow rate over subject capacity;

z = degree of congestion for cross-street traffic, cross-street traffic flow over cross-street capacity;

$f(L, x, z)$ = function of L, x, z; and

e = error term.

The parameters of the model are fitted to minimize the least square objective function, given as following:

$$s = \sum_i e_i^2 \tag{2-24}$$

where

s = sum of squared error; and

e_i = error term.

An analytical model is desirable for traffic assignment because it can be easily integrated into a transportation planning model and is efficient in computation. A suitable function form needs to be identified by studying delay-volume relationships from traffic data. Existing functional forms, such as the BPR equation, canonical equation, Akcelik equation, Dowling model, SERPM model, HCM model, *etc.*, provide clues but their inherent drawbacks need be addressed.

2.5 Summary

Currently, the travel time estimation methods in a traffic assignment model have their limitations with regard to dealing with delays at signalized intersections. Improvements in link travel time estimation for arterials may be achieved by considering intersection delays. Delay data that are needed to develop a delay model can be obtained through micro-simulation, and by considering signal control, roadway geometry, and traffic conditions. It is impractical to perform a signal design for each of intersection using a standard traffic analysis procedure in planning models.

CHAPTER 3

TRAVEL TIME ESTIMATION

Based on the literature review, the main criticism of the current travel time estimation equations is that they cannot properly predict travel time for interrupted traffic flows, such as on facilities with intersections. Important influential factors for a controlled intersection, such as signal timing plans, are either ignored or inadequately considered. The existing macroscopic delay estimation methods, such as the BPR equation, do not depict the proper spatial distribution of delay along a link. The delay in BPR equation is averaged on a link and is linearly proportional to the link length. Theoretically, a well calibrated BPR equation is only appropriate for a link of a certain length, which is the average link length from the field data collected for equation calibration. As such, delay estimation would not be accurate if link length is either too long or too short. The HCM method pays special attention to delay at an intersection node, which is a spatially important point along a link in terms of delay distribution. However, the HCM method assigns queue delays at an intersection, instead of on a link. When a link is shorter than the queue, which usually occurs in congested region or central business districts (CBD), a spillback of vehicles from downstream to upstream links is likely. However, the HCM method will assign all the estimated delay to the subject link, rather than adding the spillback delay to the impacted upstream links.

To address these problems, this dissertation is designed to develop a travel time model for planning purposes. Link travel time has two main components: free-flow travel time and delay. Free-flow time is the time that vehicles take to traverse a link at free-flow speed. This is determined by the ratio of link length and free-flow speed for a given link.

The key to travel time estimation is therefore the estimation of the delay on a link, which includes delays due to intersection control and delays due to the drop in speed that occurs as a function of increased demand on a link.

Adequate high quality data are necessary for investigating the relationship between link delay and other influential factors, such as traffic volumes, signal timing plan, facility geometry, *etc.* Field data collection is one source of information for this purpose, however, it is not an efficient way to obtain data due to the cost and the time required. Moreover, it is difficult to obtain data to cover a wide range of traffic conditions, such as a variety of traffic volume combinations, turn ratio combinations, intersection types, traffic operations, *etc.* As reviewed from the literature, microscopic simulation is able to produce realistic results given proper model calibration. This chapter describes the acquisition of delay data from simulation.

3.1 Experiment Design

An experiment is designed to extensively investigate how delays on a link and at an intersection respond to other influential factors. For the purposes of this study, an isolated intersection with four approaches is designed as a basic simulated element. Each approach has a 200-foot left-turn pocket to accommodate the left-turn movements. A signal control device is applied to manage at-grade traffic crossing at the intersection. The link for each approach is designed to be one-mile long, avoiding possible spillback of vehicles to source nodes. A sketch of simulated four-legged intersection with two lanes for each approach is presented in Figure 3.1.

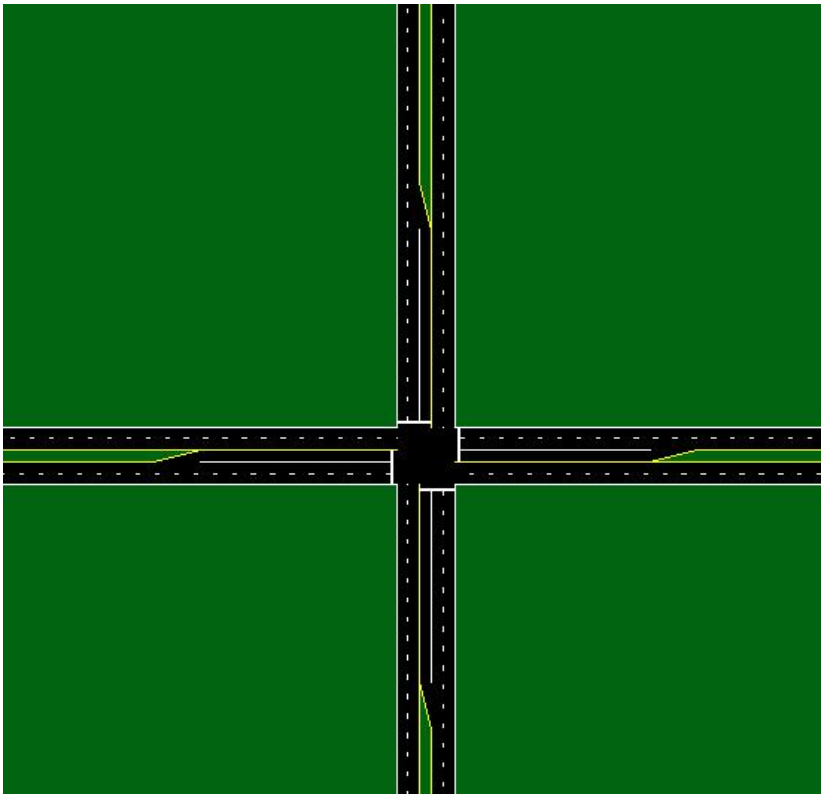

Figure 3.1 Simulated four-legged intersection.

There are several factors that affect the delay on a link connected to a signal-controlled intersection, such as traffic volumes, saturation flow rates, signal timing plan (cycle length, phase sequence, green time splits, and offset/coordination), downstream spill back, *etc*. The most significant influential factors are presented in Table 3.1, along with an explanation of how each factor is considered in this study.

Lane configurations are considered by simulating nine different configurations of the modeled intersections based on the number of lanes of the subject and cross-streets. Each of these configurations is labeled as TypeXY, with X being the number of directional lanes of the subject link and Y being that of the cross-street. The nine intersection configurations are Type11, Type12, Type13, Type21, Type22, Type23, Type31, Type32, and Type33.

Table 3.1 Influential factors on travel time delay.

Factors	Note
Lane Configurations	The lane number of both subject approach and other approaches.
Traffic Volumes	Traffic volumes for both subject approach and other approaches.
Facility Capacity	The capacity or saturation flow rate of a link.
Phasing	A four-phase signal design with leading left-turn treatment is assumed.
Cycle Length	Cycle length is optimized for a given traffic condition by TRANSYT-7F.
Green Time Splits	Green time for a given traffic condition is optimized by TRANSYT-7F.
Offset/Coordination	It is not considered. This could be considered with progression adjustment factors.
Downstream Spill-back	Delay caused by downstream spillback is assigned to the immediate upstream link.

Traffic volume is considered by simulating a large amount of variety of traffic conditions for these nine configurations. Travel delay time is produced for different scenarios of combinations of traffic flow conditions and left-turn ratios. The traffic volumes for each direction range from a very low amount (100 vphpl) up to a congested region (800 vphpl). The left-turn ratios are 10% or 20% of the link volume for a single-lane link, and 5% or 10% of link volumes for a multiple-lane link. The traffic volumes are designed to be balanced; i.e., the volumes for opposing directions, such as eastbound (EB) and westbound (WB), are assumed to be the same.

Signal timing plan is an important factor for determining the intersection delay of urban street. This study assumes that all signal timing plans are optimized for the given traffic conditions.

Default values are used for other influential factors, such as lane width, percentage of heavy vehicles, grade, parking, bus, bicycle, pedestrian blockage, *etc*. The

influence of these factors, in practice, could be included by adjusting the saturation flow rate as described in the HCM 2000.

A number of commercialized software packages are available as reviewed in the literature to conduct this experiment. For the simple design and limited requirements for this study, they are more similar than different. CORSIM microscopic simulation software is one of the most widely accepted. It supports for batch processing and provide an interface with the optimization software, TRANSYT-7F. Hence, delay data have been gleaned from the CORSIM microscopic simulation in a way designed above. TRANSYT-7F release 10 is selected to optimize signal for simulations.

3.2 Evaluation of Optimization Strategies

TRANSYT-7F provides a few options for signal optimization purposes, including two simulation engines (macroscopic or microscopic), several objective functions, and random number seeds. In this project, all of these available optimization options are investigated to evaluate the two simulation engines, select the best objective functions, and determine the role of random number seeds.

First, TRANSYT-7F provides the option of calculating the objective function by either the macroscopic engine of TRANSYT-7F or direct CORSIM simulation. TRANSYT-7F is a macroscopic engine and, as such, is faster than microscopic simulation. Micro-simulation usually gives more accurate results; however, the user should be careful when interpreting the results, especially during oversaturated conditions. For instance, CORSIM counts only vehicles that pass the stop line and calculates only delay for throughput, not demand. When the throughput of an intersection is smaller than the demand in a congested situation, the intersection delay extracted by TRANSYT-7F

from CORSIM cannot capture the excess delay experienced by vehicles at the back of the queue. Both CORSIM and TRANSYT-7F engines are evaluated in this study. The appropriate engine is selected based on whether it yields a better signal plan more often. The network-wide delay, as a performance measure, is computed by CORSIM using the signal plans that have been optimized by the objective functions with either the CORSIM or TRANSYT-7F engine.

Second, TRANSYT-7F produces signal plans by optimizing the objective functions. The objective functions for the TRANSYT-7F and CORSIM engines are slightly different. For the TRANSYT-7F engine, there are five objective functions: Control Delay, Throughput, Throughput/delay ratio, Throughput and Delay, and Queuing Ratio. An optimized signal plan may be obtained by minimizing control delay; minimizing the ratio of delay over throughput; minimizing queue ratio; maximizing throughput; or maximizing throughput and minimizing delay at the same time.

For the CORSIM simulation engine, the available objective functions in TRANSYT-7F are: Control Delay, Total Delay, Stop Delay, Queue Delay, Throughput, Percentage Stop, and Average Speed. An optimized signal plan may be obtained by minimizing control delay; minimizing stop delay; minimizing queue delay; minimizing total delay; minimizing percentage stop; maximizing throughput; or maximizing average speed. The values of the objective functions are computed by the CORSIM engine and returned to TRANSYT-7F; in turn, TRANSYT-7F performs the optimization procedure using a genetic algorithm (GA). This procedure is iterated until either an optimized result is obtained or a maximum iteration number is reached, whichever comes first. An

investigation is conducted to select a suitable objective function and the corresponding simulation engine for this study.

Third, TRANSYT-7F provides genetic algorithms as an option to optimize signal control plans. Genetic algorithms are a stochastic simulation process with the ability to go beyond a "local optimum" solution and locate a mathematically "global optimum" solution. Theoretically, given the necessary GA parameters, such as the maximum iteration number and the lowest convergence threshold, one and only one global optimum solution should be reached. The default values of GA parameters in TRANSYT-7F are suggested for use in practice; however, it appears that using different random number seeds may speed up the optimization process. This tactic may help the optimization process to avoid being stuck on a local optimum solution too long.

It should be noted that the TRANSYT-7F engine allows the user to choose from single-cycle or multi-cycle simulation, and step-wise or link-wise simulation. Single-cycle simulation only performs simulation for one cycle, the duration of which may be specified (usually 15 minutes). Compared to single-cycle, multi-cycle simulation is useful when flow is oversaturated, which improves the estimation of accurate queue blockage. When traffic flow is steady, i.e., queue length does not change between cycles, the result is identical for both multi-cycle and single-cycle simulations.

Single-cycle simulation can be performed using either step-wise or link-wise simulation, but multi-cycle simulation can only be combined with step-wise simulation. In step-wise simulation, all links within a network are simulated for one step or one second at a time, and the same procedure is repeated for all links during the analysis period. Step-wise simulation is best suited for queue-blockage and back of queue

scenarios. In link-wise simulation, each link is completely simulated before moving to the next link. Link-wise simulation is thought to be faster than the step-wise method. This project chooses multi-cycle and step-wise simulation, for TRANSYT-7F engine, to reach a realistic queue simulation for optimization purposes.

3.2.1 Objective Functions and Simulation Engines

This section presents the optimization test results for both TRANSYT-7F and CORSIM engines, obtained by applying the available objective functions. The tests have been performed for several representative traffic volume combinations of intersection Type22. Table 3.2 shows the results for an intersection with light traffic conditions for both subject and cross-street links (200 vphpl for all four approaches). The left-turn ratios for all four approaches are 10% of the total volume of each approach. The columns labeled *EW L*, *EW Th*, *NS L*, and *NS Th* represent the phases for East-West (EW) leading left-turn, EW through movement, North-South (NS) left-turn, and NS through movement. The green times in second for each phase are included in the table. *Cycle* is the cycle length in second. *Delay* is the intersection control delay in the unit of minutes per vehicle (min/veh), as derived by CORSIM simulation.

For this scenario, objective functions Control Delay, Throughput/delay, and Queue Ratio in the TRANSYT-7F engine all give the same signal timing plans and the minimal intersection delay, 0.27 min/veh. The cycle length is 80 seconds and the green times for North-South direction and East-West direction are almost the same for this balanced traffic flow. The CORSIM engine combined with the objective functions Control Delay, Total Delay, Stop Delay, Queue Delay, or Average Speed also gives fair optimization results. On the other hand, the objective functions Percentage Stop, or

Throughput combined with the CORSIM engine yield the worst results for this scenario, with the control delay time being two to five times the value of other objective functions. This shows that optimization results by different objective functions and simulation engines may vary within a large range.

Table 3.2 Optimized signal plans for an intersection with subject volume of 200 vphpl and cross-street volume of 200 vphpl.

Method		*EW L* (s)	*EW Th* (s)	*NS L* (s)	*NS Th* (s)	Cycle (s)	Delay (min/veh)
TRANSYT	Control Delay	11	30	10	29	80	0.27
	Throughput	13	18	14	75	120	0.47
	Throughput/delay	11	30	10	29	80	0.27
	Throughput & Delay	13	18	14	75	120	0.47
	Queue Ratio	11	30	10	29	80	0.27
CORSIM	Control Delay	10	24	14	37	85	0.31
	Total Delay	10	24	14	37	85	0.31
	Stop Delay	10	24	14	37	85	0.31
	Queue Delay	10	24	14	37	85	0.31
	Throughput	65	16	21	18	120	0.62
	Percentage Stop	11	94	11	9	125	1.61
	Average Speed	10	24	14	37	85	0.31

Table 3.3 presents test results for a scenario that the traffic volumes in both subject direction and cross-street direction are medium. The CORSIM engine combined with the objective functions Control Delay, Total Delay, Stop Delay, or Queue Delay yields minimal control delay of intersection. However, CORSIM engine combined with the objective functions Percentage Stop or Average Speed gives the worst result. Generally speaking, the overall optimal results from TRANSYT-7F engine are fair.

Table 3.4 presents test results for a scenario that the traffic in both subject and cross-street directions are quite heavy. The objective function of Throughput combined with the CORSIM engine yields a minimal intersection delay. The Objective functions

Control Delay, Throughput/delay, and Queue Ratio combined with the TRANSYT-7F engine give similar optimum control delay of intersection. Others give worse results.

Table 3.3 Optimized signal plans for an intersection with subject volume of 750 vphpl and cross-street volume of 750 vphpl.

Method		*EW L* (s)	EW Th (s)	*NS L* (s)	*NS Th* (s)	Cycle (s)	Delay (min)
TRANSYT	Control Delay	10	47	10	53	120	0.82
	Throughput	11	28	10	31	80	0.82
	Throughput/delay	10	47	13	50	120	0.71
	Throughput & Delay	11	30	10	29	80	0.75
	Queue Ratio	10	47	13	50	120	0.71
CORSIM	Control Delay	12	36	12	35	95	0.59
	Total Delay	12	36	12	35	95	0.59
	Stop Delay	12	36	12	35	95	0.59
	Queue Delay	12	36	12	35	95	0.59
	Throughput	12	43	13	42	110	0.69
	Percentage stop	28	84	9	9	130	3.48
	Average Speed	28	84	9	9	130	3.48

Table 3.4 Optimized signal plans for an intersection with subject volume of 1,400 vphpl and cross-street volume of 1,400 vphpl.

Method		*EW L* (s)	*EW Th* (s)	*NS L* (s)	*NS Th* (s)	Cycle (s)	Delay (min)
TRANSYT	Control Delay	10	50	12	48	120	3.62
	Throughput	22	17	30	51	120	5.35
	Throughput/delay	10	50	12	48	120	3.62
	Throughput & Delay	22	17	30	51	120	5.35
	Queue Ratio	10	50	12	48	120	3.62
CORSIM	Control Delay	27	89	10	9	135	4.31
	Total Delay	27	89	10	9	135	4.31
	Stop Delay	27	89	10	9	135	4.31
	Queue Delay	27	89	10	9	135	4.31
	Throughput	12	49	12	47	120	3.54
	Percentage stop	10	90	11	9	120	4.72
	Average Speed	22	79	10	9	120	4.24

The complete evaluation results of the objective functions and the simulation engines are included in Appendix A. After a careful examination of all test scenarios, it is

found that the objective function of Throughput/delay, when combined with the TRANSYT-7F engine, performs better in most situations. It gives optimal result for light, medium and heavy traffic conditions and the results from TRANSYT-7F engine are more stable and predictable. Furthermore, TRANSYT-7F engine consumes less computation cost than CORSIM engine, which is preferable considering most of the computation cost will be spent on signal plan optimization. Therefore, in this study, the objective function of Throughput/delay is combined with the TRANSYT-7F engine for the signal optimization for a variety of traffic flows.

3.2.2 Random Seed Number

For the selected TRANSYT-7F engine and the objective function of Throughput/delay, six different random number seeds, 1337, 2973, 5619, 9431, 7781, and 4573, are used for the optimization of each of scenario with a limited iteration (40 iterations). The best signal timing plan may be selected from one of the six optimization runs with a maximum value of performance index (PI), i.e., throughput/delay. Table 3.5 shows a sample of the optimization results using six different random number seeds. The traffic volumes for all approaches are 200 vphpl and the left-turn ratios are 10%. Column 1 lists the random number seeds. Columns 2 through 5 present the green times for EW leading left-turn phase, EW through phase, NS left phase, and NS through phase. Each phase includes, by default, three seconds of yellow time and one second of all-red time . Columns 6 through 8 present cycle length, control delay, and performance index.

For this example, the best signal timing plan is given by random number seed 4573, for which control delay is 15.9 seconds and performance index is 177.2. Appendix B lists more results from random number seed testing. From these results, it is found that

the optimized control delay and performance index are not the same for different random number seeds, which suggests that global optimal result may not be reached with one particular random number seed and a limited maximum iteration number. Another observation is that no specific random number seed is found to produce optimal results all the time. Hence it is necessary to check the optimal results of different random number seeds and find the best result, given that it is an unaffordable computation cost to run an extremely large number of iterations with a single random number seed. It is also found that the best optimal results from these test scenarios are reasonably good after six runs of optimization with six different random number seeds, which suggests that a solution near a global optimum may be reached with one of the random seeds within 40 iterations. The performance test is made for nine representative traffic combinations, including low, medium, and heavy traffic conditions. The results suggest that employing six random number seeds for each instance of optimization is appropriate because the near optimal result could be reached in most scenarios by using this tactic.

Table 3.5 Testing random seeds for the scenario that both traffic volumes from subject direction and cross-street direction are 200 vphpl.

Seed	*EW L* (s)	*EW Th* (s)	*NS L* (s)	*NS Th* (s)	Cycle (s)	Control (s)	PI
1337	12	19	9	15	55	19.6	143.6
2973	12	14	19	15	60	25.0	112.8
5619	9	25	7	19	60	18.9	149.0
9431	7	20	11	17	55	18.6	151.3
7781	7	14	9	20	50	17.5	160.7
4573	7	15	7	11	40	15.9	177.2

3.3 Simulation

Based on the optimized signal timing plans, travel time and delay for an intersection with four approaches are simulated. Due to the stochastic nature of CORSIM, it is necessary to

run the simulation multiple times with different random numbers to reflect the variability of a stochastic process. The statistical average values of delay are obtained based on ten random runs in this study. The simulation period for each of the cases is set for one hour.

Signal coordination is not considered in this study, but may be considered by incorporating a progression factor. For this purpose, the uniform distribution of departure vehicles is used in CORSIM simulation. The delay by simulation is expected to be uniform delay term in HCM method when the traffic volumes are below congestion regions (Buckholz 2008).

A dummy node design is adopted in this study to assess the spatial distribution of travel time and delay. As shown in Figure 3.2, dummy nodes are added onto a link every 200 feet to obtain the delay for each of the link segments (the segment between two dummy nodes). With this design one simulation run of a scenario could produce delay information for different distance from signalized intersection to a dummy node, therefore links of different lengths can be handled. The total delay for a link is the sum of the delays of link segments from the downstream intersection to the upstream node. Information about the spatial distribution of delays along a link explains how delays increas from an intersection to upstream. When spillback of vehicles occurs on an urban street, this information allows the delay due to spillback to be assigned to an upstream link.

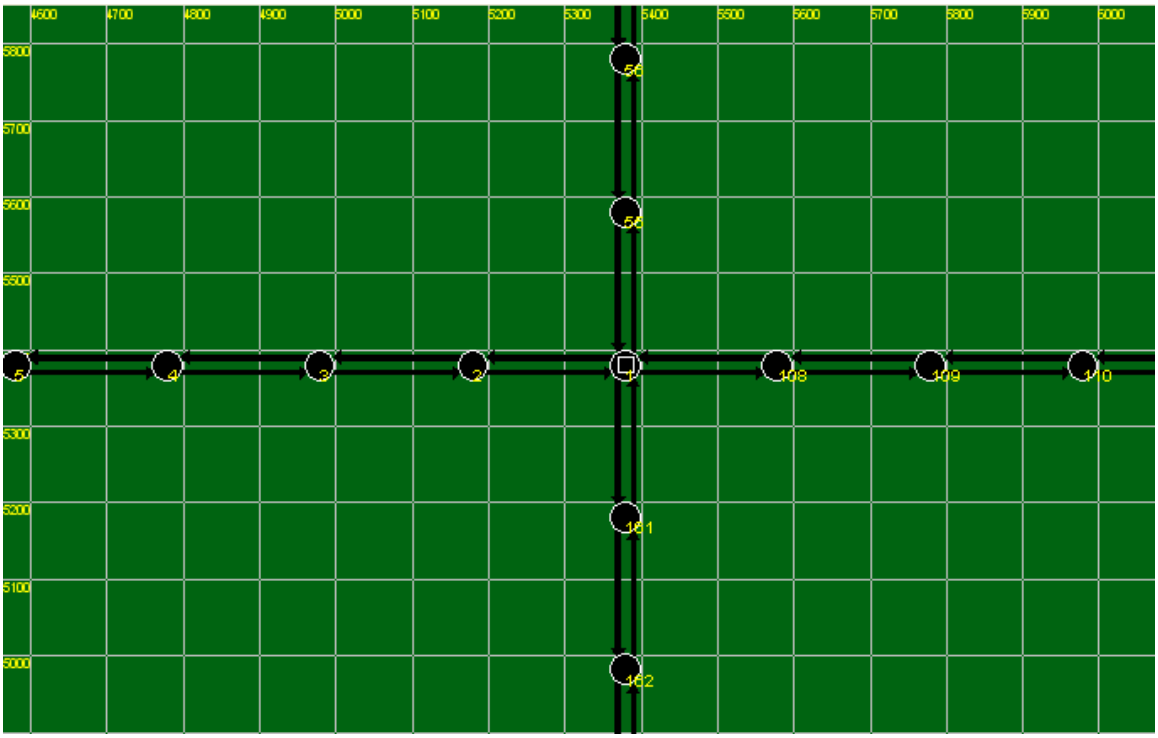

Figure 3.2 Dummy nodes designed for the links attached to an intersection.

This section presents the simulation results and their characteristics. The relations of delay and other factors, such as link length, subject volume, cross-street volume, and left turn ratio are presented. Figure 3.3 shows the spatial distribution of delay along a subject link of Type11 intersection, traffic volume ranging from 100 to 800 vphpl. The traffic volumes for the cross-street directions are 700 vphpl.

Figure 3.4 gives a close-up look of the delay spatial distribution along the segments of the first 1,400 feet. It is found that the delay experienced on the first segment (200 feet) accounts for a significant amount of total delay, and it drops when moving away from the intersection. Note that the most congested traffic condition for an intersection (800 vphpl) is still well below the saturation flow rate of a link. The delay is not sensitive to the traffic volume anymore and is nearly zero when the distance from the intersection is more than 1,000 feet, which suggests that the queue length is less than 1,

000 feet for most traffic conditions. The queue length could be represented by the decay length of the curve in the figures.

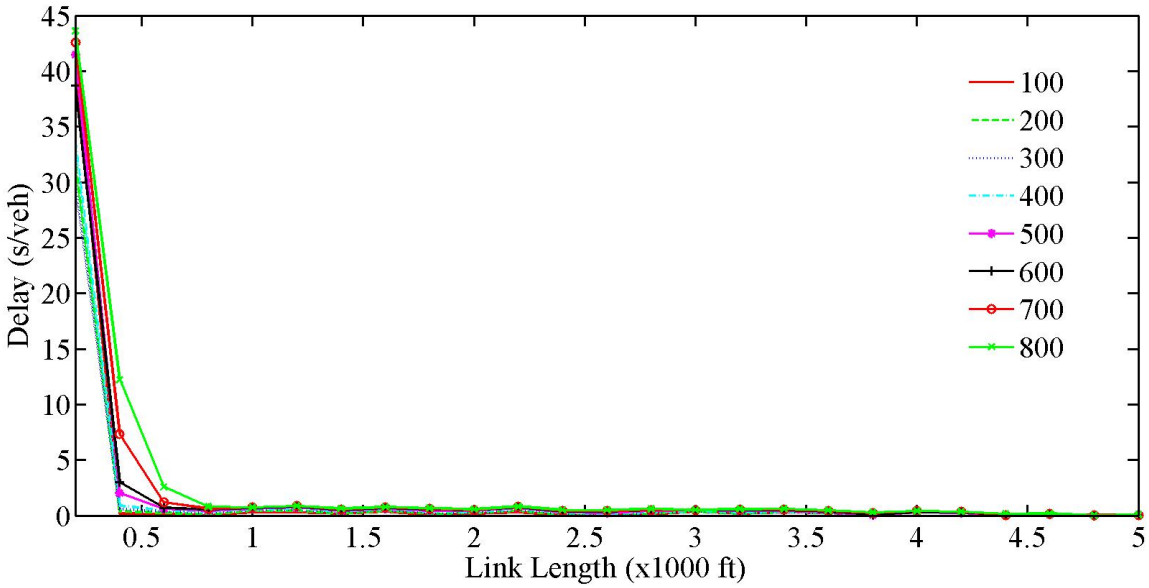

Figure 3.3 Spatial distribution of delay for different scenarios of subject traffic conditions.

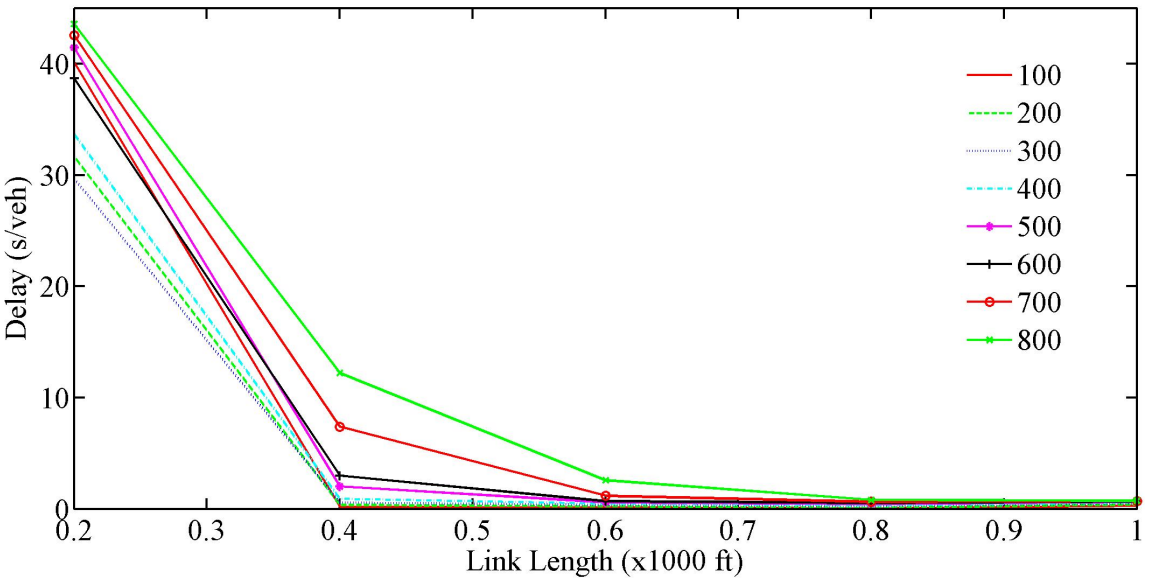

Figure 3.4 Spatial distribution of delay for different scenarios of subject traffic conditions (first 1, 000 feet).

Figure 3.5 depicts the delay-volume relationships for the first 200-foot segment. The intersection is still of the Type11 configuration. The stacked lines are the delay-

volume relations for different cross-street volumes. There is a general trend that the delay increases as the subject volume becomes larger.

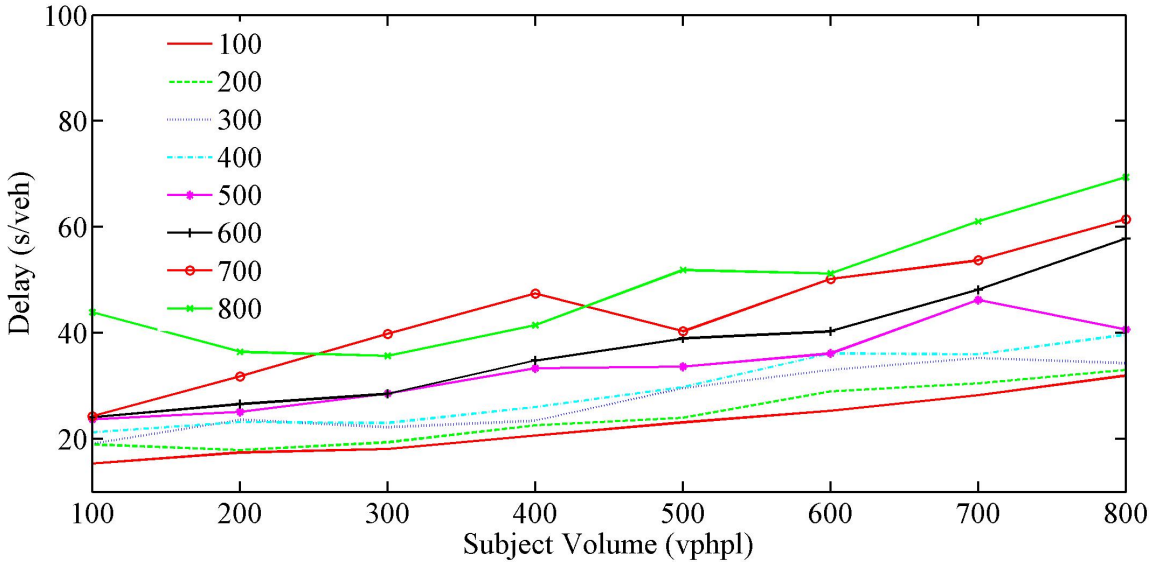

Figure 3.5 Delay-volume relations in subject direction for the different scenarios of cross-street traffic conditions for the first 200-foot segment.

It is also found that delay for a given subject volume is larger when the cross-street traffic volume is larger. The relationship between delay and cross-street volume is shown in Figure 3.6, which depicts the relationship between subject-link delay at the first segment of a link and cross-street volume. Similar to Figure 3.5, the stacked lines are the delay versus cross-street volume for different subject volumes. The general trend of lines in Figure 3.6 tells that the subject delay increases as the cross-street volume increases. It is found that the delay of a link is affected not only by subject volumes, but also by cross-street volumes.

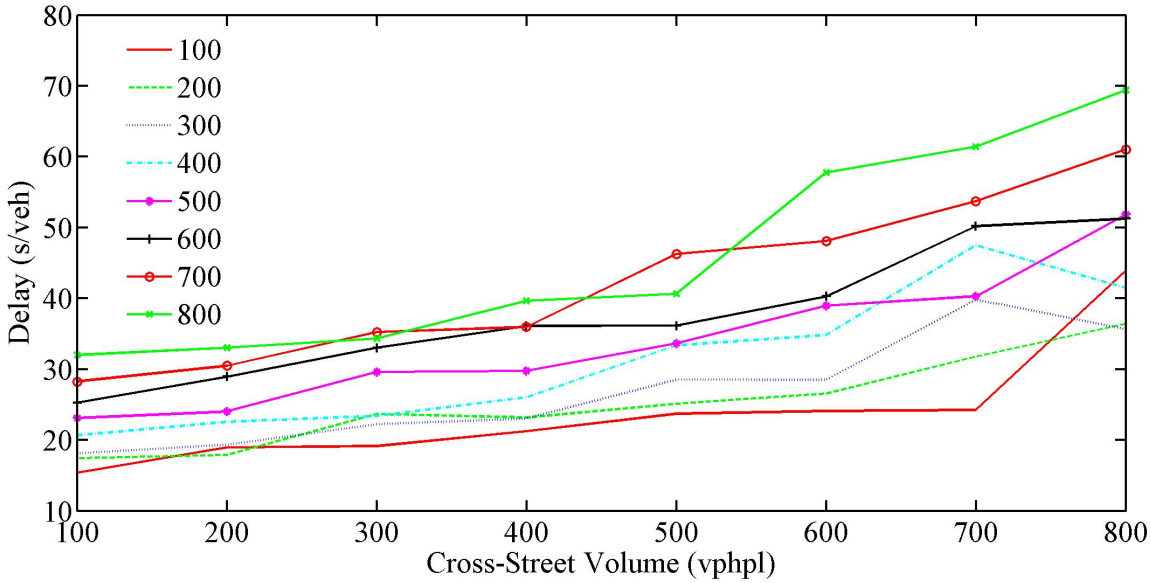

Figure 3.6 Subject delay versus cross-street volume for the different scenarios of subject traffic conditions at the first 200-foot segment.

Figure 3.7 depicts the delay spatial distribution for different left-turn ratios of subject approach. It is found that left-turn ratio most likely affects the delay on the first segment of the subject link, and the delay is larger when the left-turn ratio of the subject link increases.

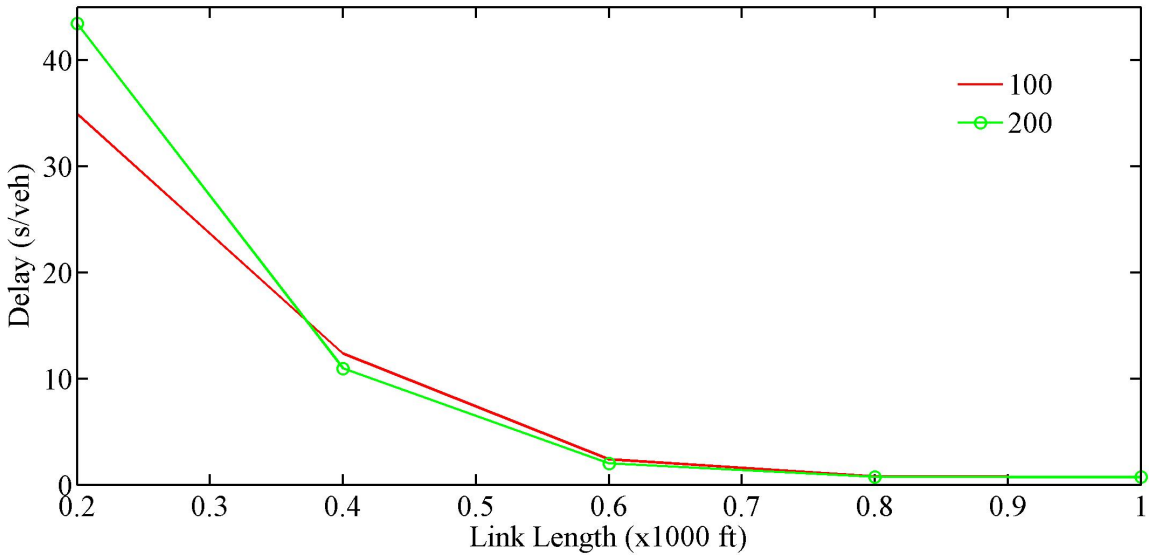

Figure 3.7 Delay spatial distribution for different subject left-turn ratios.

Figure 3.8 depicts the delay spatial distribution for different left-turn ratios of a cross-street approach. Contrary to the turning ratio of subject traffic, the turning ratio of cross-street traffic has almost no influences on the subject link delay. All these figures help to understand how delay is affected by possible influential variables, such as subject volume, cross-street volume, link length, turning ratios, and also help to develop the functional form of the travel time model.

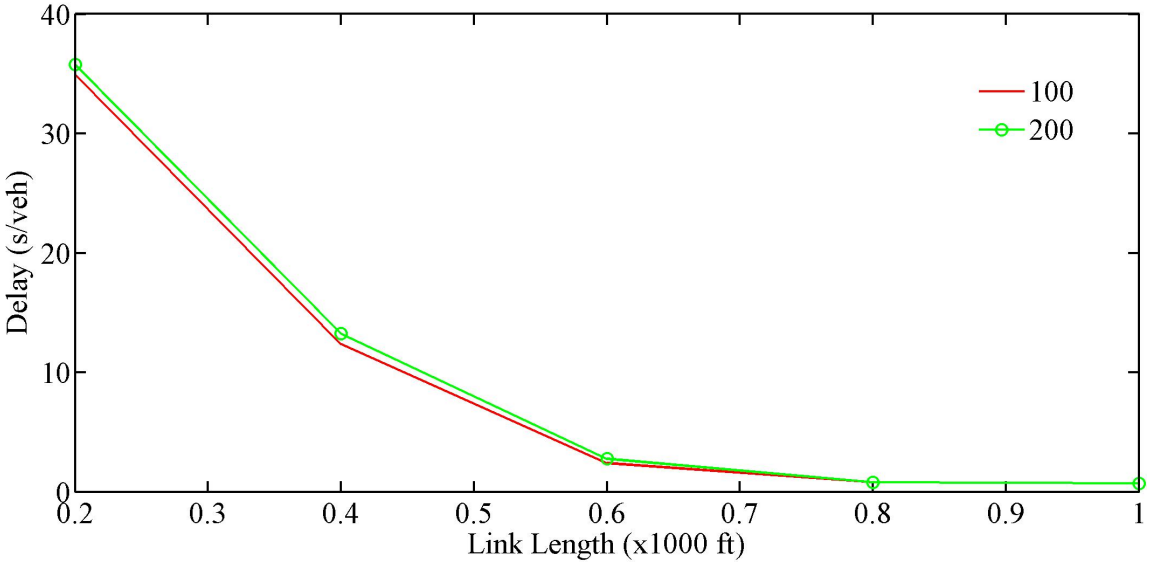

Figure 3.8 Delay spatial distribution for different cross-street left-turn ratios.

The delays from the simulation are compared to the delays predicted by the existing models reviewed in Chapter 2, as shown in Table 3.6, to assess the prediction capability of the existing models. The simulation scenario is a Type11 intersection with traffic volumes of 700 vphpl for all approaches. For the upstream segments with different distances from the intersection, as listed in the first column, delays obtained from CORSIM, standard BPR equation, Conical method, SERPM model, Dowling method and HCM method (uniform delay part), are presented in Columns 2 through 7. The capacity of the link used in all of the compared models that need capacity as an input is 750 vphpl.

Table 3.6 shows that the predicted delays by BPR and Dowling method are underestimated compared to CORSIM simulation. Overall, the delay predicted by the HCM method is better than both the BPR and Dowling method, though it is still slightly underestimated. The delays predicted by the Conical method and SERPM model show an underestimation for a shorter link and overestimation for a longer link.

Table 3.6 Comparison of delays between CORSIM simulation and existing models.

Distance from Intersection (ft)	Delay (s/veh)					
	CORSIM	BPR	Conical	SERPM	Dowling	HCM
200	38.4	0.3	2.3	4.7	15.5	28.5
400	42.9	0.7	4.6	9.4	15.5	28.8
600	43.8	1.0	6.9	14.1	15.6	29.2
800	44.4	1.4	9.3	18.8	15.7	29.5
1000	45.1	1.7	11.6	23.5	15.8	29.8
1200	46.0	2.1	13.9	28.2	15.8	30.2
1400	46.5	2.4	16.2	32.9	15.9	30.5
1600	47.3	2.8	18.5	37.6	16.0	30.9
1800	47.9	3.1	20.8	42.3	16.1	31.2
2000	48.4	3.4	23.1	47.0	16.1	31.6
2200	49.2	3.8	25.4	51.7	16.2	31.9
2400	49.6	4.1	27.8	56.4	16.3	32.3
2600	50.0	4.5	30.1	61.1	16.4	32.6
2800	50.6	4.8	32.4	65.8	16.4	33.0
3000	51.1	5.2	34.7	70.5	16.5	33.3
3200	51.6	5.5	37.0	75.2	16.6	33.6
3400	52.1	5.9	39.3	79.9	16.7	34.0
3600	52.5	6.2	41.6	84.6	16.7	34.3
3800	52.7	6.6	44.0	89.2	16.8	34.7
4000	53.1	6.9	46.3	93.9	16.9	35.0
4200	53.5	7.2	48.6	98.6	17.0	35.4
4400	53.5	7.6	50.9	103.3	17.0	35.7
4600	53.6	7.9	53.2	108.0	17.1	36.1
4800	53.7	8.3	55.5	112.7	17.2	36.4
5000	53.7	8.6	57.8	117.4	17.3	36.7
5200	53.7	9.0	60.1	122.1	17.4	37.1

Notes: The traffic volumes for all approaches of Type11 Intersection are 700 vphpl;
BPR equation: α=0.15, β=4;
SERPM model: α=0.55, β=5.05, C=90 s, g/C=0.55 (speed>=35 mph);
α=0.35, β=4.05, C=60 s, g/C=0.50 (speed<35 mph);
Conical equation: α=4.00, β=1.17; and
Dowling method: α=0.05, β=10.

3.4 Data Filtering

It should be noted that with limited iterations, optimization by TRANSYT-7F does not always give the optimized signal timing plan, which results in unexpected (unrealistic) delay from the simulation. This is also implied by random number seed testing described in Section 3.2.2 and in Appendix B, in which control delays optimized by some random number seeds are unrealistically large. Although in most instances, an optimal result could be reached by selecting one of the six results obtained from different random number seeds, there is a small chance that the best result is still far from optimum. The obvious phenomenon is that the delays for the subject and cross-street links in some scenarios are extremely unbalanced for almost equal traffic volumes from all approaches.

Although there are no existing rules to easily tell whether a signal plan is inappropriate, common sense could be employed to rule out such signal plans. For instance, it is acceptable that the per-vehicle delay for the subject approach to be larger than that of cross-street approach if the volume of the subject approach is larger. However, the ratio between the two delays should not exceed a certain threshold. This threshold could be set by the analyst to prevent unrealistic results.

There exists another possibility. The approach with the larger volume may be assigned even more green time to relief the congestion; in turn, the per-vehicle delay for that approach may be smaller than that for the cross-street approach, but the aggregated delay for the approach with the larger volume usually should not be less than the aggregated delay for the cross-street approach. Otherwise, a slight sacrifice of green time for the approach with larger volume may not increase its delay noticeably, but could significantly reduce the delay for the cross-street approach; in turn, the overall

intersection delay would be reduced. This suggests another rule, which is that the ratio of the smaller per-vehicle delay to the larger one should not be smaller than the smaller one of their volume ratios. To be conservative, the criterion ratio is set to be twice of the ratio indicated by their volumes. Hence, valid delay data satisfy the following conditions:

$$\min(\frac{1}{2R}, \frac{R}{2}) < \frac{d_{subject}}{d_{cross}} < \max(2R, \frac{2}{R}) \tag{3-1}$$

where

$d_{subject}$ = link delay per vehicle in subject direction (s/veh);

d_{cross} = link delay per vehicle in cross-street direction (s/veh); and

R = ratio of subject traffic volume (vph) and cross-street traffic volume (vph).

Based on the criterion stated above, the data are filtered and suspected outliers are excluded. The number of excluded data points is presented in Table 3.7 for each of the intersection types. Less than 5 percent of the simulation data are disregarded.

Table 3.7 Filtering of simulation data.

	Intersection Type								
	Type11	Type12	Type13	Type21	Type22	Type23	Type31	Type32	Type33
Total	6,656	12,480	17,004	10,634	22,386	35,022	15,028	31,928	44,902
Excluded	0	0	468	286	1,014	858	260	832	962
Percentage	0.0	0.0	2.8	2.7	4.5	2.4	1.7	2.6	2.1

The criterion ratios of 1.0 and 5.0 are also tested, and the number of disregarded data is not significantly different. This indicates that the discarded data are those for which the signal plan is far from optimum. Although the number of discarded data is quite small, it is significant for the development of a statistical model because inclusion of these unrealistic data would significantly degrade the model in question.

3.5 Summary of Simulation Data

The travel delay data are simulated by the microscopic simulation software, CORSIM, with signal timing plans optimized by TRANSYT-7F. The experiment designs, such as dummy node design, the selection of optimization engine, the selection of objective function, different random number seeds, and data filtering, are employed to obtain the required data with high quality. The goal is to obtain high quality travel delay data for model development in a systematic and cost effective way, as opposed to the costly and time-consuming process of field data collection.

CHAPTER 4

STATISTICAL ANALYSIS

The relationship between travel delay and its influential factors, such as traffic volumes and link length, is modeled with Statistical Analysis Software (SAS). The optimized parameters of the model are obtained by minimizing the objective function of the sum square of errors. The NLIN procedure in SAS is used with the Marquardt optimization method, which searches different domains of initial parameters.

The functional form of the model is given by Equation (4-1) and is developed based on observations of the relationship between delay and link length, traffic volumes from all movements in Section 3.3. The model is as follows:

$$t_{delay} = a_1 \times L + X_{subject}\left[a_2 + a_3 \frac{(X_{cross})^{a_4}}{(X_{subject})^{a_5}}\right]\left[1 - \exp\left(-\frac{a_6 \times L}{X_{subject}}\right)\right] \qquad (4\text{-}1)$$

where

t_{delay} = total delay on a link with a length of L (s/veh);

L = distance from intersection to the location where delay is measured (miles);

$X_{subject}$ = degree of congestion for a critical lane group in subject approaches;

X_{cross} = degree of congestion for a critical lane group in cross-street approaches; and

$a_1, a_2, a_3, a_4, a_5, a_6$ = fitted parameters.

The degrees of congestion for a subject and cross-street approach, $X_{subject}$ and X_{cross}, are defined as follows:

$$X_{subject} = \frac{v_{subject}}{c_{subject}} \tag{4-2}$$

$$X_{cross} = \frac{v_{cross}}{c_{cross}} \tag{4-3}$$

where

$X_{subject}$ = degree of congestion for a critical lane group in subject approaches;

$v_{subject}$ = per-lane volume for a critical lane group in subject approaches (vphpl);

$c_{subject}$ = per-lane capacity (or saturation flow rate) for a critical lane group in subject approaches (vphpl);

X_{cross} = degree of congestion for a critical lane group in cross-street approaches;

v_{cross} = per-lane volume for a critical lane group in cross-street approaches (vphpl); and

c_{cross} = per-lane capacity (or saturation flow rate) for a critical lane group in cross-street approaches (vphpl).

The model indicates that delay has three parts: friction delay along a link, delay right before an intersection due to signal control, and queue delay that decays exponentially with the increase in the distance from the intersection. Friction delay is the first term in the equation, i.e., $a_1 \times L$, which is proportional to the link length. The second term, $a_2 + a_3 \frac{(X_{cross})^{a_4}}{(X_{subject})^{a_5}}$, is mostly determined based on the competition between the volumes of subject and cross roads, which fundamentally determines the signal splitting.

The third term, $X_{subject}\left[1-\exp\left(-\frac{a_6 \times L}{X_{subject}}\right)\right]$, is an integral of an exponential decay function, and describes how queue delay is accumulated near the intersection. This term is approximated because segment delay nearly exponentially decreases when the link length increases, as shown in Figures 3.3 and 3.4. The decay length, $\frac{X_{subject}}{a_6}$, is determined by the degree of congestion of the subject link volume. The exponential relationship is observed and verified by the data for a variety of volume combinations. The degree of congestion is defined in two different ways in this study: one by the ratio of volume to capacity, and the other by the ratio of volume to saturation flow rate. Left-turn and right-turn ratios are considered through adjusting saturation flow rate or capacity.

4.1 Degree of Congestion Defined by the Ratio of Volume to Capacity

In practice, the capacities of links connected to the intersection can usually be estimated. The degree of congestion of a link connected to an intersection is then expressed as the ratio of volume to reduced physical capacity of the link. The simulated facility, described in the previous section, is assumed to be an intersection with divided arterial roads, which have a physical capacity of 750 vphpl (FDOT 1997). Thereafter, the model developed based on this measure of degree of congestion is cited as the capacity-based delay model (or represented by capacity-based thereafter).

Nine capacity-based models, which are for the nine intersection types, are developed based on the simulated data. The fitted parameters for nine different models are shown in Table 4.1.

Table 4.1 Fitted parameters for developed model with degree of congestion defined by volume to reduced physical capacity.

Parameters	a_1 (s/veh/mile)	a_2 (s/veh)	a_3 (s/veh)	a_4	a_5	a_6 (1/mile)
Type11-V1	6.5678	13.3733	19.2147	0.5746	1.0743	31.6264
Type11-V2	6.6336	23.5309	21.5217	1.6190	1.0564	40.8196
Type11-V3	11.5076	16.0301	27.0282	1.3844	0.7237	49.3029
Type11-V4	10.8644	27.8275	19.2703	3.1277	0.8718	41.6388
Type12-V1	6.5506	14.9922	19.3105	0.6245	1.1859	33.3889
Type12-V2	6.9174	7.2626	40.5680	1.2991	0.8497	42.0766
Type12-V3	11.7004	15.5101	33.4226	1.3461	0.5222	49.3079
Type12-V4	10.7654	31.3140	22.9674	3.5978	0.8891	38.1690
Type13-V1	6.5015	14.3359	17.0008	0.5243	1.2598	32.8687
Type13-V2	6.3975	23.9102	21.9020	1.5773	1.2138	39.5509
Type13-V3	11.6650	15.9407	31.3207	1.3978	0.5380	49.1855
Type13-V4	10.3659	36.6817	13.0402	6.0055	2.0236	42.6084
Type21-V1	8.8058	14.6038	20.8539	0.7797	1.0668	28.1592
Type21-V2	9.1033	0.0000	44.5422	1.1033	0.7326	36.1980
Type21-V3	11.8959	15.9229	45.1994	2.0627	0.0000	48.2451
Type21-V4	10.3308	36.0020	10.7427	4.1843	1.8679	38.0763
Type22-V1	8.7914	10.8203	20.0060	0.5722	1.0929	26.6629
Type22-V2	8.7709	28.4325	16.5642	1.8307	1.2725	35.9642
Type22-V3	11.7006	11.1865	24.5650	0.9851	0.7895	51.8955
Type22-V4	11.3548	20.8656	25.8819	3.0991	0.9213	41.1566
Type23-V1	8.9350	8.4788	24.3442	0.5568	1.0246	28.0850
Type23-V2	8.8655	21.1647	27.5940	1.5730	1.0446	36.3515
Type23-V3	12.0316	13.6009	42.4142	1.6348	0.0000	48.6505
Type23-V4	11.1356	34.7163	18.6581	5.4296	0.9109	36.2531
Type31-V1	9.4178	11.0442	23.2008	0.6421	1.0155	29.0569
Type31-V2	9.6044	8.0373	36.1254	1.3158	0.9009	36.7698
Type31-V3	12.5453	15.4848	42.1810	1.8062	0.2913	47.9063
Type31-V4	11.6419	35.4281	11.1351	3.7879	2.1981	39.2630
Type32-V1	9.4544	8.3498	23.0695	0.5808	1.0815	26.9064
Type32-V2	9.5068	4.9754	34.0901	1.0813	0.9689	35.8456
Type32-V3	12.6574	15.6515	37.6976	1.9333	0.6828	49.1965
Type32-V4	11.6712	35.3982	11.6688	5.0444	1.8869	40.9980
Type33-V1	9.5284	8.4488	23.2655	0.5875	1.1492	27.5086
Type33-V2	9.3962	15.7861	26.7344	1.3188	1.1488	35.5011
Type33-V3	12.6547	14.2752	36.0737	1.5547	0.6810	49.3357
Type33-V4	11.7556	36.4132	13.8689	6.1388	2.2588	41.8054

Note: a_1 to a_6 represent the parameters in Equation (4-1).

V1: $v_{subject}$ <=500 vphpl and v_{cross} <=500 vphpl;
V2: $v_{subject}$ <=500 vphpl and 500 vphpl < v_{cross} <=800 vphpl;
V3: 500 vphpl < $v_{subject}$ <=800 vphpl and v_{cross} <=500 vphpl;
V4: 500 vphpl < $v_{subject}$ <=800 vphpl and 500 vphpl < v_{cross} <=800 vphpl.

To best fit the simulation data, a model for each intersection type is developed separately for four different traffic flow ranges, represented by V1, V2, V3, and V4 (see notes for Table 4.1). Because both signal timing optimization and simulation have difficulties in extremely congested cases, the simulated delay data are obtained only for traffic volumes up to 800 vphpl, or slightly over the physical capacity.

The functional form of the developed models is investigated in terms of how delay response to the link length, subject approach volume, and cross-street volume. Figure 4.1 presents the relationship between delay predicted by Type11 model and the distance to an intersection, *L*. The subject and cross-street volumes for this example are 700 vphpl, with left-turn ratio of 10% and right-turn ratio of 10%.

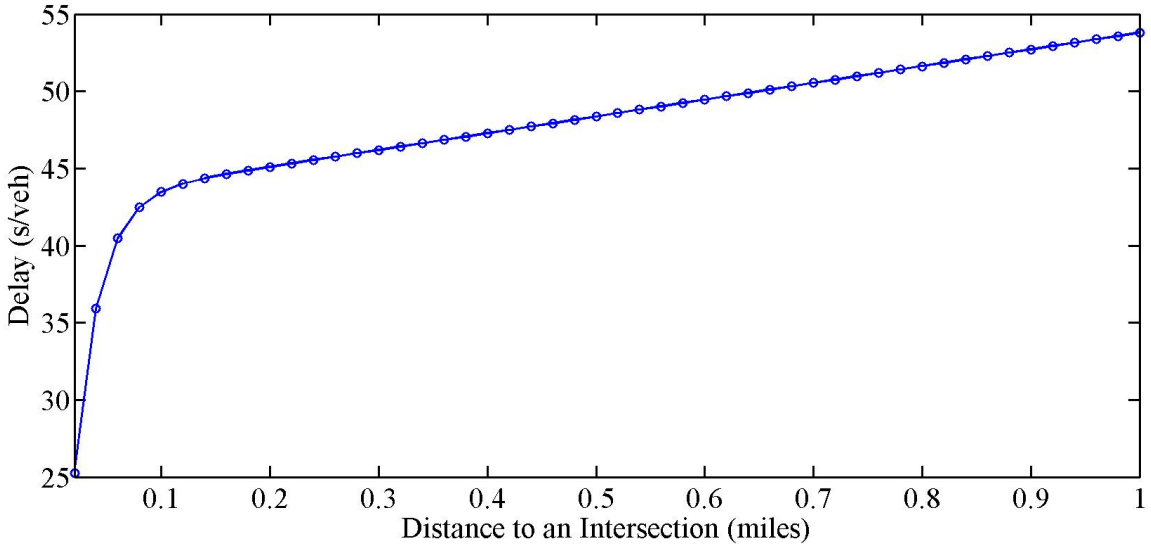

Figure 4.1 Predicted delay response to various link lengths.

As can be seen , link delay increases with the increase of the distance to an intersection. There are two different rates of change in delay with increasing of distance to an intersection. These two regions represent the queuing region (distance to

intersection, L, below about 0.11 miles) and the no-queuing region. If the subject link length is less than the queuing region length (in this case 0.11 miles), then the model assigns the extra delay from this region that is not on the subject link to upstream links.

Figure 4.2 presents the relationship of predicted delay versus degree of congestion in subject direction. The intersection type is Type11, with cross-street volumes of 700 vphpl and turn ratios of 10%. The predicted delay increases as traffic volume increases in the subject direction.

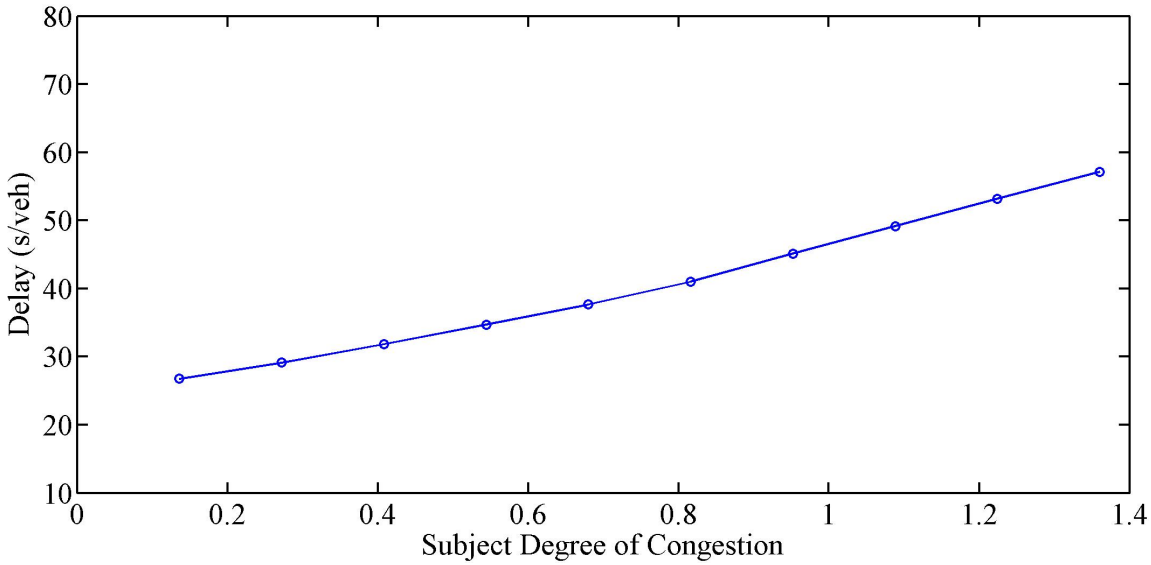

Figure 4.2 Predicted delay versus degree of congestion in subject approach.

Figure 4.3 presents a similar relationship between the predicted delay and degree of congestion in the cross-street direction. The subject volumes are 700 vphpl and other conditions apply. The predicted delay for the subject approach increases in response to the higher demand from the cross-street, given the same subject traffic conditions. The model describes almost equal influence by traffic volumes from both subject and cross-street approaches, in contrast to the existing models that only consider the effect of traffic from the subject approach.

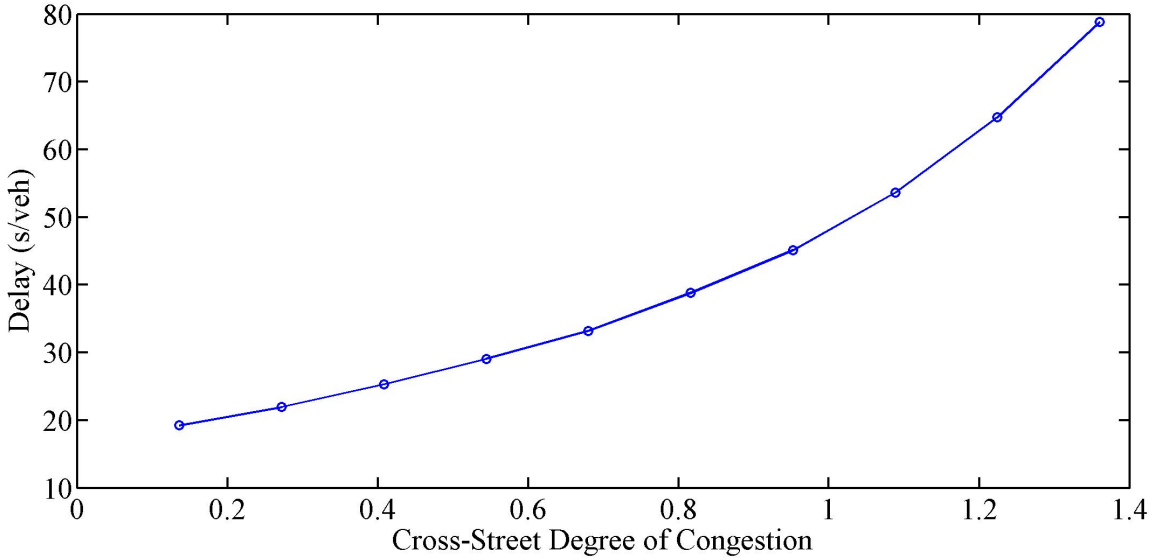

Figure 4.3 Predicted delay versus degree of congestion for cross-street.

Figure 4.4 shows the CORSIM delay data (green dots) and the predicted delays by the model (red solid line) for a link of Type11 intersection with a volume of 700 vphpl for both directions.

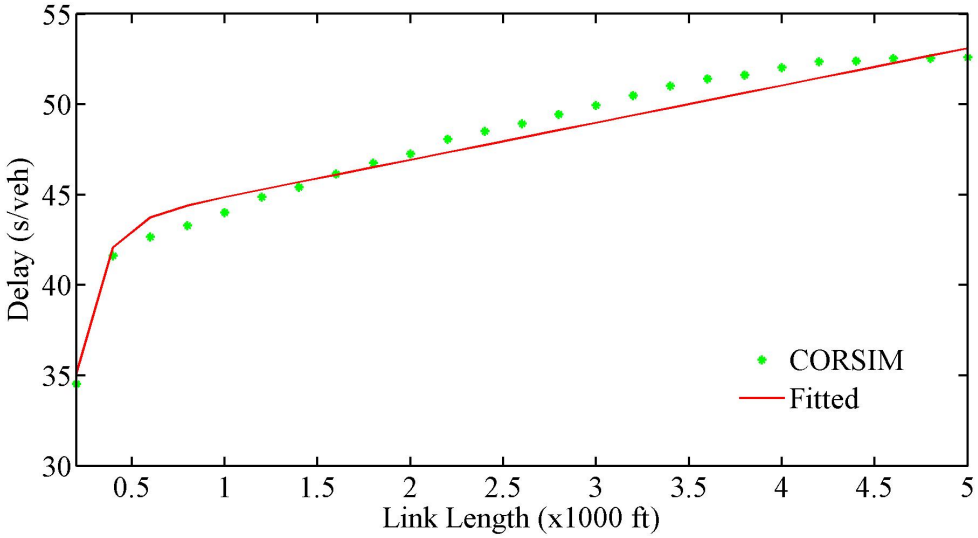

Figure 4.4 Delay distribution along a link of Type 11 intersection. Volumes for both directions are 700 vphpl.

From Figure 4.4, the predicted data are compared to simulation data for evaluating the model's fitness. The model predicted delays fit with the simulated delay data well.

The accumulated delay along a link, depicted in Figure 4.4, is not spatially uniform. Delay per vehicle within the first 200-foot segment is 34 seconds, which constitutes the largest portion of the total delay along a link, since queues are formed on this portion of the link. The queue delay within the second 200-foot segment adds another 10 seconds per vehicle to the total delay. In this scenario, as can be seen from Figure 4.4, per-vehicle delay continues to increase at a constant rate after 400 feet from an intersection, which is the end of the queue. The delay per unit length, represented by the slope of the solid line in Figure 4.4, is larger near the intersection where vehicles queue more often and is smaller as the queuing probability on the segments decreases farther away from the intersection. As previously mentioned, identifying this spatial distribution of delay by the developed model is important, because it can be used to differentiate between the delay that should be assigned to the subject link and the delay that should be assigned to upstream links. This spatial distribution is not properly accounted for in existing delay estimation methods in the literature.

With regards to the fitness of the developed models, Figures 4.5 through 4.13 present the predicted delays by the model (y-axis) against simulated delays from CORSIM (x-axis) for intersection types of Type11, Type12, Type13, Type21, Type22, Type23, Type31, Type32, and Type33, respectively. For example, the scattered points are around a straight line with an R-squared value of 0.9366 in Figure 4.5. This suggests that the model fits well with the data from CORSIM simulation. Similarly, the R-squares of

the best-fitted lines for other figures are mostly around 0.90, which suggests that all these statistical models fit well with the simulated data.

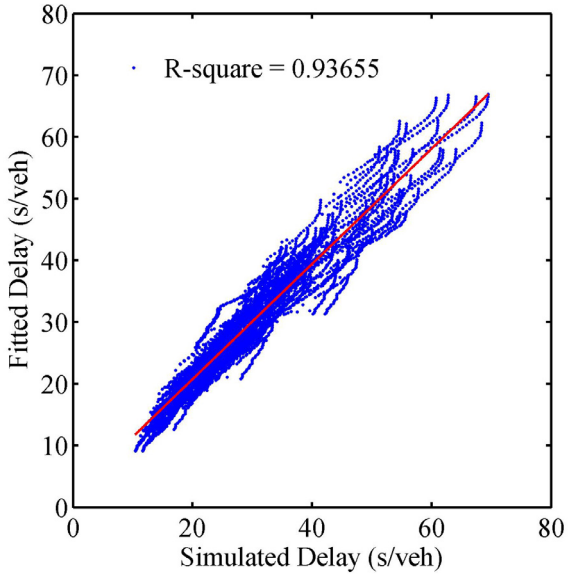

Figure 4.5 Predicted versus simulated delays for Type11 intersection by the capacity-based model.

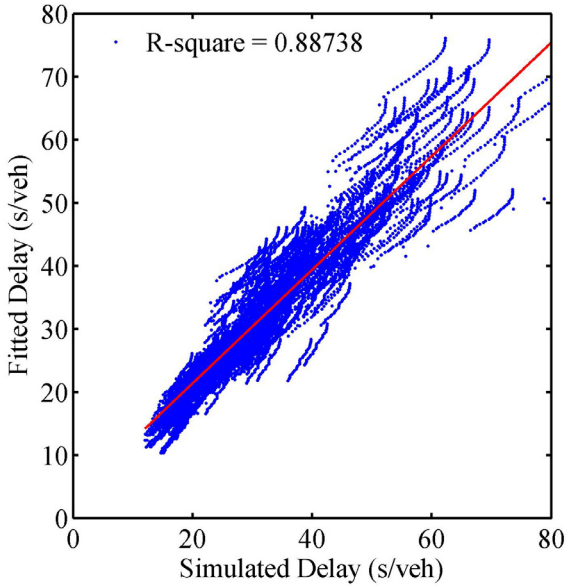

Figure 4.6 Predicted versus simulated delays for Type12 intersection by the capacity-based model.

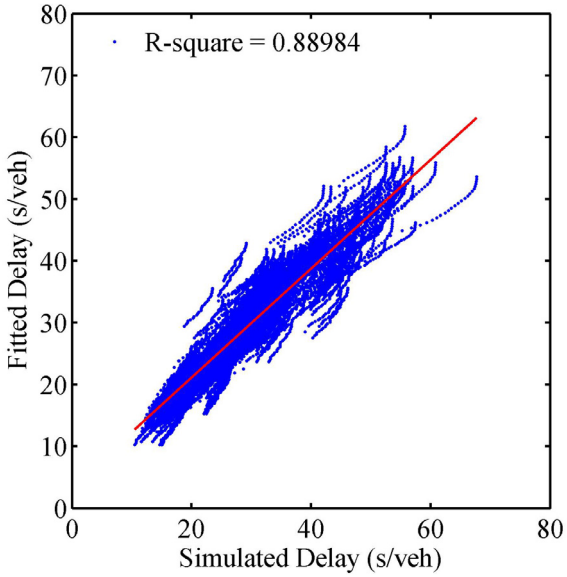

Figure 4.7 Predicted versus simulated delays for Type13 intersection by the capacity-based model.

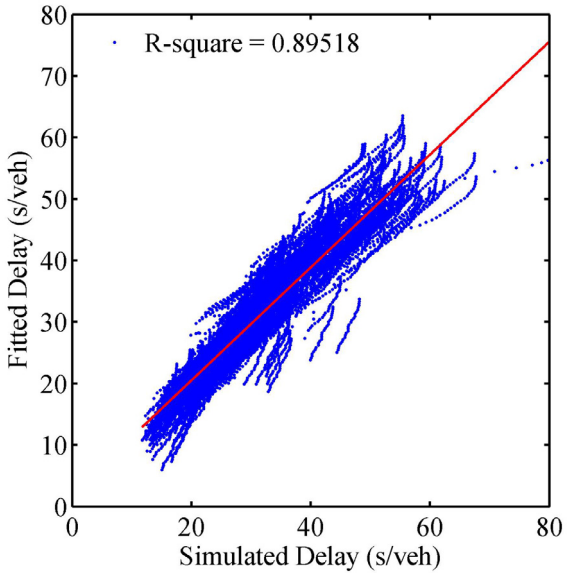

Figure 4.8 Predicted versus simulated delays for Type21 intersection by the capacity-based model.

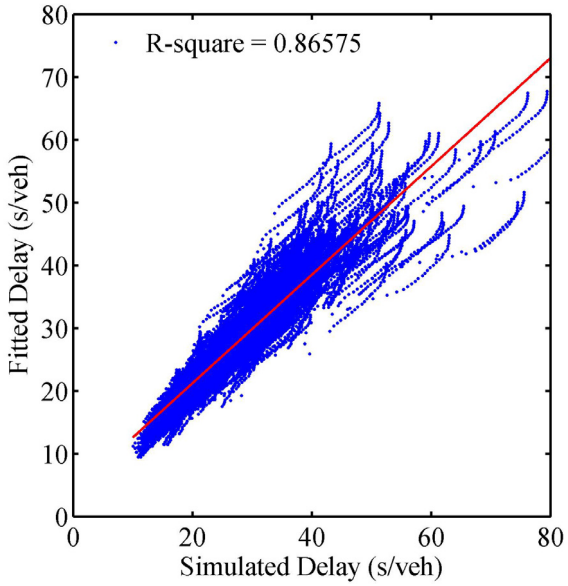

Figure 4.9 Predicted versus simulated delays for Type22 intersection by the capacity-based model.

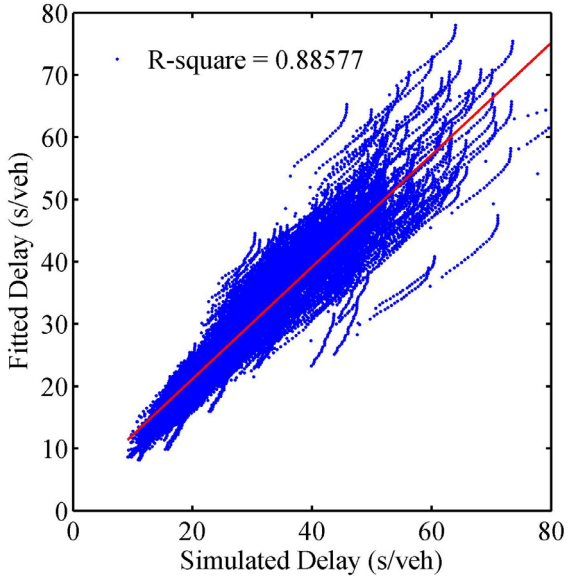

Figure 4.10 Predicted versus simulated delays for Type23 intersection by the capacity-based model.

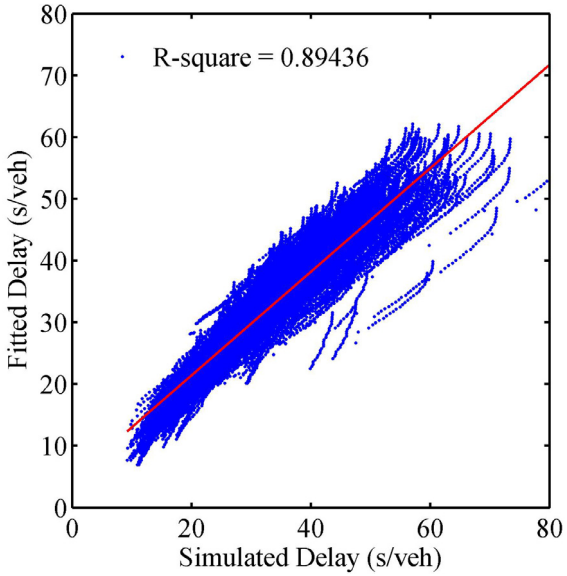

Figure 4.11 Predicted versus simulated delays for Type31 intersection by the capacity-based model.

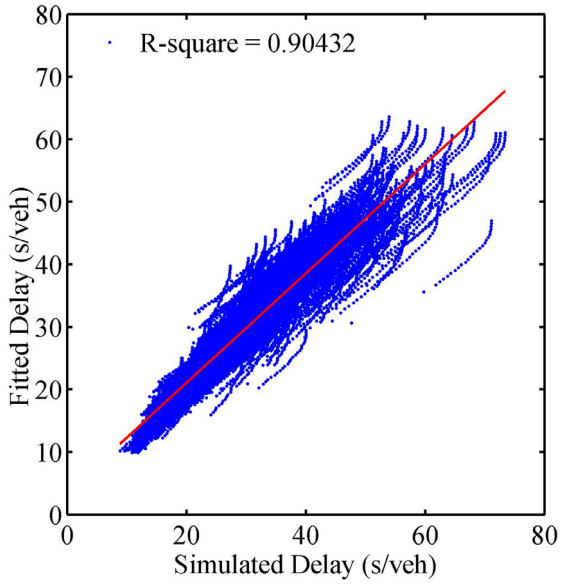

Figure 4.12 Predicted versus simulated delays for Type32 intersection by the capacity-based model.

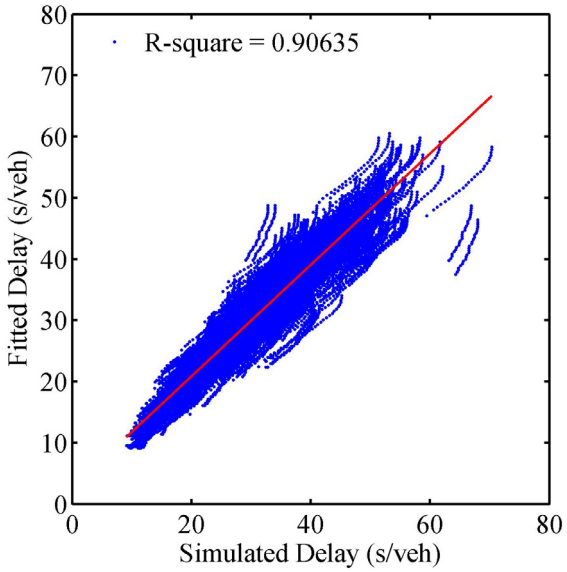

Figure 4.13 Predicted versus simulated delays for Type33 intersection by the capacity-based model.

To investigate the possibility of replacing the nine developed models with a single one for application, each of the nine developed models is applied to other eight intersection types for which they are not calibrated. This is a sensitivity analysis of delay estimations on the number of lane. If the influence of lane number is negligible, it is possible to apply a model to other intersection types, especially the intersection type not covered by the previous simulation. Their performance is evaluated by comparing their predictions to the simulated data in terms of mean absolute percentage error (MAPE). The accuracy of each model is measured by MAPE, which is defined by Equation (4-4):

$$MAPE = \frac{1}{n}\sum_{i=1}^{n}\left|\frac{d_i - d_{i,simulation}}{d_{i,simulation}}\right| \times 100\% \qquad (4\text{-}4)$$

where

$MAPE$ = mean absolute percentage error;

i = delay data point i;

n = total number of data points;

$d_{i,simulation}$ = simulated travel delay for data point *i* (s/veh); and

d_i = predicted delay by the model for data point *i* (s/veh).

The results are presented in Table 4.2. Each column shows the MAPEs of a particular delay model, which is developed for one intersection type and applied to other intersection types. The MAPEs are computed based on simulated delay data.

Table 4.2 Percentage error between nine capacity-based models and simulated data.

		Model Type								
		Type11	Type12	Type13	Type21	Type22	Type23	Type31	Type32	Type33
Data Source	Type11	**7.4**	12.6	12.5	9.5	10.1	13.3	11.3	11.9	15.9
	Type12	10.4	**8.9**	9.3	9.9	11.3	9.8	9.3	9.9	11.1
	Type13	10.0	9.0	**8.3**	9.9	10.5	9.6	9.3	9.0	10.0
	Type21	8.3	10.5	10.8	**7.1**	8.9	10.1	8.5	9.4	13.1
	Type22	10.4	13.4	12.3	10.9	**8.3**	12.0	11.9	11.0	14.1
	Type23	11.0	9.9	9.6	9.5	9.3	**8.5**	9.0	8.7	9.9
	Type31	8.9	7.9	8.8	7.0	8.3	7.5	**6.2**	7.2	10.3
	Type32	10.0	9.0	8.4	9.0	8.3	8.1	8.0	**7.0**	9.0
	Type33	12.7	9.3	8.3	11.1	10.7	8.5	9.1	7.8	**7.3**
	All	10.4	9.7	9.3	9.5	9.5	9.0	8.9	8.5	9.9

The data in the diagonal cells in Table 4.2 represent the overall percentage differences between model perditions and the simulated delay data used to calibrate the model. Theses percentage differences reflect the overall error of the models compared to the simulated data. From Table 4.2, it can be seen that the overall errors for all nine models are below 9.0%. The off-diagonal data describe the performance of the models when they are applied to different intersection configurations for which they are not originally calibrated. As shown in the second column, the errors are below 12.7% when a model, developed based on the simulated data for the Type11 intersection, is applied to other intersection configurations. The errors are slightly higher than the error when the Type11 model is applied to a Type11 intersection (7.4%). The largest error, 15.9%,

occurs when Type33 model is applied to the Type11 intersection configuration. The MAPEs of the last row show that the average percentage error is about 10% when a developed model is applied to all simulation data for the nine intersection types.

The significance of these off-diagonal tests is to provide statistical evidence that lane configurations may not significantly affect intersection delay estimations when volumes are normalized by lane number. This implies that a model developed in this study could be extended to other intersection configurations, even when the number of lanes at an intersection is greater than three for either approach. This may also mean that one single model may possibly provide acceptable accuracy for all facility types not studied in this research, i.e., intersection configurations with more than three lanes in either approach.

4.2 Degree of Congestion Defined by the Ratio of Volume to Saturation Flow Rate

Although practical capacity can be estimated based on roadway class, this estimation is crude without signal timing information. In such cases, saturation flow rate defines the physical capacity of the link under free flow conditions. The degree of congestion for a link may be defined as the ratio of traffic volume to saturation flow rate of the link. This study has also calibrated models that replace physical capacity with the degree of congestion, which are referred to as delay models with saturation flow rate, or the saturation-based models. The parameters for these models are listed in Table 4.3.

Table 4.3 Fitted parameters for the delay model with saturation flow rate.

Parameters	a_1 (s/veh/mile)	a_2 (s/veh)	a_3 (s/veh)	a_4	a_5	a_6 (1/mile)
Type11-V1	6.5678	32.0470	29.7522	0.5746	1.0743	13.1980
Type11-V2	6.6336	56.3883	84.3267	1.6190	1.0564	17.0344
Type11-V3	11.5076	38.4138	115.4000	1.3844	0.7237	20.5742
Type11-V4	10.8644	66.6846	331.6000	3.1277	0.8719	17.3759
Type12-V1	6.5506	35.9264	28.3582	0.6245	1.1859	13.9335
Type12-V2	6.9175	17.4030	144.3000	1.2991	0.8497	17.5594
Type12-V3	11.7004	37.1675	164.9000	1.3461	0.5222	20.5764
Type12-V4	10.7654	75.0391	590.4000	3.5978	0.8891	15.9280
Type13-V1	6.5015	34.3537	21.4390	0.5243	1.2598	13.7164
Type13-V2	6.3975	57.2971	72.2864	1.5773	1.2138	16.5049
Type13-V3	11.6650	38.1995	159.5000	1.3978	0.5380	20.5255
Type13-V4	10.3659	87.9020	1023.6000	6.0054	2.0236	17.7805
Type21-V1	8.8058	35.0490	38.8807	0.7797	1.0668	11.7331
Type21-V2	8.9774	0.0000	143.4000	1.0835	0.7393	15.2971
Type21-V3	11.8071	36.3844	533.6000	1.8711	0.0000	20.0269
Type21-V4	10.3307	86.4046	194.7000	4.1843	1.8679	15.8651
Type22-V1	8.7915	25.9688	30.4367	0.5722	1.0929	11.1097
Type22-V2	8.7709	68.2380	64.8040	1.8307	1.2725	14.9854
Type22-V3	11.7006	26.8477	69.9712	0.9851	0.7895	21.6232
Type22-V4	11.3548	50.0773	418.0000	3.0991	0.9213	17.1487
Type23-V1	8.9350	20.3491	38.7933	0.5568	1.0246	11.7024
Type23-V2	8.8655	50.7951	105.2000	1.5730	1.0446	15.1471
Type23-V3	11.9628	31.7426	382.5000	1.5421	0.0000	20.2176
Type23-V4	11.1356	83.3190	2339.7000	5.4296	0.9109	15.1056
Type31-V1	9.4178	26.5062	40.1184	0.6421	1.0155	12.1072
Type31-V2	9.6044	19.2896	124.4000	1.3158	0.9009	15.3208
Type31-V3	12.5453	37.1635	380.3000	1.8062	0.2913	19.9609
Type31-V4	11.6419	85.0275	106.9000	3.7879	2.1981	16.3596
Type32-V1	9.4544	20.0396	35.7180	0.5808	1.0815	11.2112
Type32-V2	9.5068	11.9409	90.2794	1.0813	0.9689	14.9358
Type32-V3	12.6574	37.5635	270.4000	1.9333	0.6828	20.4987
Type32-V4	11.6712	84.9555	444.3000	5.0443	1.8869	17.0825
Type33-V1	9.5284	20.2771	34.1477	0.5875	1.1492	11.4623
Type33-V2	9.3962	37.8866	74.4633	1.3188	1.1488	14.7925
Type33-V3	12.6547	34.2603	186.0000	1.5546	0.6810	20.5567
Type33-V4	11.7556	87.3917	944.2000	6.1388	2.2588	17.4189

Note: a_1 to a_6 represent the parameters in Equation (4-1).

V1: $v_{subject}$ <=500 vphpl and v_{cross} <=500 vphpl;
V2: $v_{subject}$ <=500 vphpl and 500 vphpl < v_{cross} <=800 vphpl;
V3: 500 vphpl < $v_{subject}$ <=800 vphpl and v_{cross} <=500 vphpl;
V4: 500 vphpl < $v_{subject}$ <=800 vphpl and 500 vphpl < v_{cross} <=800 vphpl.

Figures 4.14 through 4.22 present the fitness of saturation-based models for the nine intersection types. The aforementioned figures plot the relationship between the predicted delays against simulated delay data, and the best fitted lines in red. The R-squares of the best fitted lines show that the models fit the simulated data well, similar to the capacity-based models.

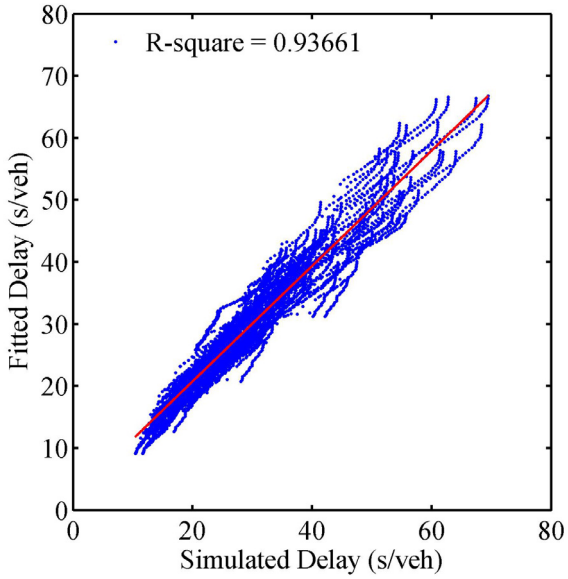

Figure 4.14 Predicted versus simulated delays for Type11 intersection by the saturation-based model.

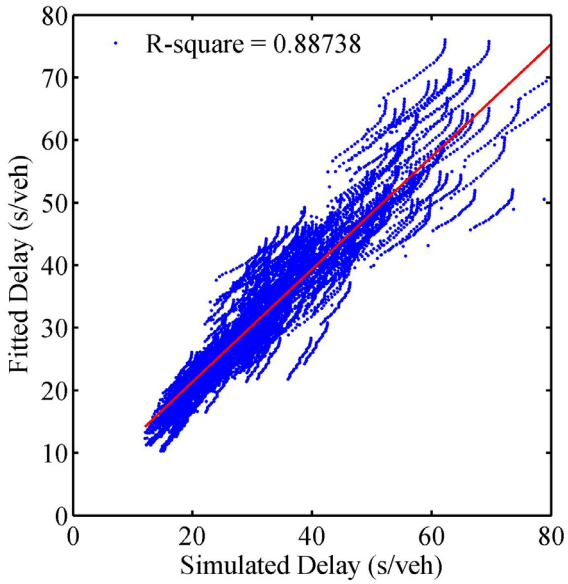

Figure 4.15 Predicted versus simulated delays for Type12 intersection by the saturation-based model.

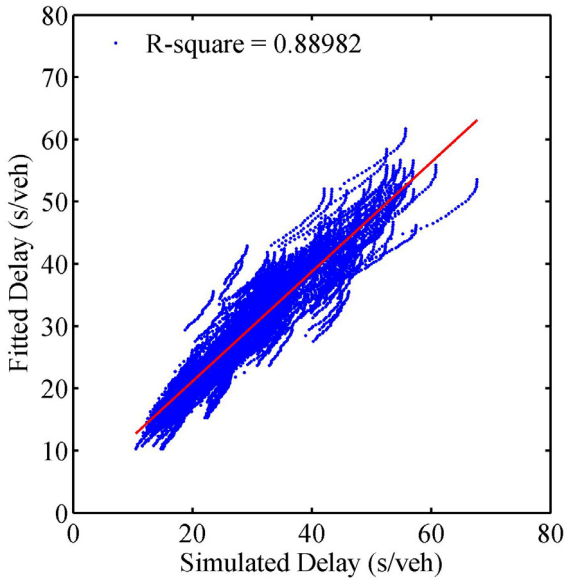

Figure 4.16 Predicted versus simulated delays for Type13 intersection by the saturation-based model.

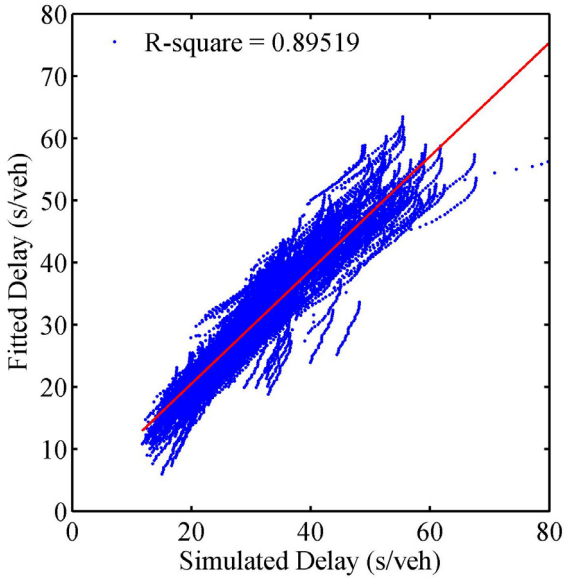

Figure 4.17 Predicted versus simulated delays for Type21 intersection by the saturation-based model.

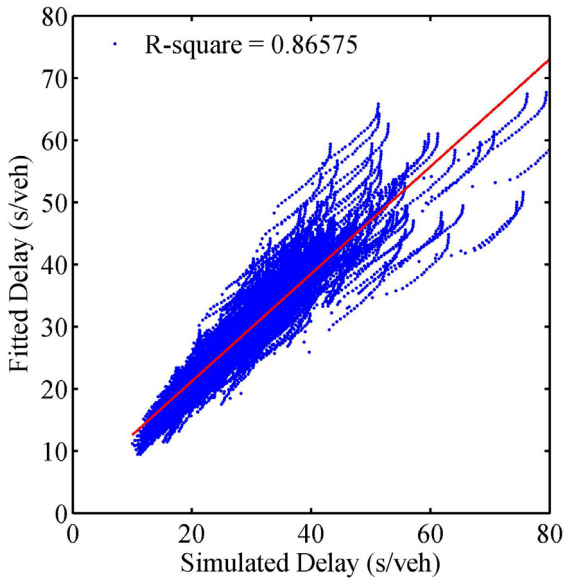

Figure 4.18 Predicted versus simulated delays for Type22 intersection by the saturation-based model.

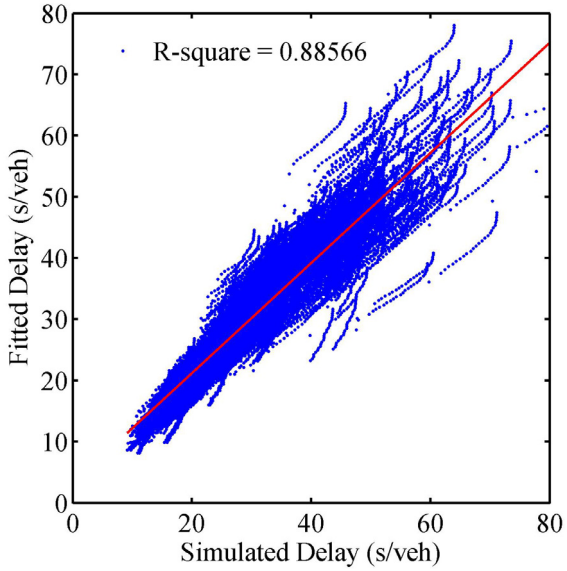

Figure 4.19 Predicted versus simulated delays for Type23 intersection by the saturation-based model.

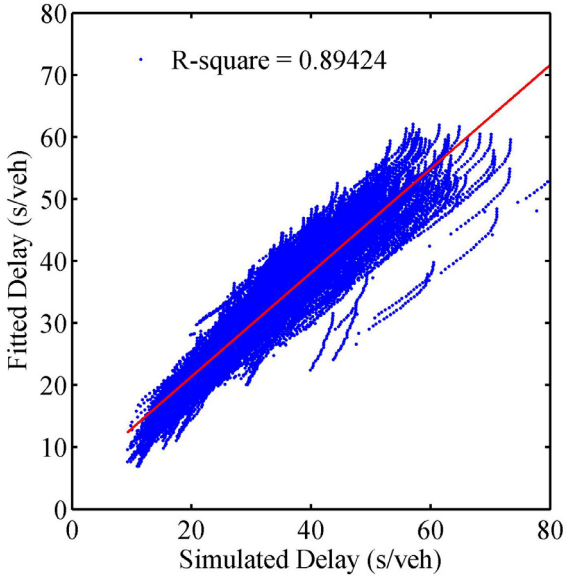

Figure 4.20 Predicted versus simulated delays for Type31 intersection by the saturation-based model.

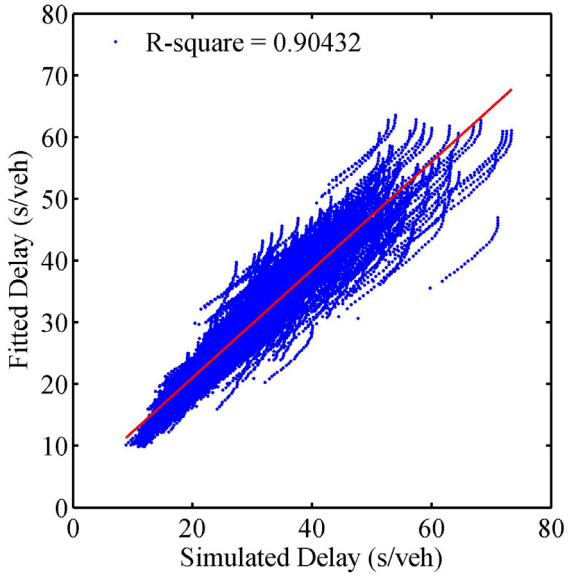

Figure 4.21 Predicted versus simulated delays for Type32 intersection by the saturation-based model.

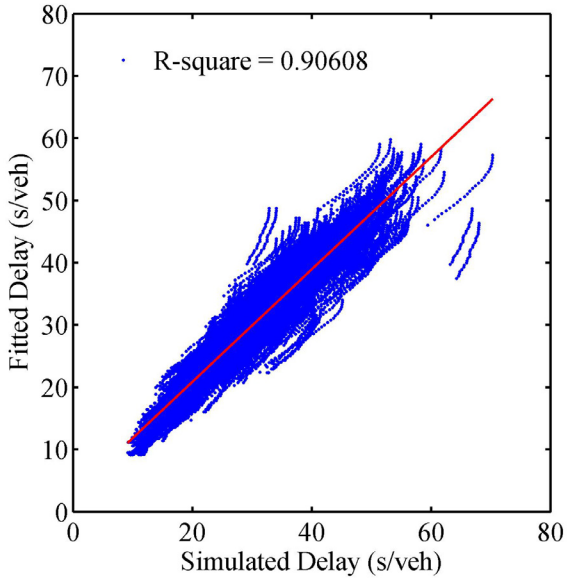

Figure 4.22 Predicted versus simulated delays for Type33 intersection by the saturation-based model.

Similar to Section 4.1, the nine saturation-based models are evaluated by comparing the predicted data to simulated data in terms of MAPE, and the results are presented in Table 4.4. The diagonal data in Table 4.4 represents the overall percentage

difference between each model and the corresponding simulated delay data. The off-diagonal data again show the average errors of these models when they are applied to different intersection configurations. The last row gives the overall MAPE of the models when they are applied to all of the nine intersection types. It is found that the sensitivity of the delay models with saturation flow rate to different intersection configuration is similar to that of the capacity-based models. The number of lanes may not be a significant factor to affect intersection delay estimations when traffic volumes are normalized by saturation flow rate. Consequently, one single model may possibly provide acceptable accuracy for all intersection configurations with three plus lanes in either approach.

Table 4.4 Percentage error between nine saturation-based models and simulated data.

		Model Type								
		Type11	Type12	Type13	Type21	Type22	Type23	Type31	Type32	Type33
Data Source	Type11	**7.4**	12.6	12.5	9.5	10.1	13.3	11.2	11.9	15.7
	Type12	10.4	**8.9**	9.3	9.9	11.3	9.8	9.3	9.9	11.0
	Type13	10.0	9.0	**8.3**	10.0	10.5	9.6	9.3	9.0	10.0
	Type21	8.3	10.5	10.8	**7.1**	8.9	10.1	8.4	9.4	13.0
	Type22	10.4	13.4	12.3	10.8	**8.3**	12.0	11.9	11.0	14.0
	Type23	11.0	9.9	9.5	9.5	9.3	**8.6**	9.0	8.7	9.8
	Type31	9.0	7.9	8.8	7.1	8.3	7.5	**6.2**	7.2	10.2
	Type32	10.1	9.0	8.4	9.0	8.3	8.1	8.0	**7.0**	9.0
	Type33	12.7	9.3	8.3	11.1	10.7	8.5	9.1	7.8	**7.3**
	All	10.5	9.7	9.3	9.4	9.5	9.0	8.9	8.5	9.8

4.3 Unified Model

With the idea that one single model may be able to achieve acceptable accuracy for different intersection configurations, a unified model is calibrated using all data point obtained from simulations for the nine intersection types. The model is developed based on both capacity and saturation flow rate. Each is fitted for four domains of traffic volumes. The model parameters are presented in Tables 4.5 and 4.6.

Table 4.5 Fitted parameters for capacity-based unified models.

Parameters	a_1 (s/veh/mile)	a_2 (s/veh)	a_3 (s/veh)	a_4	a_5	a_6 (1/mile)
Unified-V1	8.7011	10.2499	21.4451	0.5784	1.1190	28.6590
Unified-V2	8.7529	13.7745	29.5615	1.2661	1.0249	37.4402
Unified-V3	12.1799	15.0981	36.2065	1.6570	0.4470	49.5398
Unified-V4	11.2062	31.2239	17.8689	3.6033	1.2801	39.9628

Note: a_1 to a_6 represent the parameters in Equation (4-1).

V1: $v_{subject}$ <=500 vphpl and v_{cross} <=500 vphpl;
V2: $v_{subject}$ <=500 vphpl and 500 vphpl < v_{cross} <=800 vphpl;
V3: 500 vphpl < $v_{subject}$ <=800 vphpl and v_{cross} <=500 vphpl;
V4: 500 vphpl < $v_{subject}$ <=800 vphpl and 500 vphpl < v_{cross} <=800 vphpl.

Table 4.6 Fitted parameters for unified models with saturation flow rate.

Parameters	a_1 (s/veh/mile)	a_2 (s/veh)	a_3 (s/veh)	a_4	a_5	a_6 (1/mile)
Unified-V1	8.7011	24.5998	32.0611	0.5784	1.1190	11.9415
Unified-V2	8.7529	33.0590	87.6315	1.2661	1.0249	15.6002
Unified-V3	12.1799	36.2352	250.6000	1.6570	0.4470	20.6417
Unified-V4	11.2062	74.9369	327.8000	3.6033	1.2801	16.6512

Note: a_1 to a_6 represent the parameters in Equation (4-1).

V1: $v_{subject}$ <=500 vphpl and v_{cross} <=500 vphpl;
V2: $v_{subject}$ <=500 vphpl and 500 vphpl < v_{cross} <=800 vphpl;
V3: 500 vphpl < $v_{subject}$ <=800 vphpl and v_{cross} <=500 vphpl;
V4: 500 vphpl < $v_{subject}$ <=800 vphpl and 500 vphpl < v_{cross} <=800 vphpl.

Figure 4.23 presents the fitness of the unified model for all simulation data points for the nine intersection types. This figure plots predicted delay by the capacity-based unified model against the simulated data and the best fitted line. (Note that there is no difference between the capacity-based and saturation-based unified model.) The R-square of the best fitted lines is 0.8768, which shows that the model fits the simulated data well.

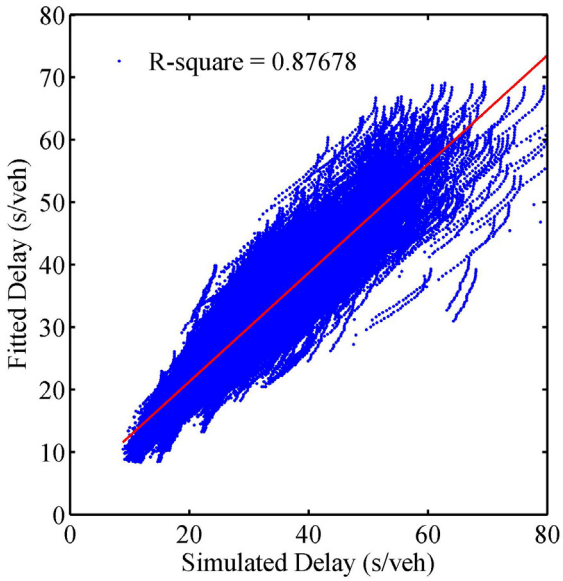

Figure 4.23 Predicted versus simulated delays for unified model.

The two unified models (capacity-based and saturation-based) are evaluated by comparing model predictions to the simulation data in terms of MAPE. The MAPEs for both versions of the unified models are presented in Table 4.7.

Table 4.7 Percentage error between unified models and simulated data.

		Model Type	
		Capacity-based	Saturation-based
Data Source	Type11	11.8	11.8
	Type12	9.4	9.4
	Type13	8.7	8.7
	Type21	9.3	9.3
	Type22	11.2	11.2
	Type23	8.5	8.5
	Type31	7.1	7.1
	Type32	7.2	7.2
	Type33	7.9	7.9
	All	**8.5**	**8.5**

It is found that the unified models have an overall MAPEs of 8.5%. When the unified models are applied to the data of a particular intersection type, the MAPEs range

from 7.9% to 12%. It is recommended that the unified model be applied to an intersection with more than three lanes in either approach, the intersection not simulated in this study.

4.4 Effect of Speed

Besides the influence of the number of lanes of a facility, free flow speed may be another factor that affects delay. The models described previously are based on the assumption of a free-flow speed of 45 mph. In this section, the effect of speed is studied for a Type22 intersection, with free flow speed of 40 mph and 30 mph investigated. The results are presented for the different speed models with different definitions of degree of congestion in the next two subsections.

4.4.1 Degree of Congestion Defined by the Ratio of Volume to Capacity

The fitted parameters for a model calibrated using Type22 simulation data are presented in Table 4.8. There are three sets of parameters, which are developed based on three free flow speeds of 45 mph, 40 mph, and 30 mph, and are labeled as Speed45, Speed40, and Speed30, respectively. The degree of congestion is defined by the ratio of volume to capacity.

Figures 4.24 and 4.25 show the model fitness of two developed models for different free flow speed, 40 mph and 30 mph, respectively. It was found that the predicted data fit well with simulated data.

Table 4.8 Fitted parameters for capacity-based models for different free flow speeds.

Parameters	a_1 (s/veh/mile)	a_2 (s/veh)	a_3 (s/veh)	a_4	a_5	a_6 (1/mile)
Speed45-V1	8.7914	10.8203	20.0060	0.5722	1.0929	26.6629
Speed45-V2	8.7709	28.4325	16.5642	1.8307	1.2725	35.9642
Speed45-V3	11.7006	11.1865	24.5650	0.9851	0.7895	51.8955
Speed45-V4	11.3548	20.8656	25.8819	3.0991	0.9213	41.1566
Speed40-V1	8.8952	10.9799	17.2728	0.6005	1.1981	34.4219
Speed40-V2	8.7800	29.3438	14.0885	1.9361	1.3662	44.0890
Speed40-V3	11.5681	12.0369	25.5679	1.1211	0.4933	54.5882
Speed40-V4	11.5970	23.7156	26.6412	4.2020	0.4533	39.5827
Speed30-V1	9.5114	12.5421	16.1046	0.6148	1.2245	36.8930
Speed30-V2	9.3124	31.6277	13.0703	2.0617	1.3914	46.5121
Speed30-V3	14.5778	12.9480	27.5684	1.1518	0.3017	50.7363
Speed30-V4	13.7583	15.0789	40.0055	2.4843	0.2271	36.3981

Note: a_1 to a_6 represent the parameters in Equation (4-1).

V1: $v_{subject}$ <=500 vphpl and v_{cross} <=500 vphpl;
V2: $v_{subject}$ <=500 vphpl and 500 vphpl < v_{cross} <=800 vphpl;
V3: 500 vphpl < $v_{subject}$ <=800 vphpl and v_{cross} <=500 vphpl;
V4: 500 vphpl < $v_{subject}$ <=800 vphpl and 500 vphpl < v_{cross} <=800 vphpl.

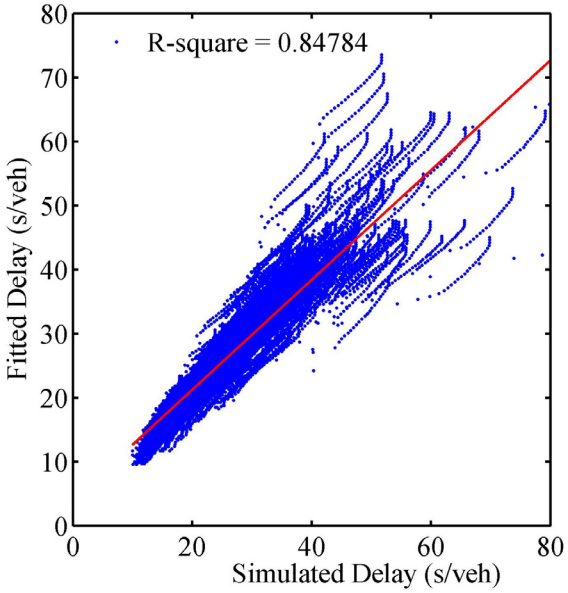

Figure 4.24 Predicted versus simulated delays for Type22 intersection with free flow speed of 40 mph by the capacity-based model.

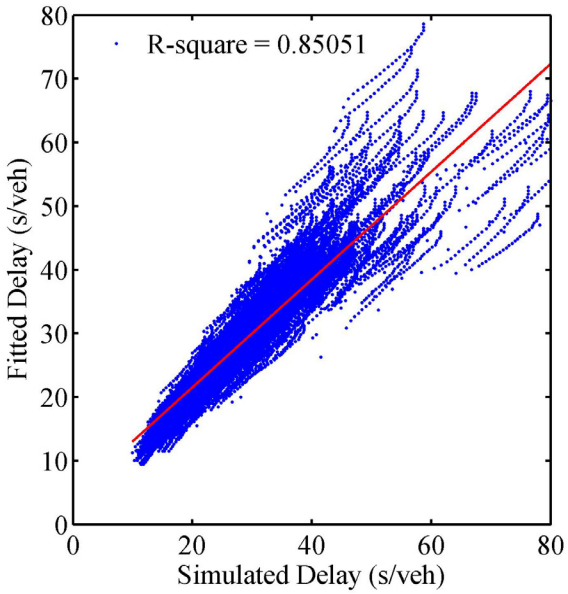

Figure 4.25 Predicted versus simulated delays for Type22 intersection with free flow speed of 30 mph by the capacity-based model.

The errors of the models for different speeds are investigated by comparing the model predictions to the simulated data. The MAPEs of the models are presented in Table 4.9. Delays for the facility with the free-flow speed of 40 mph are predicted by its own model, Speed40, and by the Speed45 model, which result in MAPEs of 8.2% and 8.9%, respectively. When the Speed45 model is applied to the facility with the free-flow speed of 30 mph, MAPE is 9.2%, comparable to 8.4%, a MAPE by Speed30 model. It is found that when applying the model that has been developed based on a free flow speed of 45 mph to intersections with a link free flow speed of 40 mph or 30 mph, no significant errors result. This suggests that delay models developed in this study are capable of predicting delay for facilities with different free flow speeds, and that free flow speed is not a significant factor in travel delay estimation for a facility with signal-controlled intersections. The conclusion is not inconsistent with the fact that free flow speed is proportional to free flow time, a significant factor of travel time.

The unified model is also tested here, which gives larger errors. The larger errors suggest that the speed effect on delay estimation is less compared to the influence of lane configurations.

Table 4.9 Percentage error between the capacity-based models and simulated data for different speeds.

		Model Type			
		Unified Model (45 mph)	Speed45	Speed40	Speed30
Data Source	Speed40	12.5	**8.9**	**8.2**	10.4
	Speed30	10.7	**9.2**	9.0	**8.4**

4.4.2 Degree of Congestion Defined by the Ratio of Volume to Saturation Flow Rate

The effect of speed is also investigated for the models developed with the degree of congestion defined as the ratio of volume to saturation flow rate. The fitted parameters are presented in Table 4.10 for different speed models.

Table 4.10 Fitted parameters for saturation-based models for different free flow speeds.

Parameters	a_1 (s/veh/mile)	a_2 (s/veh)	a_3 (s/veh)	a_4	a_5	a_6 (1/mile)
Speed45-V1	8.7915	25.9688	30.4367	0.5722	1.0929	11.1097
Speed45-V2	8.7709	68.2380	64.8040	1.8307	1.2725	14.9854
Speed45-V3	11.7006	26.8477	69.9712	0.9851	0.7895	21.6232
Speed45-V4	11.3548	50.0773	418.0000	3.0991	0.9213	17.1487
Speed40-V1	8.8952	26.3516	24.5689	0.6005	1.1981	14.3428
Speed40-V2	8.7800	70.4250	55.6857	1.9361	1.3662	18.3708
Speed40-V3	11.5681	28.8886	106.3000	1.1211	0.4933	22.7452
Speed40-V4	11.597	56.9171	1702.4000	4.2020	0.4533	16.4928
Speed30-V1	9.5114	30.1011	22.6647	0.6148	1.2245	15.3723
Speed30-V2	9.3124	75.9063	56.4089	2.0617	1.3914	19.3808
Speed30-V3	12.5453	37.1635	380.3000	1.8062	0.2913	19.9609
Speed30-V4	11.6419	85.0275	106.9000	3.7879	2.1981	16.3596

Note: a_1 to a_6 represent the parameters in Equation (4-1).

V1: $v_{subject}$ <=500 vphpl and v_{cross} <=500 vphpl;
V2: $v_{subject}$ <=500 vphpl and 500 vphpl < v_{cross} <=800 vphpl;
V3: 500 vphpl < $v_{subject}$ <=800 vphpl and v_{cross} <=500 vphpl;
V4: 500 vphpl < $v_{subject}$ <=800 vphpl and 500 vphpl < v_{cross} <=800 vphpl.

Figures 4.26 and 4.27 show the fitness of Speed40 and Speed30 models, respectively. The models fit the simulated data well.

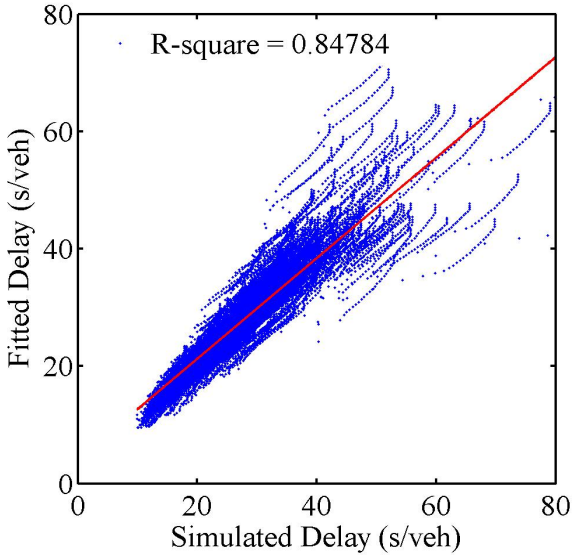

Figure 4.26 Predicted versus simulated delays for Type22 intersection with free flow speed of 40 mph by the saturation-based model.

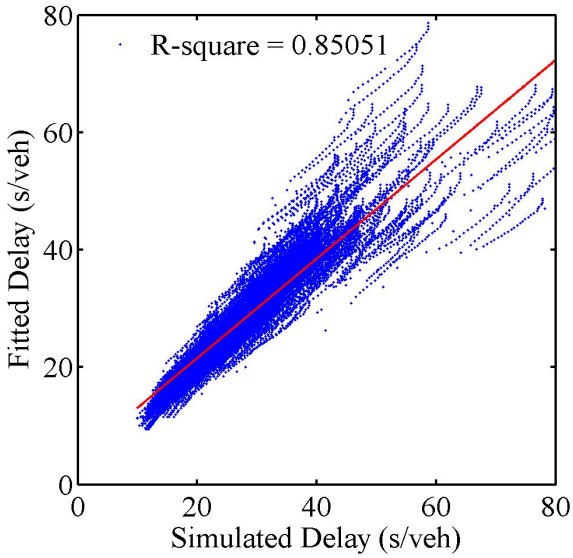

Figure 4.27 Predicted versus simulated delays for Type22 intersection with free flow speed of 30 mph by the saturation-based model.

Similar to the capacity-based models, the errors of the saturation-based models for different speeds are investigated by comparing the model predictions to the simulated

data. The MAPEs of the models are presented in Table 4.11. Similar to previous findings, there is no significant difference when the model, developed for a facility with a free flow speed of 45 mph, is applied when free flow speed is 40 mph or 30 mph. The MAPEs are less than 10%, which is acceptable. This suggests that the nine models developed in previous sections are applicable to a facility with a free flow speed different from 45 mph.

Table 4.11 Percentage error between the saturation-based models and simulated data for different speeds.

		Model Type			
		Unified Model (45 mph)	Speed45	Speed40	Speed30
Data Source	Speed40	12.5	**8.9**	**8.2**	10.4
	Speed30	10.7	**9.2**	9.0	**8.4**

4.5 Summary of Model Development

Two versions of delay model are developed for signal-controlled facility in this study, with the degree of congestion defined by the ratio of volume to reduced capacity of a link and by the ratio of volume to saturation flow rate of a link. The delay model based on saturation flow rate is a universal model for links connected to an intersection, typically when the link practical capacity cannot be estimated. Otherwise, when link capacity can be estimated, the capacity-based model may be used. In terms of model fitness, the MAPEs of both models and corresponding delay data are similar, less than 10% in most cases.

It is found that the delay models are insensitive to free flow speed, which suggests that the model developed based on free flow speed of 45 mph can be applied to facilities with other free flow speeds. Since the relationship between free flow time and free flow speed is well understood, a travel time model could be developed based on a good delay

model and free flow time. This is why this study is focused on delay estimation, instead of directly attempting the development of a travel time model.

The number of lanes of a link has slightly more influence on delay estimation. When a model developed for an intersection type is applied to another type of intersection, additional prediction errors are introduced, but they are insignificant. It is recommended that the model for a given facility type be applied for planning applications, but a unified model or one of the nine models be extended to other intersection configurations with four or more lanes for either approach.

In summary, capacity-based and saturation-based delay models are applicable for signal-controlled facilities with different lane numbers and different free flow speeds. The total travel time for a link is computed as the sum of the delay from the developed models and free flow travel time.

CHAPTER 5

MODEL EVALUATION

The accuracy of the developed models (capacity-based and saturation-based models) presented in the previous section are evaluated using field data from the Minnesota Department of Transportation (MDOT), as well as CORSIM simulation data for US-1 in Miami-Dade County, Florida. Mean absolute percentage error (MAPE) is defined in Equation (5-1), which reflects the prediction accuracy of a model. Other methods from the literature, such as BPR equation, conical equation, Dowling method, SERPM model, and HCM method, are also included in the evaluation. The MAPE is defined as follows:

$$MAPE = \frac{1}{n}\sum_{i=1}^{n}\left|\frac{TT_{i,predicted} - TT_i}{TT_i}\right| \times 100\% \quad (5\text{-}1)$$

where

$MAPE$ = mean absolute percentage error;

i = data collection site i;

n = total number of data collection sites;

TT_i = travel time for site i from MDOT or US-1 (s/veh); and

$TT_{i,predicted}$ = predicted travel time for site i by the developed models, BPR, conical, SERPM, Dowling, and HCM method (s/veh).

5.1 Evaluation Based on Minnesota Data

The MDOT conducted a study to evaluate the existing travel time estimation methods, including the BPR equation, Conical, Dowling, and HCM methods (Davis 2007). Field data were collected because no suitable data were available in the literature. The original report (Davis 2007) included data for 50 sites. Data from 20 sites are not used in this

evaluation because of aggressive driving behavior (average speed passing an intersection is over the speed limit). For the remaining 30 sites, Table 5.1 presents the capacity, speed limit, link length, traffic volume, cycle length, green time, total travel time per vehicle, and number of lane in Columns 2 to 9, respectively.

Table 5.1 Field collected data from MDOT (Davis 2007).

Site ID	Capacity (vph)	Speed Limit (mph)	Link Length (mile)	Volume (vph)	Cycle Length (s)	Green Time (s)	Travel Time (s/veh)	Number of Lanes
2	650	30	0.21	388	90	45	40.64	1
3	750	35	0.51	268	93	35	84.32	1
8	750	40	0.35	268	146	30	91.11	1
25	1300	40	0.32	529	80	44	49.02	2
30	650	30	0.37	200	65	22	73.23	1
32	650	30	0.29	212	87	29	55.40	1
34	650	30	0.24	146	90	26	51.64	1
35	1300	35	0.24	539	90	60	33.40	2
36	650	30	0.24	200	56	18	43.91	1
40	1700	45	0.76	815	50	24	74.55	2
50	550	40	0.19	357	120	40	63.09	1
51	750	35	0.34	306	100	22	55.24	2
53	1300	30	0.15	274	90	40	37.59	2
64	750	35	0.51	212	122	34	94.07	1
66	750	30	0.47	124	88	28	70.24	1
67	750	30	0.37	146	76	9	67.06	1
68	750	30	0.48	214	52	12	76.05	1
81	1700	40	0.24	571	86	65	33.82	2
83	1900	50	0.45	603	80	32	44.60	2
86	850	45	0.83	246	112	26	115.14	1
96	650	30	0.14	276	90	25	39.81	1
97	650	30	0.13	111	90	44	43.80	1
98	1300	30	0.24	966	90	70	46.46	2
100	1300	30	0.25	733	94	50	42.10	2
109	650	30	0.26	301	88	54	44.97	1
111	1300	30	0.23	876	90	36	50.45	2
130	1500	30	0.24	157	62	14	47.34	2
140	1900	45	0.38	513	86	30	55.50	2
146	2250	35	0.49	334	90	33	63.20	3
148	1400	35	0.20	1098	62	44	31.27	2

These data represent light traffic conditions, with an average traffic volume of 266 vphpl, and an average capacity of 711 vphpl. The traffic volumes are well below the intersection capacity. The average link length is about 0.34 mile, with an average speed limit of 35 mph. The average travel time is about 170 seconds per mile, which translates into an average speed of 21.2 mph.

5.1.1 Capacity-Based Travel Time Models

In practice, travel time instead of delay is usually collected. Travel time is also required in planning models. In this study, travel time is the sum of free flow link travel time and delay at the downstream intersection predicted by the developed models:

$$TT_{predicted} = \frac{L}{FFS} \times 3600 + t_{delay} \tag{5-2}$$

where

$TT_{predicted}$ = travel time predicted by developed models (s/veh);

L = link length (miles);

FFS = free flow speed (mph); and

t_{delay} = delay predicted by the developed models (s/veh).

As introduced in Chapter 4, two versions of delay models have been developed. In this section, the capacity-based delay models are first evaluated with the MDOT field data. The MDOT data are compared to the travel time predicted by the developed models, as well as by other existing planning models. Table 5.2 presents the travel times from the MDOT (field), the capacity-based model, BPR, Conical, SERPM, Dowling, and HCM methods in Columns 3 to 9, respectively. The formula of travel time calculation for the

existing planning models is referred to in the literature review. The parameters used in the models are given as notes following the table.

Table 5.2 Travel time calculated by different planning models for the MDOT data.

Site ID	Model Evaluated	Field (s/veh)	Capacity -based (s/veh)	BPR (s/veh)	Conical (s/veh)	SERPM (s/veh)	Dowling (s/veh)	HCM (s/veh)
2	Type11	40.64	46.27	25.68	30.52	31.95	36.46	41.24
3	Type11	84.32	74.23	52.59	56.95	68.59	66.96	73.35
8	Type11	91.11	75.59	31.58	34.20	44.18	60.50	81.23
25	Type22	49.02	44.66	28.92	31.82	40.51	37.80	39.24
30	Type11	73.23	63.09	44.46	47.47	54.12	55.15	60.28
32	Type11	55.40	54.44	34.86	37.41	42.45	49.30	56.49
34	Type11	51.64	46.04	28.81	30.11	35.03	44.80	53.13
35	Type22	33.40	37.51	24.80	27.35	32.39	32.19	31.60
36	Type11	43.91	46.81	28.84	30.79	35.11	38.30	43.11
40	Type22	74.55	83.98	61.28	69.18	91.65	67.30	69.58
50	Type11	63.09	50.04	17.56	21.46	25.40	37.12	51.13
51	Type22	55.24	59.04	35.12	38.65	45.86	54.47	68.39
53	Type22	37.59	30.21	18.01	18.76	21.89	30.50	33.32
64	Type11	94.07	76.02	52.51	55.68	68.44	74.46	86.91
66	Type11	70.24	72.49	56.41	58.17	68.56	71.40	77.99
67	Type11	67.06	83.69	44.41	46.09	53.99	61.15	74.63
68	Type11	76.05	81.48	57.66	61.18	70.16	67.60	74.07
81	Type22	33.82	31.57	21.64	23.29	30.27	26.85	25.04
83	Type22	44.60	54.13	32.45	34.74	51.02	44.40	48.89
86	Type11	115.14	100.09	66.47	70.61	98.87	87.90	101.80
96	Type11	39.81	43.46	16.88	18.68	20.64	33.05	43.41
97	Type11	43.80	25.15	15.60	16.11	18.96	27.10	28.43
98	Type22	46.46	43.77	30.12	39.18	38.68	33.89	34.07
100	Type22	42.10	49.38	30.45	35.62	37.71	41.01	44.71
109	Type11	44.97	46.48	31.42	35.25	38.51	39.70	40.38
111	Type22	50.45	58.59	28.45	35.30	35.92	41.14	49.78
130	Type22	47.34	43.83	28.80	29.33	35.00	40.80	47.83
140	Type22	55.50	52.09	30.42	32.16	45.25	44.40	50.53
146	Type33	63.20	68.55	50.40	51.79	65.70	64.65	69.49
148	Type22	31.27	34.34	21.74	29.24	31.14	25.18	26.46

Notes:
BPR equation: $\alpha = 0.15$, $\beta = 4$;
SERPM model: $\alpha = 0.55$, $\beta = 5.05$, $C = 90$ *s*, $g/C = 0.55$ (speed >= 35 mph);
$\alpha = 0.35$, $\beta = 4.05$, $C = 60$ *s*, $g/C = 0.50$ (speed <35 mph);
Conical equation: $\alpha = 4.00$, $\beta = 1.17$;
Dowling method: $\alpha = 0.05$, $\beta = 10$.

In the dataset in Table 5.2, the turn volumes for all approaches, lane number, and volume for cross-streets are not available. However, they are needed in the calculation using the developed models. The traffic volume for the cross-street is approximated based on the green splitting for the subject approach and cross-street. It is assumed that the turn volume is 10% of approach volume and that the lane number of cross-street is same as that of the subject approach. Hence, the models that are evaluated are Type11, Type22, and Type33 models, as indicated in Column 2. The evaluation of these models may shed light on the overall performance of all developed models since the difference between the models is insignificant, as concluded in Chapter 4.

In SERPM, the default signal timing based on function class is usually taken for application. The Dowling and HCM method take advantage of available actual signal timing plan collected from the field. Note that the developed model is designed to reproduce uniform delay of the HCM method; it is fair to compare these model prediction values to uniform delay of HCM. Hence, the delay computed for the HCM method in this chapter is only the uniform delay. For the Dowling method, the portion of vehicles arriving on green from the field data is not used and is assumed as 50%, considering that this information is usually unavailable in general applications.

Table 5.3 presents the absolute percentage errors for the capacity-based model, BPR equation, Conical equation, SERPM, Dowling method, and HCM method. The last row of the table gives the mean absolute percentage error for each of the methods.

Table 5.3 Mean absolute percentage error for different planning models in comparison with MDOT data.

Field (s/veh)	Percentage						
	Capacity-based (%)	BPR (%)	Conical (%)	SERPM (%)	Dowling (%)	HCM (%)	Capacity-based - HCM (%)
40.64	14	37	25	21	10	1	12
84.32	12	38	32	19	21	13	1
91.11	17	65	62	52	34	11	7
49.02	9	41	35	17	23	20	14
73.23	14	39	35	26	25	18	5
55.40	2	37	32	23	11	2	4
51.64	11	44	42	32	13	3	13
33.40	12	26	18	3	4	5	19
43.91	7	34	30	20	13	2	9
74.55	13	18	7	23	10	7	21
63.09	21	72	66	60	41	19	2
55.24	7	36	30	17	1	24	14
37.59	20	52	50	42	19	11	9
94.07	19	44	41	27	21	8	13
70.24	3	20	17	2	2	11	7
67.06	25	34	31	19	9	11	12
76.05	7	24	20	8	11	3	10
33.82	7	36	31	10	21	26	26
44.60	21	27	22	14	0	10	11
115.14	13	42	39	14	24	12	2
39.81	9	58	53	48	17	9	0
43.80	43	64	63	57	38	35	12
46.46	6	35	16	17	27	27	28
42.10	17	28	15	10	3	6	10
44.97	3	30	22	14	12	10	15
50.45	16	44	30	29	18	1	18
47.34	7	39	38	26	14	1	8
55.50	6	45	42	18	20	9	3
63.20	8	20	18	4	2	10	1
31.27	10	30	6	0	19	15	30
MAPE	**13**	**39**	**32**	**23**	**16**	**11**	**11**

Notes: BPR equation: $\alpha = 0.15$, $\beta = 4$;
SERPM model: $\alpha = 0.55$, $\beta = 5.05$, $C = 90$ *s*, $g/C = 0.55$ (speed >= 35 mph);
$\alpha = 0.35$, $\beta = 4.05$, $C = 60$ *s*, $g/C = 0.50$ (speed <35 mph);
Conical equation: $\alpha = 4.00$, $\beta = 1.17$;
Dowling method: $\alpha = 0.05$, $\beta = 10$.

It is found that overall the MAPEs for the BPR and Conical equations are 39% and 32%, respectively, which are the largest among all of the planning methods considered here. Compared to the BPR and Conical methods, which do not consider signal timing plans, SERPM uses default signal timing settings and shows prediction improvement in terms of MAPE, 23%. The Dowling method shows further improvement with the application of actual signal timing plans collected from the field, which gives an MAPE of 16%. The HCM gives the best results with the consideration of the available actual signal timing settings, with an MAPE of 11%.

The MAPE for the capacity-based model, which does not require timing plans as input, is 13%, which is only slightly worse than the 11% given by the HCM method. With the HCM results as a reference, the overall mean absolute percentage difference between the capacity-based model and HCM is 11%, which implies that the accuracy level of the capacity-based model is comparable to that of uniform delay of HCM method, which uses actual signal timing information in delay prediction.

The statistical test of correlation between field travel time data and the predictions by the models is conducted, which is presented in Table 5.4. Seven pairs of data are compared and each of them has 30 data points because of the limited data. Note that the number of data points is quite small, merely meeting the minimal requirement for this statistical test. The statistical inference of correlation and significance are presented in Column 3 and Column 4, respectively.

Based on the values of correlation, the seven data pairs are positively correlated with each other. At a significance level of 0.05, the null hypothesis that data pairs are not correlated can be rejected. The predictions by the capacity-based model, Dowling, and

HCM methods, are highly correlated to the field data, and have a stronger correlation to the field data than the predictions by the BPR, Conical, and SERPM methods. The test of correlation between the capacity-based model and HCM method shows that their predictions are consistent with the highest correlation inference score, 0.950.

Table 5.4 Correlations between paired samples by the models and from MDOT field data.

		N	Correlation	Significance
Pair 1	Capacity-based & Field	30	0.896	0.000
Pair 2	BPR & Field	30	0.802	0.000
Pair 3	Conical & Field	30	0.782	0.000
Pair 4	SERPM & Field	30	0.810	0.000
Pair 5	Dowling & Field	30	0.918	0.000
Pair 6	HCM & Field	30	0.934	0.000
Pair 7	Capacity-based & HCM	30	0.950	0.000

The paired *t*-test, presented in Table 5.5, also provides indications as whether the predicted value and field data differ or not. Column 3 gives the mean value of differences between each set of the paired data. Column 4 is the standard error of the mean value in Column 3. Column 5 and Column 6 are the lower and upper bounds of the 95% confidence interval for each of the mean values, respectively. Columns 7 through 9 give *t* value, degree of freedom, and two-tailed significance for the statistical test.

The mean difference of paired data between the prediction by the capacity-based model and field data is -1.40 ± 1.64 s/veh. The 95% confidence interval of the difference is [-4.75, 1.95]. At a significance level of 0.05, the null hypothesis that there is no significant difference between predicted travel time by the developed model and field collected data cannot be rejected. This suggests that the model prediction is not significantly different from the field data. However, at a significance level of 0.05, the null hypothesis that there is no significant difference between the predicted travel time by

the models in the literature and field collected data can be rejected. It suggests that the capacity-based model is the best model among all planning methods considered here.

Table 5.5 Statistical test for the paired difference based on MDOT field data.

Pair		Paired Differences				t	df	Significance (two-tailed)
		Mean (s/veh)	Std. Error (s/veh)	95% Confidence Interval of the Difference				
				Lower (s/veh)	Upper (s/veh)			
1	Capacity-based - Field	-1.40	1.64	-4.75	1.95	-0.85	29	0.40
2	BPR - Field	-22.36	2.24	-26.93	-17.78	-10.00	29	0.00
3	Conical - Field	-19.06	2.31	-23.79	-14.34	-8.25	29	0.00
4	SERPM - Field	-11.37	2.25	-15.98	-6.76	-5.04	29	0.00
5	Dowling - Field	-9.45	1.52	-12.56	-6.34	-6.22	29	0.00
6	HCM - Field	-3.08	1.33	-5.79	-0.37	-2.33	29	0.03
7	Capacity-based - HCM	1.68	1.12	-0.62	3.98	1.50	29	0.15

Taking HCM as a reference, the paired difference test shows that the mean difference between the capacity-based model and the HCM model is 1.68 s/veh. At a significance level of 0.05, the null hypothesis that there is no significant difference between predicted travel time by the developed model and HCM method cannot be rejected. Again, this suggests that the delay predicted by the developed model is similar to the uniform delay of the HCM method.

5.1.2 Saturation-Based Travel Time Model

This section presents the evaluation of the saturation-based model. The travel time predicted by the saturation-based model is presented in Column 5 in Table 5.6, which is compared to the MDOT field data, given in Column 2, and the travel time by the capacity-based model, in Column 3. The absolute percentage differences between the

models and the field travel time are presented in Columns 4 and 6. The last row of the table gives the average value of each version of the models.

It is found that the predicted values by both capacity-based and saturation-based models are close to each other. The mean absolute percentage error for the saturation-based model is 12%, which is close to the 13% for the capacity model.

Correlation test is conducted for three data pairs: predictions by the saturation-based model and the field data, predictions by the saturation-based model and by the HCM model, and predictions by the saturation-based model and by the capacity-based model. The result is presented in Table 5.7.

The statistical test shows that the correlation between predicted values by the saturation-based models and the field data is high, similar to the capacity-based model. At a significance level of 0.05, the null hypothesis that the model predictions are not correlated to field data is rejected. The saturation-based model is also highly related to the HCM method, as well as to the capacity-based model, with correlation inference of 0.948 and 0.999, respectively.

Table 5.6 Travel time by different models in comparison with the MDOT data.

Site ID	Field (s/veh)	Capacity-based		Saturation-based	
		Travel Time (s/veh)	Percentage (%)	Travel Time (s/veh)	Percentage (%)
2	40.64	46.27	14	45.29	11
3	84.32	74.23	12	74.21	12
8	91.11	75.59	17	75.50	17
25	49.02	44.66	9	44.18	10
30	73.23	63.09	14	62.64	14
32	55.40	54.44	2	53.97	3
34	51.64	46.04	11	45.75	11
35	33.40	37.51	12	36.98	11
36	43.91	46.81	7	46.36	6
40	74.55	83.98	13	84.55	13
50	63.09	50.04	21	46.12	27
51	55.24	59.04	7	57.89	5
53	37.59	30.21	20	30.01	20
64	94.07	76.02	19	76.00	19
66	70.24	72.49	3	72.48	3
67	67.06	83.69	25	83.61	25
68	76.05	81.48	7	81.47	7
81	33.82	31.57	7	32.01	5
83	44.60	54.13	21	54.75	23
86	115.14	100.09	13	100.81	12
96	39.81	43.46	9	42.18	6
97	43.80	25.15	43	24.90	43
98	46.46	43.77	6	42.74	8
100	42.10	49.38	17	48.69	16
109	44.97	46.48	3	45.71	2
111	50.45	58.59	16	56.36	12
130	47.34	43.83	7	43.83	7
140	55.50	52.09	6	52.55	5
146	63.20	68.55	8	68.55	8
148	31.27	34.34	10	33.71	8
Average	**57.30**	**55.90**	**13**	**55.46**	**12**

Table 5.7 Correlation between three travel time models based on MDOT data.

		N	Correlation	Significance
Pair 1	Saturation-based & Field	30	0.895	0.000
Pair 2	Saturation-based& HCM	30	0.948	0.000
Pair 3	Saturation-based & Capacity-based	30	0.999	0.000

The paired *t*-test also provides a measure to indicate whether the predicted and field data differ or not. Table 5.8 presents paired difference test for three data pairs: saturation-based model and field data, saturation-based model and HCM model, and saturation-based model and capacity-based model. The mean difference of paired data between predictions by the saturation-based model and the field data is -1.84 ± 1.65 s/veh. The 95% confidence interval of the difference is [-5.21, 1.53]. At a significance level of 0.05, the null hypothesis that the travel time predictions by the saturation-based model are the same as field collected data cannot be rejected.

Similar to the capacity-based model, the mean difference between the saturation-based model and the HCM method is expected to be zero. At a significance level of 0.05, the null hypothesis that there is no significant difference between the saturation-based model and the HCM method cannot be rejected. However, the values predicted by the saturation-based model are systematically lower than those predicted by the capacity-based model, although the mean difference between them is as low as -0.44 s/veh. Due to the high degree of correlation between predicted values from both models, the standard error of mean difference is as low as 0.17 s/veh. At a significance level of 0.05, the null hypothesis that there is no difference between the means of the twomodel can be rejected. The predicted values by the saturation-based model are lower than those predicted by the capacity-based model.

Table 5.8 Statistical test for the paired differences under light traffic.

		Paired Differences				t	df	Significance (two-tailed)
		Mean (s/veh)	Std. Error Mean (s/veh)	95% Confidence Interval of the Difference				
				Lower (s/veh)	Upper (s/veh)			
Pair 1	Saturation-based - Field	-1.84	1.65	-5.21	1.53	-1.12	29	0.27
Pair 2	Saturation-based - HCM	1.24	1.14	-1.08	3.57	1.09	29	0.28
Pair 3	Saturation-based - Capacity-based	-0.44	0.17	-0.78	-0.10	-2.65	29	0.01

5.2 Evaluation Based on Miami-Dade County Data

Considering the field data collected from the MDOT are mostly well below congestion conditions, the data are also collected from US-1 in Miami-Dade County, Florida, where traffic during peak periods is congested. The area for this case study is along US-1 and between SW 98 Street and SW 136 Street in Miami, Florida. Real-time operation parameters, such as cycle length, green time, traffic volume in peak time, *etc*., are available. However, travel times are not directly available. Because it is time-consuming and expensive to collect such data for urban streets, CORSIM simulation is conducted to generate travel time for each link. Table 5.9 presents operation parameters for each link, as well as the travel time from simulation. The identification number of each site is presented in the first column. Columns 2 through 11 present capacity (*c*), speed limit, length of link (*L*), volume (*v*), left turn portion, right turn portion, number of lanes (*N*), cycle length (*Cycle*), green time (*g*), and total travel time per vehicle.

These data represent a heavy traffic situation with a traffic volume of 565 vphpl, and a capacity of 738 vphpl in average. The average link length is about 0.23 mile and

the average speed limit is 45 mph. The average travel time per mile is about 415 seconds, which translates into an average speed of 8.7 mph during peak period.

Table 5.9 Operational parameters of 7 intersections along US-1 in Miami-Dade.

Site ID	c (vph)	Speed Limit (mph)	L (mile)	v (vph)	Left Turn Ratio	Right Turn Ratio	N	Cycle (s)	g (s)	Travel Time (s/veh)
136-NB	2,250	45	0.103	1,939	0.15	0.04	3	170	104	38.7
136-SB	2,250	45	0.224	3,065	0.04	0.1	3	170	104	66.5
136-EB	2,250	45	0.126	820	0.25	0.34	3	170	38	130.2
136-WB	2,250	45	0.092	709	0.47	0.07	3	170	38	63.5
132-NB	2,250	45	0.224	1,788	0.11	0.00	3	180	140	46
132-SB	2,250	45	0.327	2,625	0.00	0.04	3	180	140	64.9
132-EB	1,500	45	0.087	666	0.12	0.88	2	180	24	50.3
128-NB	2,250	45	0.327	1,682	0.04	0.03	3	170	103	71.6
128-SB	2,250	45	0.277	2,774	0.01	0.06	3	170	103	35
128-EB	592	45	0.057	192	0.45	0.10	1	170	39	244.8
128-WB	592	45	0.058	266	0.29	0.12	1	170	39	57.9
124-NB	2,250	45	0.277	1,653	0.03	0.05	3	170	107	45
124-SB	2,250	45	0.829	2,888	0.04	0.04	3	170	107	125
124-EB	750	45	0.079	229	0.31	0.25	1	170	36	137.8
124-WB	1,060	45	0.082	348	0.36	0.13	2	170	36	58.2
112-NB	2,250	45	0.829	1,556	0.12	0.03	3	177	112	125.8
112-SB	2,250	45	0.547	3,068	0.03	0.06	3	177	112	75.3
112-EB	750	45	0.098	225	0.40	0.27	1	177	38	358.6
112-WB	750	45	0.08	325	0.16	0.17	1	177	38	62.5
104-NB	2,250	45	0.547	1,482	0.08	0.02	3	180	111	85.8
104-SB	2,250	45	0.106	3,292	0.07	0.09	3	180	111	55.1
104-EB	1,500	45	0.099	599	0.00	0.23	2	180	41	203.6
104-WB	2,250	45	0.108	492	0.22	0.00	3	180	41	69.1
98-NB	2,250	45	0.193	683	0.09	0.03	3	140	97	41.3
98-SB	2,250	45	0.188	2,385	0.07	0.12	3	140	97	124.5
98-EB	750	45	0.067	225	0.35	0.19	1	140	29	50.3
98-WB	750	45	0.083	162	0.22	0.34	1	140	29	48.8

5.2.1 Capacity-Based Model

The evaluation of the capacity-based models is conducted following the same procedure as described in Section 5.1. The travel time predictions by the capacity-based delay model are evaluated first, which are presented in the third column in Table 5.10. The travel time predictions by the BPR, Conical, SERPM, Dowling, and HCM methods are

presented in Columns 4 through 8, respectively. The travel time predictions are compared to the US-1 travel times in Column 2. The models evaluated by the dataset in Table 5.9 are Type13, Type23, Type31, Type32 and Type33.

Table 5.10 Travel time calculated by different planning models in comparison with US-1 data.

Site ID	Model Evaluated	US-1 (s/veh)	Capacity-based (s/veh)	BPR (s/veh)	Conical (s/veh)	SERPM (s/veh)	Dowling (s/veh)	HCM (s/veh)
136-NB	Type33	38.70	50.14	8.92	12.94	15.43	25.02	35.32
136-SB	Type33	66.50	48.77	27.19	74.29	96.61	72.41	50.92
136-EB	Type33	130.20	63.89	10.11	10.97	15.04	43.08	65.87
136-WB	Type33	63.50	63.35	7.37	7.88	10.96	40.36	62.48
132-NB	Type32	46.00	57.56	18.99	25.78	31.25	28.06	29.56
132-SB	Type32	64.90	56.99	33.43	74.39	85.53	44.61	46.16
132-EB	Type23	50.30	53.65	7.00	7.80	10.45	45.96	78.81
128-NB	Type31	71.60	84.69	27.39	35.76	43.85	43.03	50.31
128-SB	Type31	35.00	57.61	29.85	72.26	85.24	54.75	55.66
128-EB	Type13	244.80	56.31	4.57	4.90	6.80	37.31	59.09
128-WB	Type13	57.90	51.78	4.67	5.21	6.97	37.39	60.91
124-NB	Type31	45.00	75.15	23.13	29.90	36.78	38.00	43.87
124-SB	Type31	125.00	105.49	93.36	238.60	290.38	132.05	97.82
124-EB	Type13	137.80	56.06	6.33	6.75	9.41	39.82	62.78
124-WB	Type23	58.20	61.47	6.57	7.06	9.78	40.06	63.32
112-NB	Type31	125.80	129.05	68.60	86.09	107.10	82.67	87.55
112-SB	Type31	75.30	84.14	66.48	181.83	236.76	126.90	76.26
112-EB	Type13	358.60	69.04	7.85	8.36	11.68	42.59	66.18
112-WB	Type13	62.50	60.14	6.43	7.14	9.60	41.15	66.58
104-NB	Type32	85.80	81.03	45.00	55.31	69.44	61.06	66.03
104-SB	Type32	55.10	39.19	14.30	41.31	59.95	83.39	42.98
104-EB	Type23	203.60	69.95	7.95	8.73	11.84	42.67	66.97
104-WB	Type33	69.10	77.98	8.64	9.02	12.85	43.39	65.12
98-NB	Type31	41.30	46.25	15.46	16.49	23.00	26.19	23.81
98-SB	Type31	124.50	39.59	17.89	34.06	38.88	28.10	36.54
98-EB	Type13	50.30	44.30	5.37	5.72	7.98	33.11	52.28
98-WB	Type13	48.80	50.07	6.64	6.93	9.88	34.39	52.70

Absolute percentage errors between predicted values and US-1 data in Miami-Dade are presented in Table 5.11. The capacity-based model is also compared to the HCM method. The absolute percentage errors are presented in Column 8. Mean absolute

percentage errors (MAPEs) for different planning methods are provided in the last row of the table.

Table 5.11 Mean absolute percentage error for different planning models in comparison with US 1 data.

US-1 (s/veh)	Percentage						
	Capacity-based (%)	BPR (%)	Conical (%)	SERPM (%)	Dowling (%)	HCM (%)	Capacity-based - HCM (%)
38.70	30	77	67	60	35	9	42
66.50	27	59	12	45	9	23	4
130.20	51	92	92	88	67	49	3
63.50	0	88	88	83	36	2	1
46.00	25	59	44	32	39	36	95
64.90	12	48	15	32	31	29	23
50.30	7	86	84	79	9	57	32
71.60	18	62	50	39	40	30	68
35.00	65	15	106	144	56	59	4
244.80	77	98	98	97	85	76	5
57.90	11	92	91	88	35	5	15
45.00	67	49	34	18	16	3	71
125.00	16	25	91	132	6	22	8
137.80	59	95	95	93	71	54	11
58.20	6	89	88	83	31	9	3
125.80	3	45	32	15	34	30	47
75.30	12	12	141	214	69	1	10
358.60	81	98	98	97	88	82	4
62.50	4	90	89	85	34	7	10
85.80	6	48	36	19	29	23	23
55.10	29	74	25	9	51	22	9
203.60	66	96	96	94	79	67	4
69.10	13	87	87	81	37	6	20
41.30	12	63	60	44	37	42	94
124.50	68	86	73	69	77	71	8
50.30	12	89	89	84	34	4	15
48.80	3	86	86	80	30	8	5
MAPE	**29**	**71**	**73**	**74**	**43**	**31**	**24**

Notes: BPR equation: $\alpha = 0.15$, $\beta = 4$;
SERPM model: $\alpha = 0.55$, $\beta = 5.05$, $C = 90$ *s*, $g/C = 0.55$ (speed >= 35 mph);
$\alpha = 0.35$, $\beta = 4.05$, $C = 60$ *s*, $g/C = 0.50$ (speed <35 mph);
Conical equation: $\alpha = 4.00$, $\beta = 1.17$;
Dowling method: $\alpha = 0.05$, $\beta = 10$.

The capacity-based model in this study gives the best performance for saturated traffic condition with a MAPE of 29%, which is slightly better than that of the HCM method (31%). The other models, such as the BPR equation, conical equation, SERPM, and Dowling method, give large errors of 71%, 73%, 74%, and 43%, respectively. Although the parameters are from field operation of US-1, there is still the concern that the travel time is not directly collected from the field. Considering that HCM method is a widely accepted industry standard, the travel time predicted by the model is also evaluated against the uniform delay from the HCM. The overall percentage difference between the capacity-based model and HCM method is about 24%.

Statistical tests of correlation between the US-1 simulated travel time data and the predictions by the capacity-based models are conducted, and the results are presented in Table 5.12. Seven pairs of data are compared and each of them has 27 data points. The statistical inference of correlation and significance are presented in Columns 4 and 5, respectively.

Table 5.12 Correlations between paired samples by the models and from US-1 data.

		N	Correlation	Significance
Pair 1	Capacity-based & US-1	27	0.203	0.309
Pair 2	BPR & US-1	27	-0.036	0.858
Pair 3	Conical & US-1	27	-0.049	0.808
Pair 4	SERPM & US-1	27	-0.050	0.804
Pair 5	Dowling & US-1	27	0.030	0.881
Pair 6	HCM & US-1	27	0.316	0.108
Pair 7	Capacity-based & HCM	27	0.680	0.000

At a significance level of 0.05, the null hypothesis that model predictions are not correlated to US-1 data cannot be rejected for the first six pairs. This suggests that all models have a poor performance under congested conditions. On the other hand, there is

a strong positive correlation between the predictions from the capacity-based model and HCM method, and the correlations between the predictions by these two models and the US-1 data are much stronger than that for the other models. Some models, such as the BPR, Conical, and SERPM model have negative correlation between their predictions and US-1 data. This raises the doubt about the ability of these models to accurately predict travel time under congested conditions. Note that both the capacity-based model and HCM method are applied here to predict uniform delay. It is expected that the model performance under congested conditions is not satisfactory. However, it should be noted that the results from the capacity-based model are well correlated to those from the HCM method. At a significance level of 0.05, the null hypothesis that the capacity-based model predictions are not correlated to the HCM predictions under a congested condition is rejected. This means that the predictions by the capacity-based model and HCM method are consistent. The model is considered to be improved in the future when appropriate progression factors are available.

A paired t-test is only conducted for the correlated pair of models: the capacity-based model and HCM method. The mean difference of paired data between the predictions by the capacity-based model and HCM is 6.21 ± 2.90 s/veh. The 95% confidence interval of the difference is [0.25, 12.18]. At a significance level of 0.05, the null hypothesis that the predicted travel times by the capacity-based model are the same as the HCM prediction can be rejected. However, the small mean difference is in favor of the similarity of predicted delays and uniform delays of the HCM.

The statistical test reveals the difficulty in travel time prediction under congested traffic conditions. The capacity-based model provides better predictions, compared to current models in literature, but can still be improved.

5.2.2 Saturation-Based Travel Time Models

The travel time prediction method based on the saturation-based delay model is evaluated using the US-1 data in Miami-Dade County, Florida. US-1 travel times are presented in the second column in Table 5.13. The travel times predicted by both capacity and saturation-based models are presented in Columns 3 and 5. The absolute percentage errors are presented in Columns 4 and 6, respectively.

It is found that the values predicted by both travel time models are close to each other. The overall MAPE for the saturation-based model is 27%, which is close to the MAPE of 29% for the capacity-based model.

Table 5.13 Comparison of travel time by two developed models with US-1 data.

Site ID	US-1 (s/veh)	Capacity-based		Saturation-based	
		Travel Time (s/veh)	Percentage (%)	Travel Time (s/veh)	Percentage (%)
136-NB	38.70	50.14	30	50.14	30
136-SB	66.50	48.77	27	48.77	27
136-EB	130.20	63.89	51	63.90	51
136-WB	63.50	63.35	0	63.35	0
132-NB	46.00	57.56	25	57.56	25
132-SB	64.90	56.99	12	56.99	12
132-EB	50.30	53.65	7	53.66	7
128-NB	71.60	84.69	18	69.72	3
128-SB	35.00	57.61	65	53.11	52
128-EB	244.80	56.31	77	56.83	77
128-WB	57.90	51.78	11	51.51	11
124-NB	45.00	75.15	67	65.57	46
124-SB	125.00	105.49	16	103.27	17
124-EB	137.80	56.06	59	56.06	59
124-WB	58.20	61.47	6	60.11	3
112-NB	125.80	129.05	3	128.93	2
112-SB	75.30	84.14	12	84.11	12
112-EB	358.60	69.04	81	69.05	81
112-WB	62.50	60.14	4	60.14	4
104-NB	85.80	81.03	6	81.03	6
104-SB	55.10	39.19	29	39.19	29
104-EB	203.60	69.95	66	69.96	66
104-WB	69.10	77.98	13	77.98	13
98-NB	41.30	46.25	12	46.23	12
98-SB	124.50	39.59	68	39.57	68
98-EB	50.30	44.30	12	44.30	12
98-WB	48.80	50.07	3	50.07	3
Average	**93.93**	**64.21**	**29**	**63.00**	**27**

A statistical test of the correlation between the US-1 travel time data and predictions by the saturation-based model is conducted, which is presented in Table 5.14.

Table 5.14 Correlation between three travel time models based on MDOT data.

		N	Correlation	Significance
Pair 1	Saturation-based & US-1	27	0.241	0.227
Pair 2	Saturation- based & HCM	27	0.721	0.000
Pair 3	Saturation- based & Capacity- based	27	0.986	0.000

At a significance level of 0.05, the null hypothesis that model predictions are not correlated to US-1 data cannot be rejected. It suggests that the saturation-based model has poor prediction under congested conditions, just as the capacity-based model does. However, it should be noted that the saturation-based model is highly correlated to the HCM method and capacity-based model. At a significance level of 0.05, the null hypothesis that the predictions by the saturation-based model are not correlated to the HCM predictions under congested traffic conditions is rejected. This means that the predictions by the developed model and HCM method are consistent. At a significance level of 0.05, the null hypothesis that the model predictions by both capacity and saturation-based models are not correlated under congested conditions is rejected. Both models are highly correlated, with a correlation inference as high as 0.986.

The paired *t*-test is conducted for the correlated pairs, i.e., the saturation-based model and HCM method, as well as the saturation-based model and capacity-based model. The test results are presented in Table 5.15.

Table 5.15 Statistical test for the paired differences for three models under congested traffic.

		Paired Differences				t	df	Significance (two-tailed)
		Mean (s/veh)	Std. Error Mean (s/veh)	95% Confidence Interval of the Difference				
				Lower (s/veh)	Upper (s/veh)			
Pair 1	Saturation-based - HCM	5.01	2.65	-0.44	10.46	1.89	26	0.070
Pair 2	Saturation-absed - Capacity-based	-1.20	0.66	-2.56	0.15	-1.83	26	0.079

The statistical test between the saturation-based model and HCM method indicates that the mean difference between the developed model and HCM method is 5.01 s/veh. At a significance level of 0.05, the null hypothesis that there is no significant difference between the saturation-based model and HCM method cannot be rejected.

The predictions by the saturation-based model are lower than those predicted by the capacity-based model. The mean difference between them is low at -1.20 s/veh. At a significance level of 0.05, the null hypothesis that there is no significance difference between the means of both versions of the model cannot be rejected.

5.3 Summary of Evaluation

Two versions of the developed model, one capacity-based and the other saturation-based, are evaluated using two sets of operational travel time data. Generally speaking, both models are highly correlated with each other, with correlation coefficient as high as 0.99 under both uncongested and congested conditions. The travel times predicted by the delay model with saturation flow rate are slightly lower than those by the capacity-based model in average. The mean differences of predicted travel times by both models are 0.44 s/veh for uncongested traffic conditions, and 1.20 s/veh for congested conditions. The mean prediction differences between the two models are small compared to the average travel time of 55 s/veh or 94 s/veh. In conclusion, the two models are similar, which suggests that any of them could be applied in planning applications without causing significant difference in travel time prediction.

The developed models provide a better travel time prediction than most of the existing planning models in the literature for both uncongested and congested traffic conditions. The MAPE of the developed model is 13% for uncongested conditions, and

29% for congested conditions, which is comparable to the prediction accuracy of the HCM uniform delay model. This performance is achieved without requiring signal timing as input, as opposed to the HCM model, which requires operational signal timing plans.

Note the developed models only include the uniform delay that is not adjusted for signal coordination and oversaturation. The models are expected to predict a lower travel time under congested conditions. The developed models need to be adjusted by incorporating progression factors when they are available.

CHAPTER 6

MODEL APPLICATION FOR TRAFFIC ASSIGNMENT

To investigate whether the developed models have the potential to be applied for planning and to identify technical challenges, the developed models for different lane configurations (calibrated based on a free flow speed of 45 mph) are tested for traffic assignment in a travel demand forecasting process. When the number of lanes of any approaches is more than three, the Type11 model is applied. As previously discussed, all models or unified models can substitute for Type11 model without significant deterioration in performance. The test is implemented with the Cube software, which is a product of Citilabs. It supports transportation planning and provides modules for trip generation, trip distribution, modal split, and traffic assignment. Cube Voyager provides function modules, such as Network, Matrix, and Highway modules. The Network module assists in network building based on a link and node text file. The Matrix module supports OD (origin-destination) matrix manipulation. The Highway module performs traffic assignment for a given network and OD matrix. Traditional assignment methods are available, including equilibrium, average, weighted average, incremental, and the all-or-nothing assignment method. Default cost functions are available, which may be replaced by user definitions.

Although the developed model does not require signal timing information, it requires traffic volumes from the cross-street direction, which presents several challenges to a general purpose software package, such as Cube. In current practices, traffic assignment is conducted on a link by link basis, and both traffic volumes and travel costs are updated link by link during each iteration. To apply the model developed in this study,

the update of travel cost for a link requires the traffic volumes from other approaches connected to the same intersection. These other volumes need to be coded as the attributes of the subject link, but they are usually unavailable due to the design of data structure of the software. Second, the convergence of traffic assignment using multi-approach volumes presents another challenge as reviewed in the literature, i.e., the monotonicity requirement of the link travel cost function is not satisfied.

The solution process is illustrated by the flow chart in Figure 6.1. The only difference in the process is that travel cost is now provided by the developed model, which provides new travel time estimation for links with traffic controlled intersections.

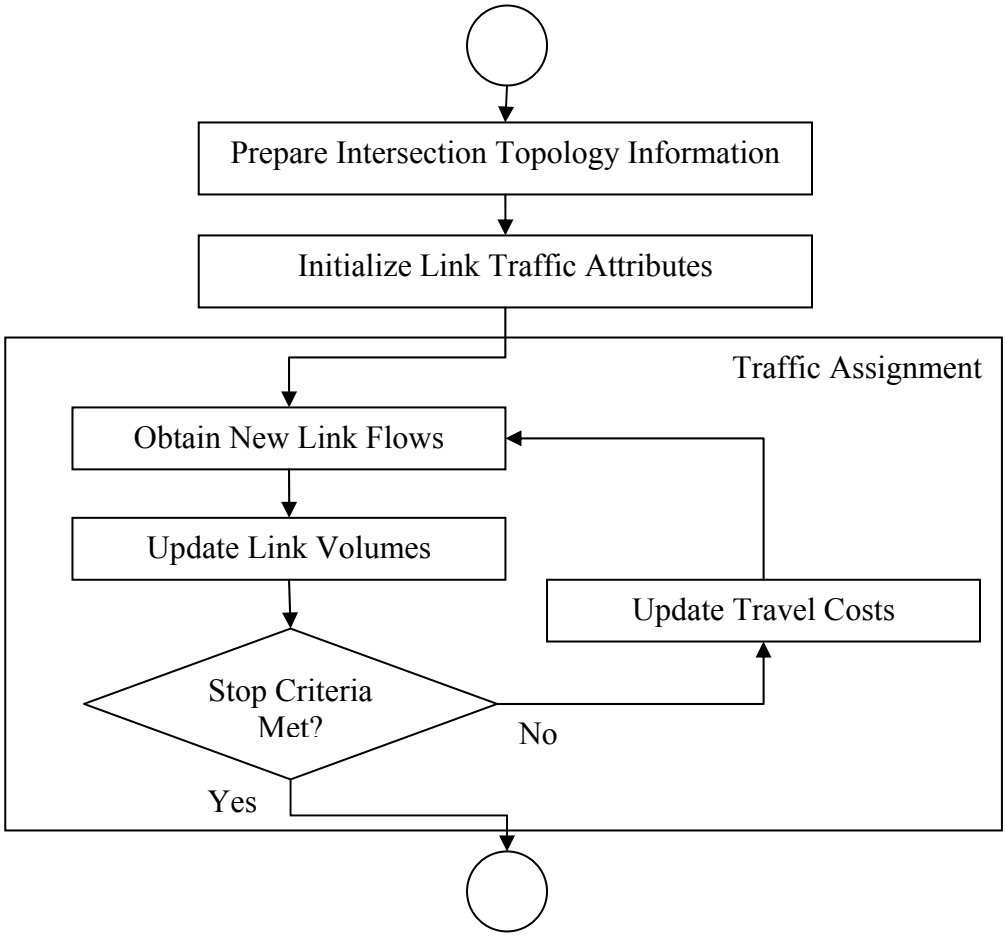

Figure 6.1 A flow chart of assignment process with new developed travel time model.

6.1 Technical Issues of Model Application

6.1.1 Preparing Intersection Topology Information

The first application issue is to make the information required by the developed model available. Cube does not provide cross-street volumes for a subject link, but it does provide a turning volume file. The data structure of the turning volume file includes records such as Node A, Node B, Node C, and turning volume from Node A, through Node B, to Node C. The turning volume file provides the information about how links are connected through a junction node, which can be used to assemble cross-street volumes for a given subject link. To illustrate the assembling method, Figure 6.2 presents a schematic drawing of a four-legged intersection with approaches of *subject1*, *subject2*, *cross1* and *cross2*.

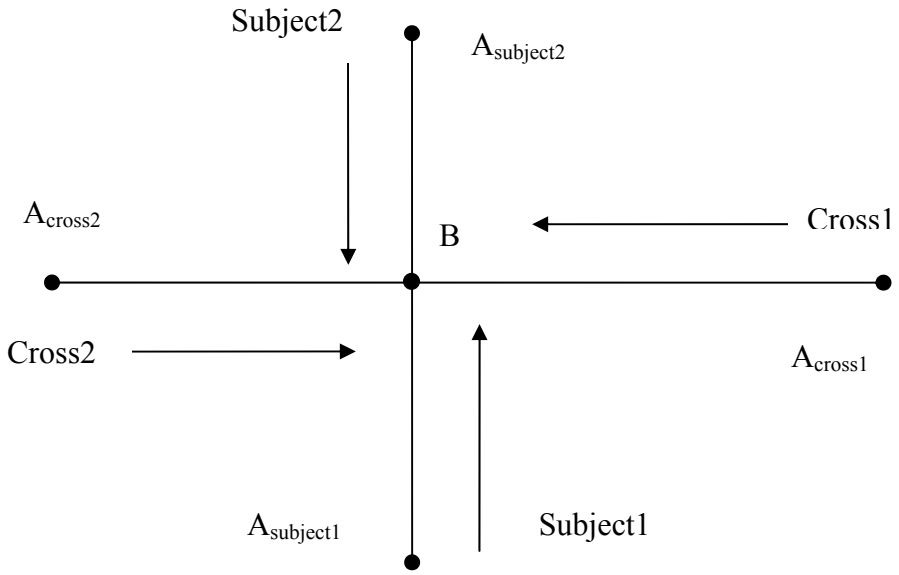

Figure 6.2 Schematics drawing of four-leg intersection with approaches of *subject1*, *subject2*, *cross1* and *cross2*.

In Figure 6.2, four approaches share the same junction node, B, with four starting turning nodes, $A_{subject1}$, A_{cross1}, $A_{subject2}$, and A_{cross2}. Each of the links has attributes such as volume, link length, speed, travel time, travel cost, starting node, ending node, *etc.* Let *subject1* represent subject direction of link $A_{subject1}B$. Because the required traffic volumes for other links, such as V_{cross1} for link $A_{cross1}B$, $V_{subject2}$ for link $A_{subject2}B$, and V_{cross2}, for link $A_{cross2}B$, are not attributes of link $A_{subject1}B$, therefore are unavailable. These volumes need to be coded as the attributes of the subject link $A_{subject1}B$. Hence, it is necessary to define Node A_{cross1}, $A_{subject2}$, and A_{cross2} for a given subject link $A_{subject1}B$. From the topology shown in Figure 6.2, A_{cross1}, $A_{subject2}$, and A_{cross2} are actually the ending node of right-turn, through, and left-turn movements of link $A_{subject1}B$, respectively. As presented in Figure 6.3, the turn attribute is defined as left, through, or right based on the angle of $\angle ABC$. If the angle $\angle A_{subject1}BC$ for a turning movement for link $A_{subject1}B$, is less than 120°, the turn is defined as a left-turn, and the ending node C is the starting node of *cross2* traffic, A_{cross2}. If the angle $\angle A_{subject1}BC$ is between 120°and 240°, the turn is defined as through traffic, and the ending node C is the starting node of *subject2* traffic, $A_{subject2}$. Similarly, if the angle $\angle A_{subject1}BC$ is between 240°and 360°, the turn is defined as a right-turn, and the ending node C is the starting node of *cross1* traffic, A_{cross1}. A Cube script is written to define the attributes of the ending note of turning movements and code the attributes on a subject link. The script is given in Appendix C.

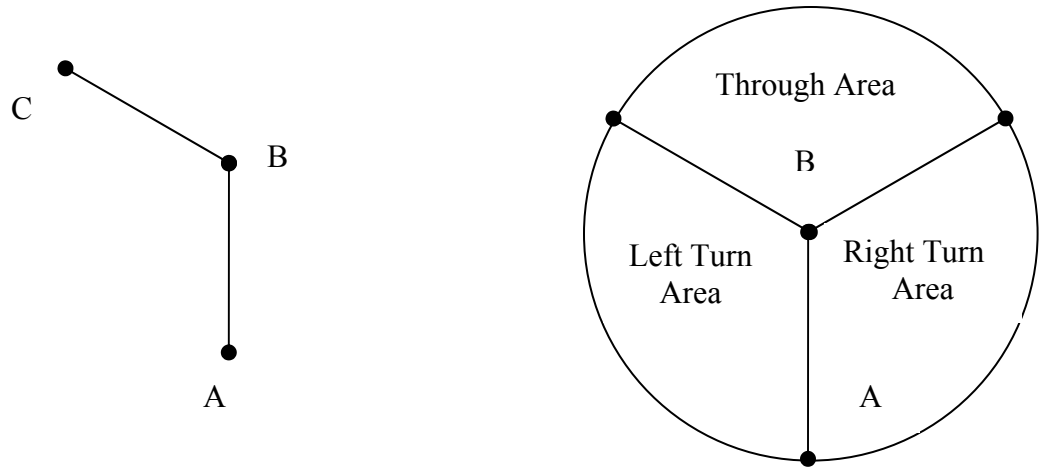

Figure 6.3 Turn attribute definition for ending node *C*.

In practice, a four-leg intersection is the most common type of intersections. However, the number of approach of intersection may be more than four. For example, there may be two left-turn legs based on the definition above. Only the one with larger turning volume is defined as left-turn leg in the treatment of this study. The model is unable to handle intersections with five or more legs.

6.1.2 Updating Link Traffic Attributes

With the definition of ending nodes for right-turn, through, and left-turn movements of link $A_{subject1}B$, which should be nodes A_{cross1}, $A_{subject2}$, and A_{cross2}, the turning volumes $V_{A_{cross1}BA_{subject1}}$, $V_{A_{cross1}BA_{cross2}}$, and $V_{A_{cross1}BA_{subject2}}$ can be looked up in a turning volume file, which is a Cube output file. The cross-street volume in *cross1* direction is defined as follows and coded as an attribute of subject link:

$$V_{cross1} = V_{A_{cross1}BA_{subject1}} + V_{A_{cross1}BA_{cross2}} + V_{A_{cross1}BA_{subject2}} \quad (6\text{-}1)$$

where

V_{cross1} = traffic volume in *cross1* direction (vph);

$V_{A_{cross1}BA_{subject1}}$ = turning volume from Node A_{cross1} through B to $A_{subject1}$ (vph);

$V_{A_{cross1}BA_{cross2}}$ = turning volume from Node A_{cross1} through B to A_{cross2} (vph); and

$V_{A_{cross1}BA_{subject2}}$ = turning volume from Node A_{cross1} through B to $A_{subject2}$ (vph).

Similarly, the traffic volume in the *subject2* direction in Figure 6.2 is defined as follows and coded as an attribute of subject link:

$$V_{subject2} = V_{A_{subject2}BA_{cross1}} + V_{A_{subject2}BA_{subject1}} + V_{A_{subject2}BA_{cross2}} \quad (6\text{-}2)$$

where

$V_{subject2}$ = traffic volume in *subject2* direction (vph);

$V_{A_{subject2}BA_{cross1}}$ = turning volume from Node $A_{subject2}$ through B to A_{cross1} (vph);

$V_{A_{subject2}BA_{subject1}}$ = turning volume from Node $A_{subject2}$ through B to $A_{subject1}$ (vph); and

$V_{A_{subject2}BA_{cross2}}$ = turning volume from Node $A_{subject2}$ through B to A_{cross2} (vph).

The traffic volume in *cross2* direction in Figure 6.2 is defined as follows and coded as an attribute of subject link:

$$V_{cross2} = V_{A_{cross2}BA_{subject2}} + V_{A_{cross2}BA_{cross1}} + V_{A_{cross2}BA_{subject1}} \quad (6\text{-}3)$$

where

V_{cross2} = traffic volume in *cross2* direction (vph);

$V_{A_{cross2}BA_{subject2}}$ = turning volume from Node A_{cross2} through B to $A_{subject2}$ (vph);

$V_{A_{cross2}BA_{cross1}}$ = turning volume from Node A_{cross2} through B to A_{cross1} (vph); and

$V_{A_{cross2}BA_{subject1}}$ = turning volume from Node A_{cross2} through B to $A_{subject1}$ (vph).

Note that the simulation experiment in Chapter 3 is designed with balanced traffic volumes, in which the traffic volumes in the opposite direction are the same. The purpose is to significantly reduce the computation need to acquire large amounts of delay data for different combinations of traffic volumes. However, the traffic volumes of different approaches through a junction node may not be balanced in practice. This problem could be solved by introducing the concept of critical lane group. The normalized subject volume is still the per lane volume for subject link, $V_{subject1}$, but the per lane cross-street volume is defined as the larger of the two per lane cross-street volumes, V_{cross1}, and V_{cross2}:

$$V_{cross} = Maximum(V_{cross1}, V_{cross2}) \quad (6\text{-}4)$$

where

V_{cross} = volume per lane in the cross-street used in the developed model (vphpl);

V_{cross1} = volume per lane in approach *cross1* (vphpl); and

V_{cross2} = volume per lane in approach *cross2* (vphpl).

A Cube script is written to implement the above definition, which is attached in Appendix D.

6.1.3 Method of Successive Average

Delays predicted by the developed model not only depend on subject traffic, but also cross-street traffic. Because delay for a link is not monotonically related to its own traffic volume in this model, convergence may become problematic for a conventional equilibrium assignment method (Horowitz 1991). The literature suggests that the method of successive average (MSA) may solve the convergence problem (Horowitz 1991). For

the purpose of updating travel costs, the traffic volume for the next iteration is the average of the volumes from previous iterations. The equation is as follows:

$$V_{n+1} = \frac{F_n}{n} + \left(1 - \frac{1}{n}\right) V_n \tag{6-5}$$

where

V_{n+1} = traffic volume in the $(n + 1)^{th}$ iteration (vph);

F_n = assigned traffic volume in the n^{th} iteration (vph);

n = iteration number; and

V_n = traffic volume in the n^{th} iteration (vph).

MSA is implemented on Cube platform, and the script is attached in Appendix E.

6.1.4 Spillback Delay from Downstream to Upstream

The developed model captures the spatial distribution of delay on a link, which helps to improve the link delay estimation for a variety of link lengths. When the queue extends beyond the subject link, the extra delay due to the queue extension to the other links should be assigned to the upstream links. In this study, a procedure has been developed to assign the extra delay that does not occur on the downstream subject link to an upstream link. Considering that most spillback vehicles are likely a part of through traffic, the receiving link is assumed to be the immediate upstream link. The additional delay on the upstream link due to spillback delay is expressed as the portion of delay experienced by vehicles on the segment between distance of L_{down} to distance of $L + L_{down}$ from the intersection, as follows:

$$t_{spillback} = X_{subject}\left[a_2 + a_3 \frac{(X_{cross})^{a_4}}{(X_{subject})^{a_5}}\right]\left\{\exp\left(-\frac{a_6 \times L_{down}}{X_{subject}}\right) - \exp\left[-\frac{a_6 \times (L + L_{down})}{X_{subject}}\right]\right\}$$

(6-6)

where

$t_{spillback}$ = additional delay spilled from downstream link (s/veh);

L = link length of upstream receiving spillback delay (miles);

L_{down} = link length for a downstream link (miles);

$X_{subject}$ = degree of congestion defined in Equation (4-2);

X_{cross} = degree of congestion defined in Equation (4-3); and

a_2, a_3, a_4, a_5, a_6 = downstream fitted parameters.

With the technical problems for implementation solved, the assignment processes with the developed models are implemented, for which a Cube script is written and is attached in Appendix F.

6.2 Model Application for a Hypothetical Network

The model is tested first on a hypothetical network, as shown in Figure 6.4. The network is a 5 × 5 grid with signal controls at the nodes numbered 200 to 224. All the links are two-lane roads with a lane width of 12 feet. The link length between signal-controlled nodes is 0.2 miles, except that the link length between Nodes 202 and 222 is 0.8 miles, and the link lengths between Nodes 206 and 208, between Nodes 211 and 213, and between Nodes 216 and 218 are 0.4 miles. The link length is designed to have some links less interrupted. The nodes 300 through 315 are designed to accommodate trips that may be spilled back from the signalized intersections. The length between the 3xx (300 – 319) node and adjacent 2xx (200 – 225) node is one mile long.

It is assumed that there are 16 centroid nodes, i.e., Nodes 1 to 16, where trips begin or end. The OD matrix for this hypothetical network is given in Table 6.1. The

traffic flows are generated and attracted between Node 1 and Node 8, between Node 11 and Node 17, and between Node 4 and Node 14. The traffic is congested, with 1,500 vehicles per hour (vph) for a two-lane road.

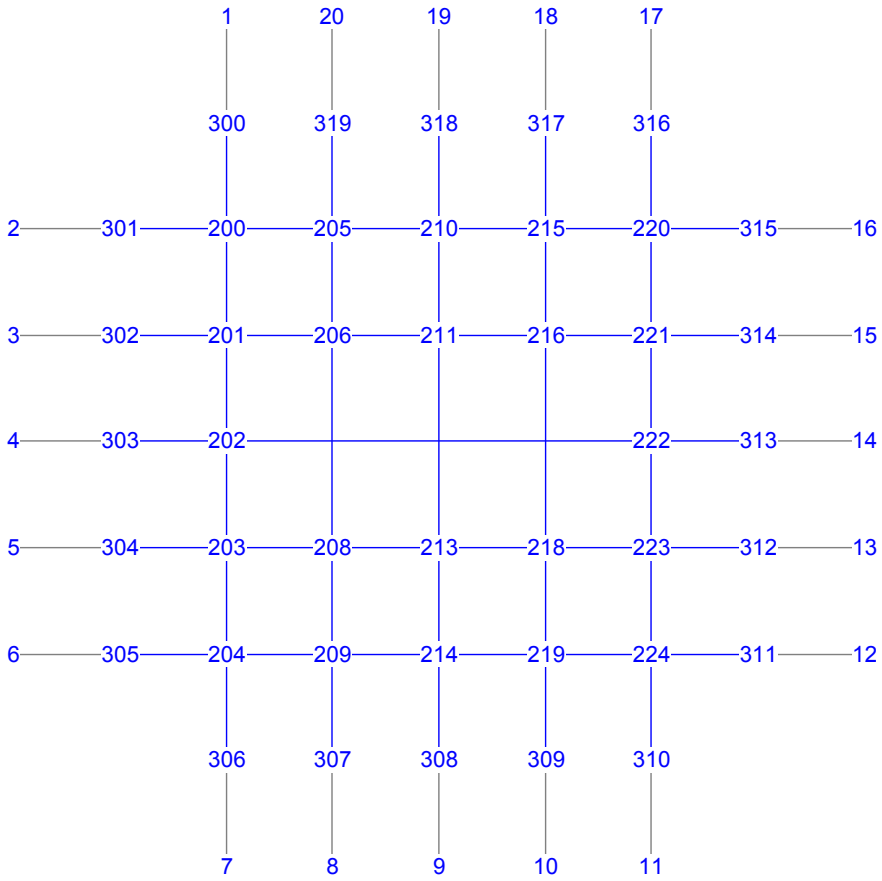

Figure 6.4 A hypothetical network.

Table 6.1 OD trip matrix for hypothesis test case.

Origins	Destinations					
	1	4	8	11	14	17
1	0	0	1,500	0	0	0
4	0	0	0	0	1,500	0
8	1,500	0	0	0	0	0
11	0	0	0	0	0	1,500
14	0	1,500	0	0	0	0
17	0	0	0	1,500	0	0

The assignment for the given OD-matrix is accomplished first using BPR equation as the travel time estimation method. The loaded network after assignment is

presented in Figure 6.5. It is found that the traffic flows from Node 4 to 14 and from Node 14 to Node 4 take straight routes through Node 202 and Node 222. The traffic flows from Node 17 to Node 11 and from Node 11 to Node 17 also take straight routes through Nodes 220, 221, 222, 223, and 224, crossing other traffic streams at Node 222. However, the trips from Node 1 to Node 8 are split into two branches, one through Nodes 300, 200, 201, 202, 203, 204, 209, and 307, crossing other traffic streams at Node 202, and another going to Node 8 without crossing any traffic streams. The traffic from Node 8 to Node 1 takes a similar path to that from Node 1 to Node 8, but in the opposite direction. The method using BPR equation does not recognize the benefit of less interrupted routes.

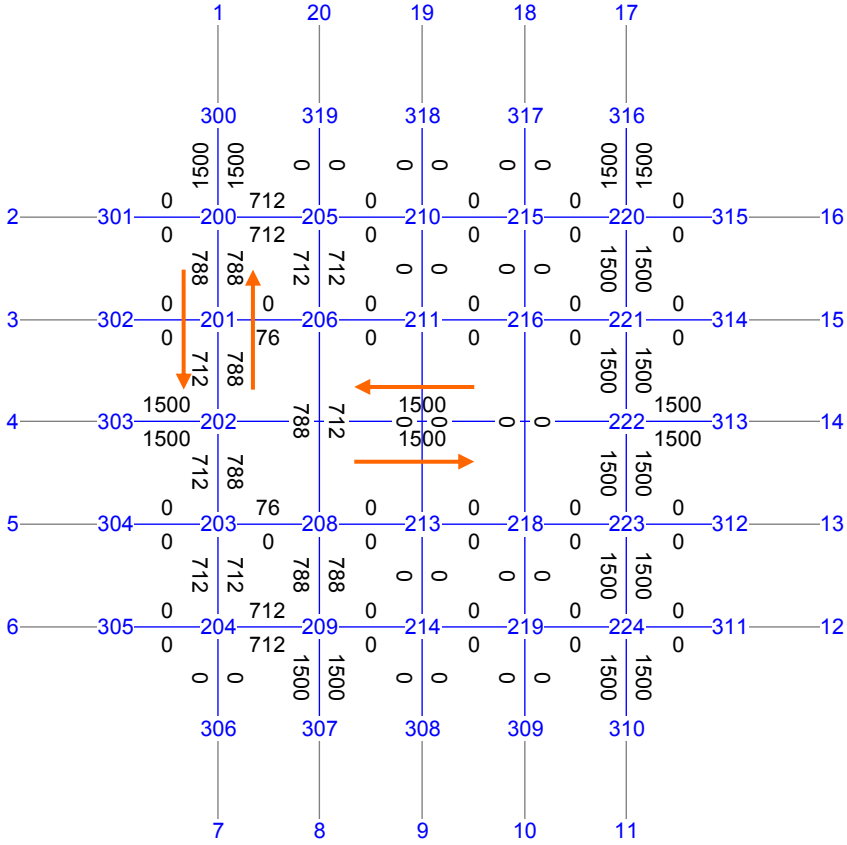

Figure 6.5 Assignment results based on the BPR equation.

The assignment with the newly developed travel time model is also conducted, and the results are presented in Figure 6.6. The developed model applied in this test case is the saturation-based travel time model, since link capacity cannot be estimated without signal settings for this hypothetical network.

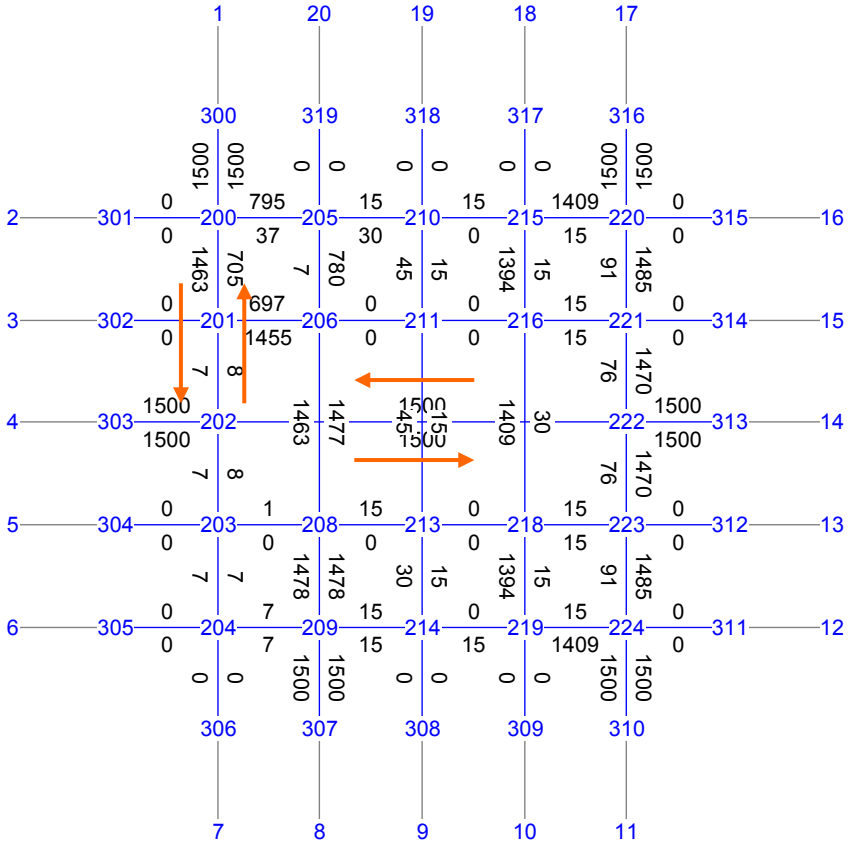

Figure 6.6 Assignment results based on the developed model.

The traffic between Node 4 and Node 14 takes the shortest straight path, as in the assignment result based on the BPR equation. The traffic from Node 1 to Node 8 mainly takes the less interrupted route through Nodes 200, 201, 206, 208, and 209, which avoids the crossing traffic streams at Node 202. The trips from Node 8 to Node 1 not only avoid the traffic crossing at Node 202, but also split into two branches at Node 206 to reduce congested cost. Most trips from Node 17 to Node 11 take a longer route to its destination

to avoid crossing other traffic streams. However, the traffic from Node 11 to Node 17 does not take the detour path as the traffic from Node 17 to Node 11 does. This may imply that the straight path outperforms the detour path, because the reduction of one crossing conflict at Node 222 may introduce the right-turn and left-turn merge conflicts at Node 215 and Node 219. It should be noted that merge conflict is actually not as serious as crossing conflict. However, they are not distinguished in the algorithm. Attention should be paid when the model is applied where there are heavy turning volumes.

A significant difference between the assignment results produced by the developed model and those produced by the BPR equation is that the traffic assigned using the new delay model avoids heavy traffic crossing at an intersection and takes less interrupted routes. With less interruption, the traffic assigned using the new delay model behaves like freeway flow, which would avoid suffering a large amount of delay at intersection. In this specific case the assignment process using the developed model is able to forecast the appropriate user selection, i.e. using the road with low cross-street volume. In comparison the assignment using BPR equation would be unable to predict this network loading. The assignment results show that the new travel time model bring improvements and that the developed model is better in dealing with delay estimation for an intersection.

The test also shows that the assigned traffic quickly converges to the equilibrium result. Figure 6.7 shows that the traffic volume on a link between Nodes 201 and 202 converges with iterations. After 20 iterations, the assigned traffic reaches convergence. Figure 6.8 shows that the traffic on the link between Nodes 206 and 208 converges to the final assigned volume after 20 iterations.

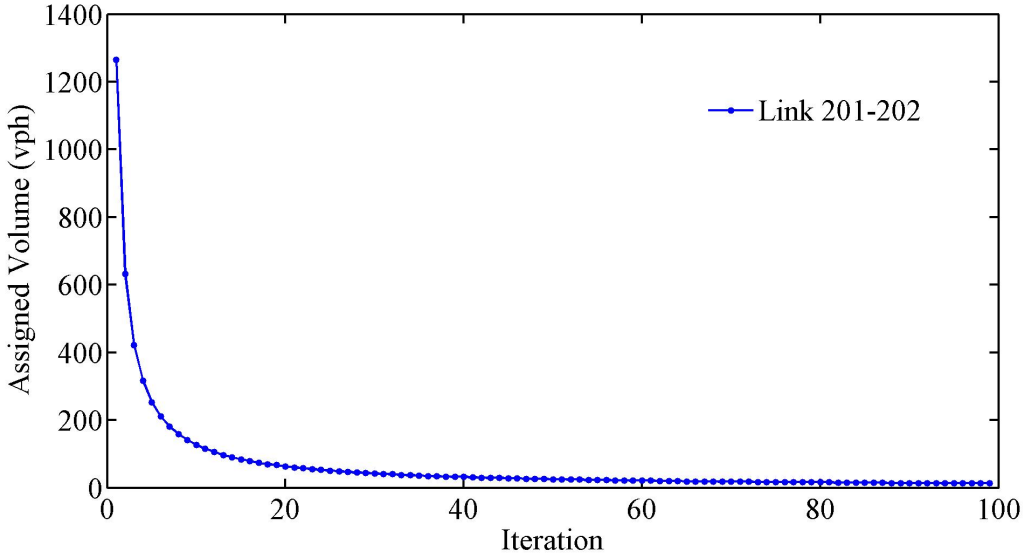

Figure 6.7 Loaded traffic on the link between Nodes 201 and 202.

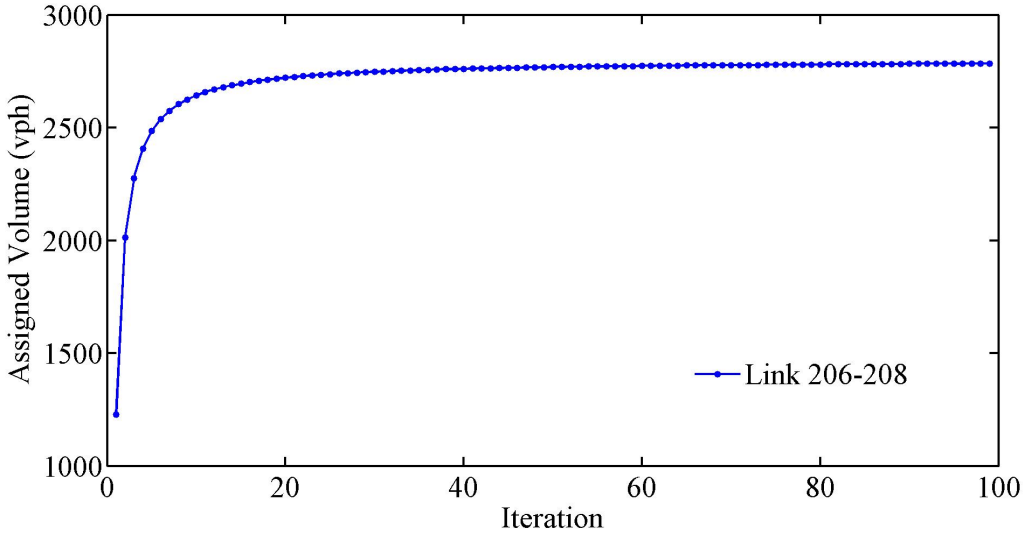

Figure 6.8 Loaded traffic on the link between Nodes 206 and 208.

The assignment test on the small hypothetical network with a simple OD matrix shows that the developed model outperforms the traditional BPR equation with a reasonable assignment result.

6.3 Model Application in the SERPM Model

The Southeast Regional Planning Model (SERPM) is a multimodal travel demand forecasting model currently adopted by the MPOs in Miami-Dade, Broward, and Palm Beach counties in Southeast Florida. Version 6.5 of SERPM (SERPM6.5) is the latest version. It uses Cube-Voyager (CV) and TRNBUILD as the new FSUTMS modeling platform for highway and transit demand analysis. The SERPM6.5 model has been implemented using Cube version 4.2.2 (Dec 12th, 2007) and has taken advantage of Cube's parallel-processing capability, or Cube Cluster, by running on a computer with a multi-core processor.

SERPM6.5 includes time-of-day and all-day (24-hour) models. After mode choice, the highway peak period trips are subdivided into AM-peak (6:30 AM - 9:30 AM), PM-peak (3:30 PM - 6:30 PM), and off-peak periods (other hours). The assignments for peak periods and off-peak periods are then combined into an all-day model. To evaluate the peak period model, period specific traffic counts have also been assembled and entered into the network database for the evaluation of assigned volumes. SERPM6.5 includes a large network of 47, 898 links and 31, 062 nodes. There are 24,890 signal-controlled links, among which 3,544 links have actual measured traffic counts. The network of SERPM is shown in Figure 6.9.

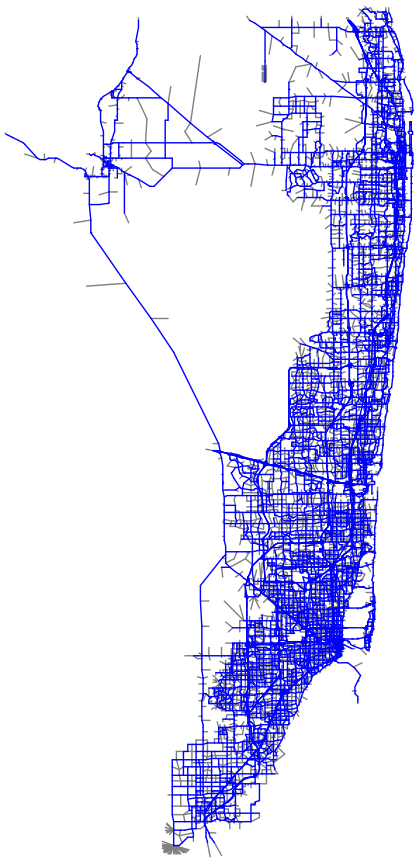

Figure 6.9 Network of Southeast Regional Planning Model.

In the current assignment process of SERPM6.5, the warm-up assignments are run for a fixed 15 equilibrium iterations and the final period assignments are allowed to run for a maximum of 50 iterations or until equilibrium process meets the convergence criterion, GAPS, which is 0.0005. The actual iteration number of the final assignment is 40 for the AM peak-period, 49 for the PM peak-period, and 31 for the off-peak period. Travel time is estimation by the current SERPM method, which is a modified BPR equation (see Equation 2-6 to 2-9).

The developed model replaces the current travel time estimation method in SERPM6.5 in the final assignment process for the AM peak-period model. A Cube application layer to implement the new model is presented in Figure 6.10.

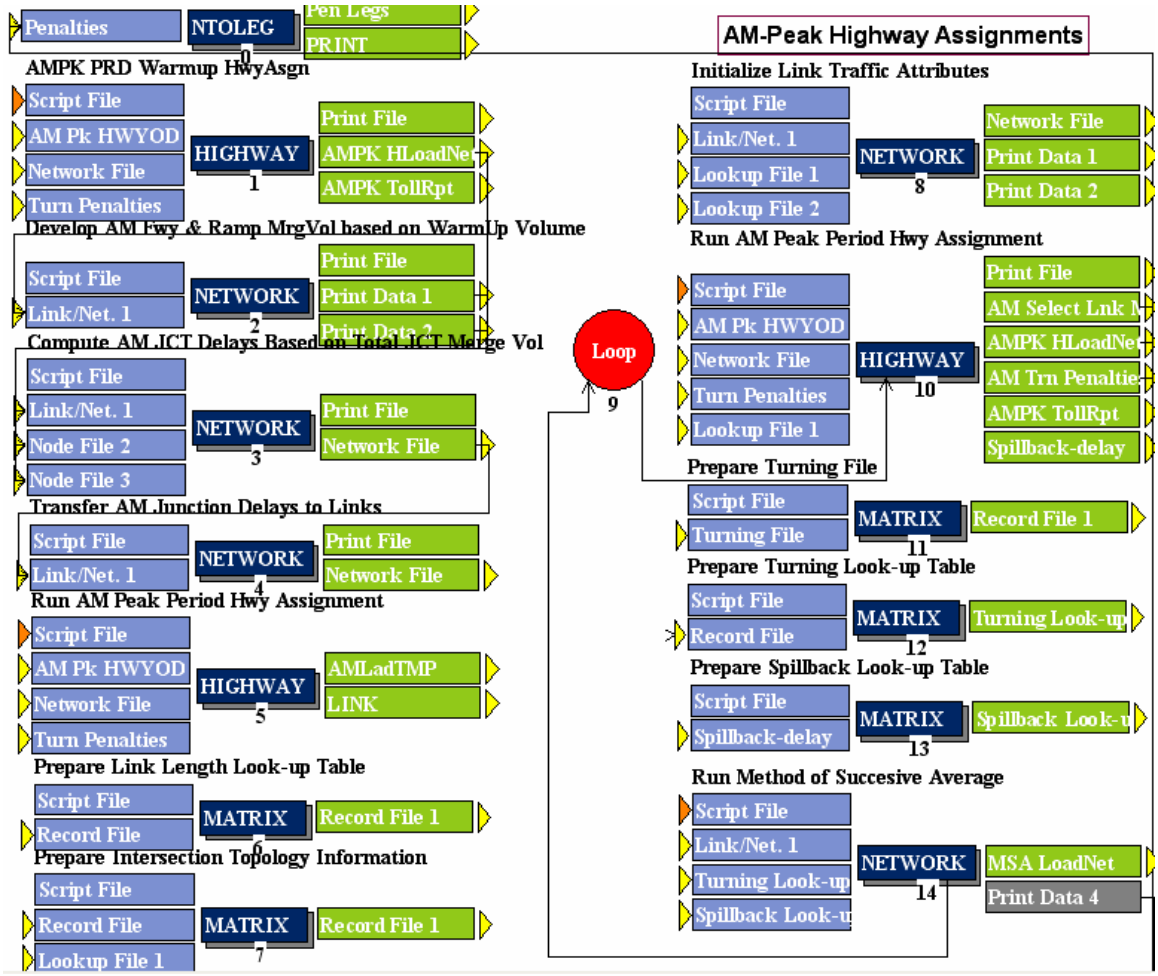

Figure 6.10 A script layer of assignment process with the developed model applied for the AM-peak period in SERPM.

In Figure 6.10, Step 1 to 5 are the warm-up processes in the SERPM6.5. The scripts are modified to create the turning volume file, link information file, and node information file. The core scripts to handle the technical issues in Chapter 6.1 are scripts 7, 8, 10, and 14, which are attached in Appendix C, D, F, and E, respectively.

The scripts 7 and 8 are to retrieve the required traffic information from other

approaches connected to the same intersection of a subject link. Figure 6.11 shows the turning volumes at junction Node 15848. This is a four-legged intersection with 12 movements heading to center node of 15848.

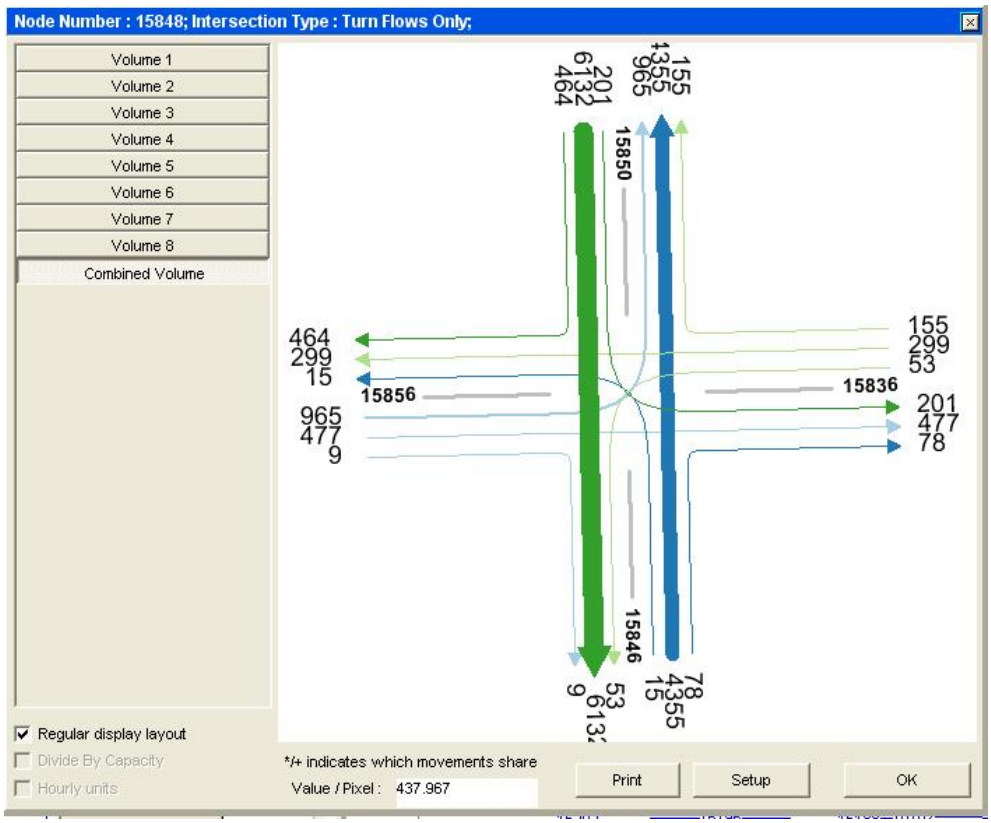

Figure 6.11 Turning volumes at junction node 15848.

After running the script 8, presented in Appendix D, the traffic volumes on the links connected to junction Node 15848 are coded for the subject link from Node 15846 to Node 15848, as illustrated in Figure 6.12, which is a screen capture of the network with the related link attributes displayed. For example, the volume on the approach from nodes 15836 to 15848 is 507 vph and is coded as VOLCROSS1. Similarly, the volume on the approach from nodes 15850 to 15848 is 6,797 vph and is coded as VOLSUB2. This script is used to initialize the link attributes for intersections. The same function for traffic volume update in the assignment loop is also included in Appendix E.

AY/BY	659419	661304
A	15846	15848
B	15848	15846
LS1_B	15848	0
LS1_C	15856	0
LEFTSUB1	15	0
THS1_A	15846	15848
THS1_B	15848	15846
THS1_C	15850	15844
THROUGHSUB1	4355	5786
RS1_A	15846	0
RS1_B	15848	0
RS1_C	15836	0
RIGHTSUB1	78	0
UP_NODE	15844	15850
VOLSUB1	4448	5786
LEFTCROSS1	53	0
THROUGHCROSS1	299	0
RIGHTCROSS1	155	0
VOLCROSS1	507	0
LEFTCROSS2	965	0
THROUGHCROSS2	477	0
RIGHTCROSS2	9	0
VOLCROSS2	1451	0
LEFTSUB2	201	0
THROUGHSUB2	6132	3975
RIGHTSUB2	464	0
VOLSUB2	6797	3975
LNCROSS1	2	0
LNCROSS2	2	0
LNSUB2	3	3
UP_LENGTH	0.41	0.33

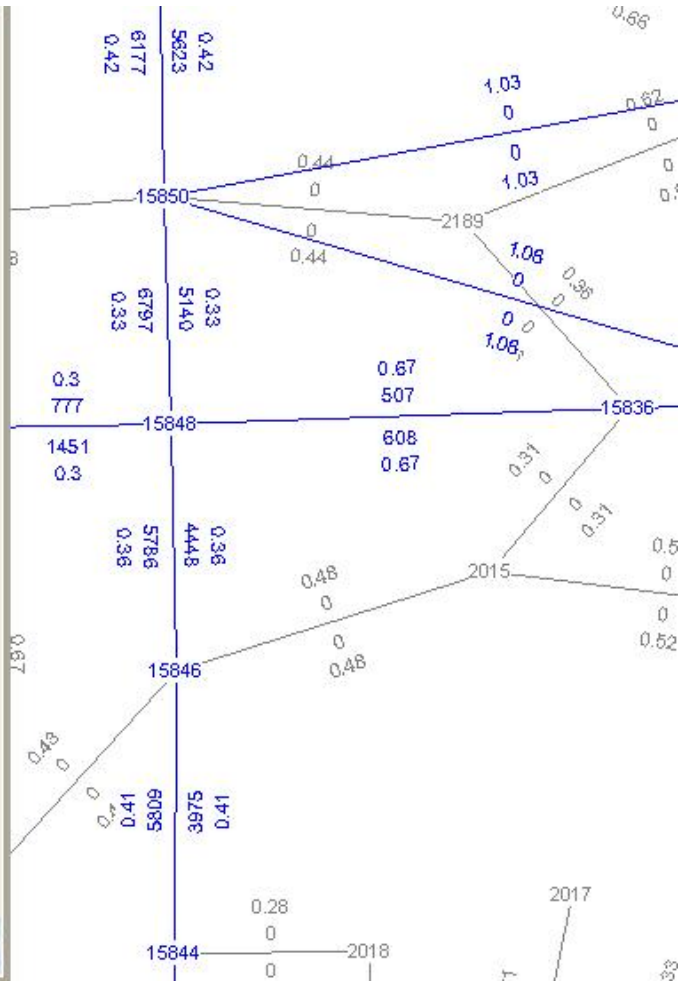

Figure 6.12 Turning volume definition for the link from Node 15846 to Node 15848.

In the script 10 in Figure 6.10, the equilibrium method is used for the assignment process. In SERPM6.5, the default number of iteration is 40. In this implementation, the iteration number is set to 5 since the loop control is now handled by the script 9 (which repeats the process 80 times). In the assignment process, an All-Or-Nothing assignment is usually performed during each iteration (based on the updated link travel cost, and it produces a new set of link volumes. In this test, the script 10 performs additional four iterations (for a total iterations of five) after a new set of link volumes are obtained. In each of the additional four iterations, the link cost for urban streets remain the same, but

that for freeway links are updated using the modified BPR equation. It is found that these additional iterations result in improved assignment results.

Scripts 10 through 14 are iterated 80 times to obtain the final equilibrium assignment solution. During each of the 80 iterations, two tasks are carried out by script 14. First, the added attributes for cross-street traffic need to be updated. Second, the traffic volume used to update travel cost is not the assigned traffic in the previous iteration, but a combination of the previously assigned volume and most recently assigned flow.

For a large network, such as that in SERPM, the efficiency of a script is important to reducing the computer running time. The topology information of a junction node, such as starting and ending nodes for all turns at a junction node, are recorded as the attributes of a link initially. And no updates are needed later. This saves the computer running time spent to look up all of the connecting nodes within each iteration. By sorting turning volumes, the computational efficiency of the traffic update process improves from an $O(n^2)$ algorithm to an $O(n)$ algorithm. In other words, the complexity of the algorithm is proportional to the size of the network. In comparison, a straightforward algorithm is a $n \times n$ nested loop, with the complexity of the quadratic of the network size.

The computer running time of the traffic update process by the improved algorithm for a network with 47, 898 links is about 30 minutes for each loop on a computer with two 3.4GHz Pentium CPUs. The computer running time of one iteration of equilibrium assignment is about seven minutes. The total computer running time is 80 loops × (30 minutes + 5 iterations × 7 minutes/iteration) = 5,200 minutes or

approximately 87 hours for AM-peak period assignment if the equilibrium assignment process is run five iterations each loop. The current assignment process in SERPM6.5 takes 40 iterations. With seven minutes per iteration, the total time required is approximately five hours. The required extra computer running time is acceptable, considering the existing computing power.

The capacity-based travel time model is applied, with the default values of capacity based on the function class of the roadways. The assigned volumes are compared to the traffic counts collected. The performance of the developed model is then compared to that of the current SERPM travel time estimation model. The results are presented in Table 6.2. There are 3,544 signal controlled links that have actual collected traffic counts for the AM period. The links are classified into three groups based on the traffic counts. Group 1 has the traffic up to 5,000 vph, Group 2 has traffic between 5,001 vph and 10,000 vph, and Group 3 has traffic between 10,001-20,000 vph. The majority of links fall into Group 1, for which the mean absolute percentage error (MAPE) by the developed model is 34.4%, while MAPE by the SERPM model is 39.2%. Overall MAPE by the developed model is 33.7%, which is also lower than the MAPE by SERPM6.5, 37.7%. Note that the performance is achieved without fine-tuning the developed model, which implies that further improvement is possible. The total traffic volume assigned to the signal controlled links by the developed model is 99% of the total collected traffic counts on the links. In comparison, the total assigned traffic volumes by SERPM6.5 model is 102% of the total collected traffic counts on the links.

Table 6.2 MAPE of assigned traffic volumes for the developed model and SERPM model.

Volume Group (vph)	Number of Count Station	MAPE	
		Model	SERPM
1- 5,000	3,287	34.4%	39.2%
5,001-10,000	255	24.0%	19.1%
10,001-20,000	2	34.4%	0.9%
Total	3,544	33.7%	37.7%

A correlation test is conducted between the assigned traffic volumes and actual traffic counts. The assigned traffic volumes based on the developed travel time model are highly correlated to the actual counts with a correlation statistic of 0.823. The correlation between assigned volumes by SERPM model and actual counts is also high, with a correlation statistic of 0.829, as presented in Table 6.3.

Table 6.3 Paired samples correlations for developed model and SERPM model.

		N	Correlation	Significance
Pair 1	Model & count	3,544	0.823	0.000
Pair 2	SERPM & count	3,544	0.829	0.000

The paired difference test is conducted for assigned traffic volume and actual counts. The results are presented in Table 6.4.

Table 6.4 Paired samples test for developed model and SERPM.

		Paired Differences				t	df	Significance (two-tailed)
		Mean (vph)	Std. Error Mean (vph)	95% Confidence Interval of the Difference				
				Lower (vph)	Upper (vph)			
Pair 1	Model - count	36	17	4	68	2.19	3,543	0.029
Pair 2	SERPM - count	111	17	78	144	6.62	3,543	0.000

The mean difference between the traffic volumes obtained based on the developed travel time model and actual counts is 36 vph. In comparison, the mean difference

between traffic volumes by the SERPM model and actual counts is 111 vph. The newly developed model shows better overall assignment results than the existing travel time model. However, at a significance level of 0.05, the hypothesis that volumes obtained by employing the developed travel time model and the BPR equation have no significant difference from the actual counts is rejected for both models.

6.4 Convergence of Assignment

This section investigates whether MSA will produce convergent solutions for the model with independent variables from multiple approaches of an intersection and how the number of iterations required for convergence changes with network size. Assignments are conducted for seven networks with 48, 168, 468, 736, 12,013, 19,181, and 47,898 links, respectively. The SERPM model network has 47,898 links and other smaller networks are extracted from the network of SERPM. The OD matrix tables for the smaller network are extracted from SERPM as well. As an example, Figure 6.13 presents the smallest network with 48 links.

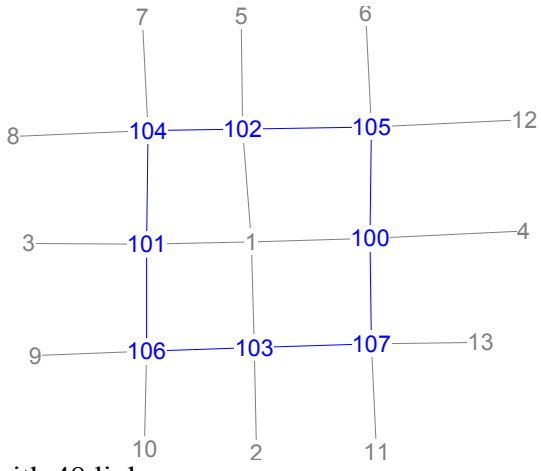

Figure 6.13 Network with 48 links.

Figures 6.14 through 6.17 present the total travel costs of each network at different iterations. The assignment process is conducted with a maximum of five

iterations, which is then iterated with a fixed number of 80 iterations (loops), as shown in Figure 6.1.

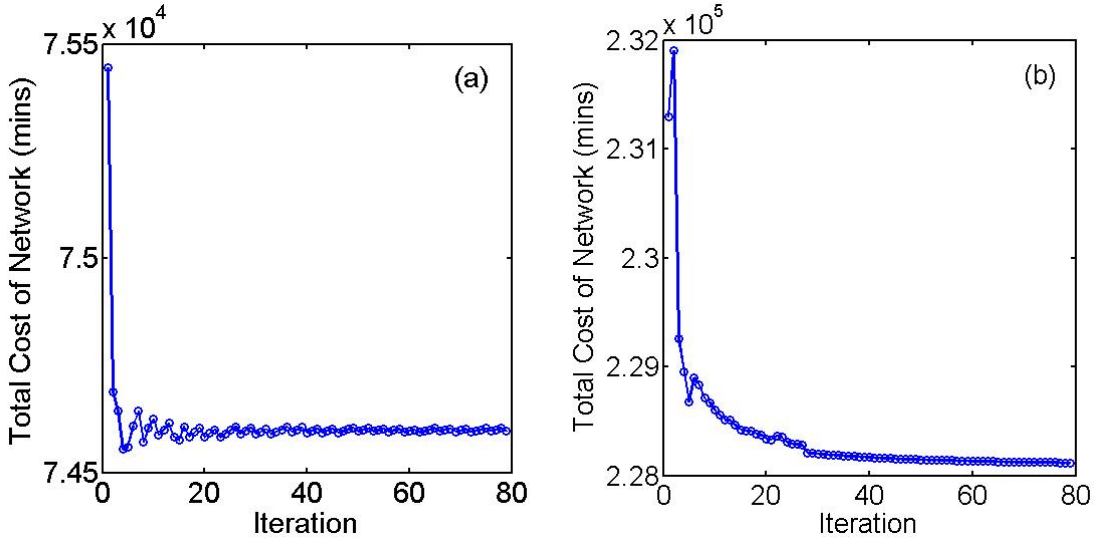

Figure 6.14 Network travel cost changes with assignment iterations for (a) network with 48 links; (b) network with 168 links.

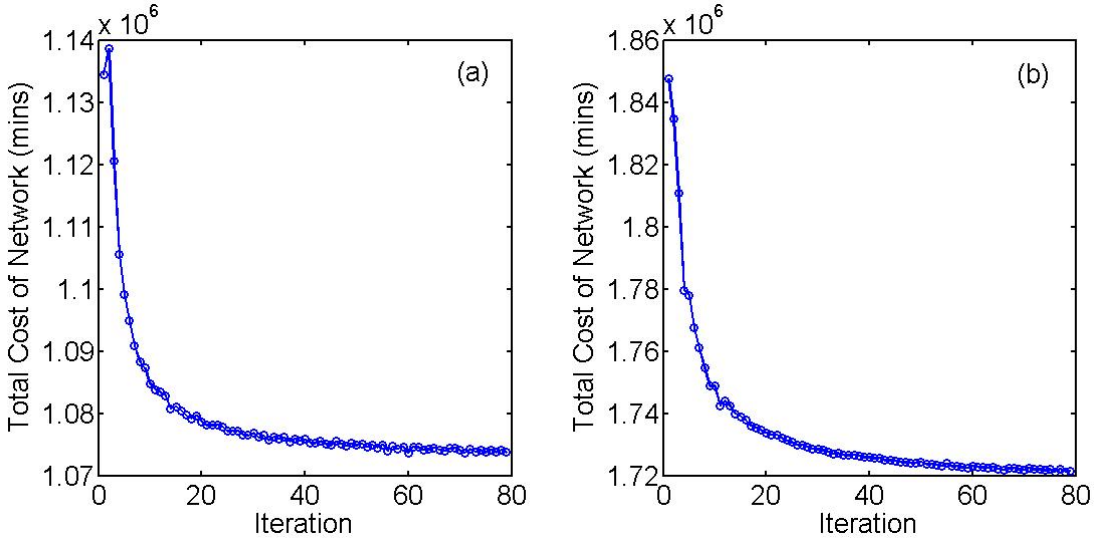

Figure 6.15 Network travel cost changes with assignment iterations for (a) network with 468 links; (b) network with 736 links.

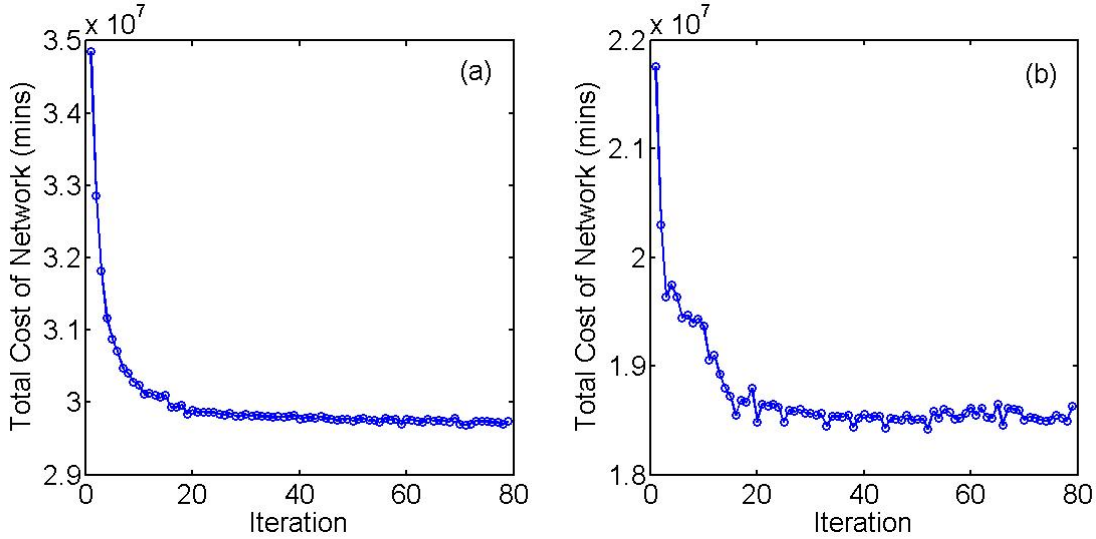

Figure 6.16 Network travel cost changes with assignment iterations for (a) network with 12,013 links; (b) network with 19,181 links.

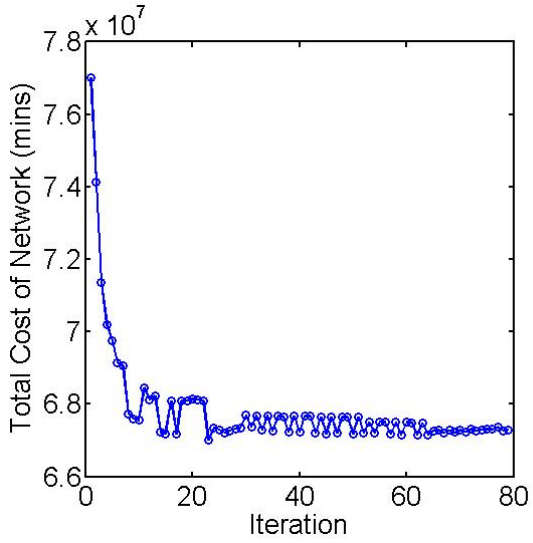

Figure 6.17 Network travel cost changes with assignment iterations for SERPM network with 47,898 links.

It is found that the total travel costs of networks reach convergence after 80 iterations. The SERPM network using the developed travel time estimation method reaches multiple equilibrium solutions (Horowitz 1997) after 30 iterations, and continue to converge toward a single point after 70 iterations. Due to fluctuations in travel cost, the

average of differences, computed using Equation (6-7) for 10 consecutive iterations is computed to check for convergence, as follows:

$$C_{i+10} = \frac{1}{10} \times \left| \frac{TC_{i+10} - TC_i}{TC_i} \right| \tag{6-7}$$

where

C_{i+10} = average percentage difference;

i = iteration number;

TC_i = network-wide travel cost for the i^{th} iteration (minutes); and

TC_{i+10} = network wide travel cost for the $(i + 10)^{th}$ iteration (minutes).

The required iteration for convergence is defined as $i + 10$ if C_{i+10} is less than 0.0005. Due to the existence of multiple solutions at convergence, convergence is considered to be achieved if occasionally C_n is larger than 0.0005, but no more than two successive C_n are larger than 0.0005. The required iterations for seven tested networks are presented in Table 6.5 and Figure 6.18. A quantitative analysis of the convergence criterion of 0.0005 shows that the required iterations linearly increase with the logarithm of the network size, i.e., number of links on the network.

Table 6.5 Required iterations for convergence by network size.

Number of Links	48	168	468	736	12,013	19,181	47,898
Required Iterations	12	13	22	24	34	29	33

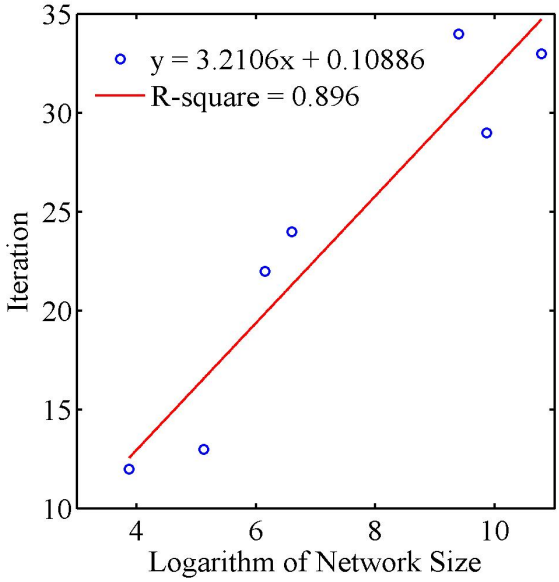

Figure 6.18 Required iterations for convergence increase with network size.

The convergence of assigned traffic volumes is checked for several links in the SERPM network. Figures 6.19 through 6.21 present the assigned traffic volumes of a typical link for 80 iterations. Through an examination of several representative links, it is found that the traffic volumes become stable after 80 iterations at the link level.

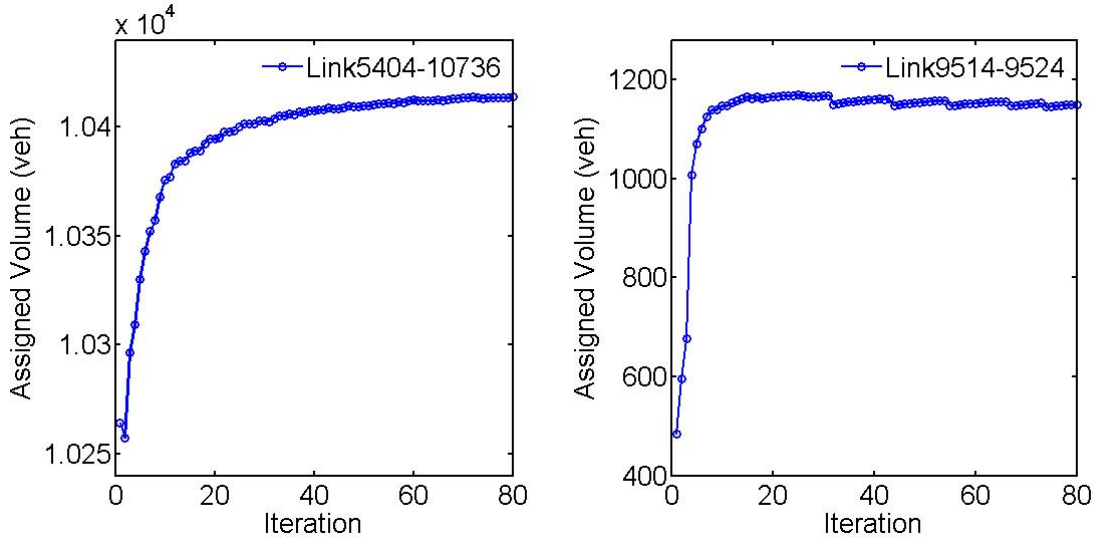

Figure 6.19 Assigned traffic volumes for links between Nodes 5404 and 10736, and 9514 and 9524.

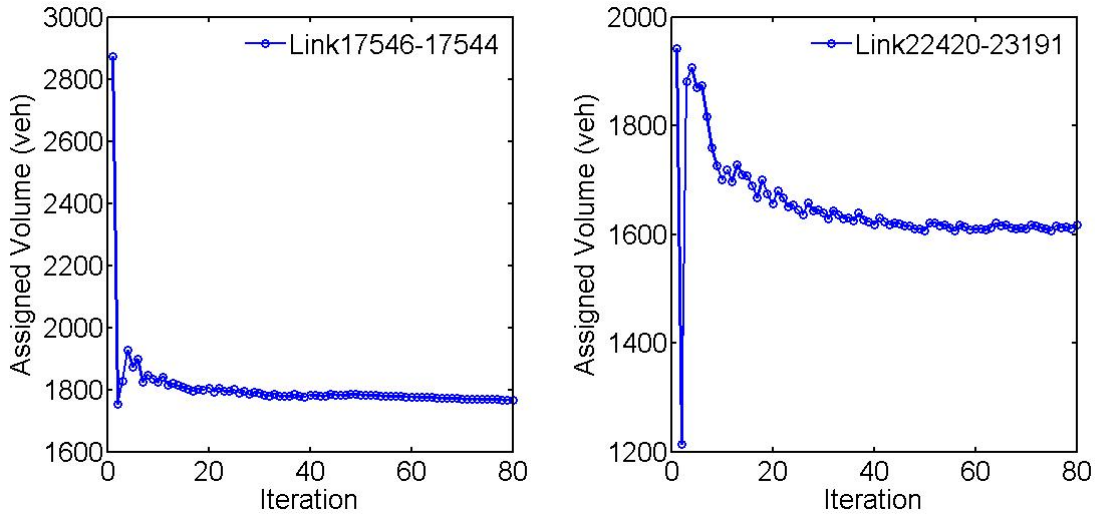

Figure 6.20 Assigned traffic volumes for links between Nodes 17546 and 17544, and 22420 and 23191.

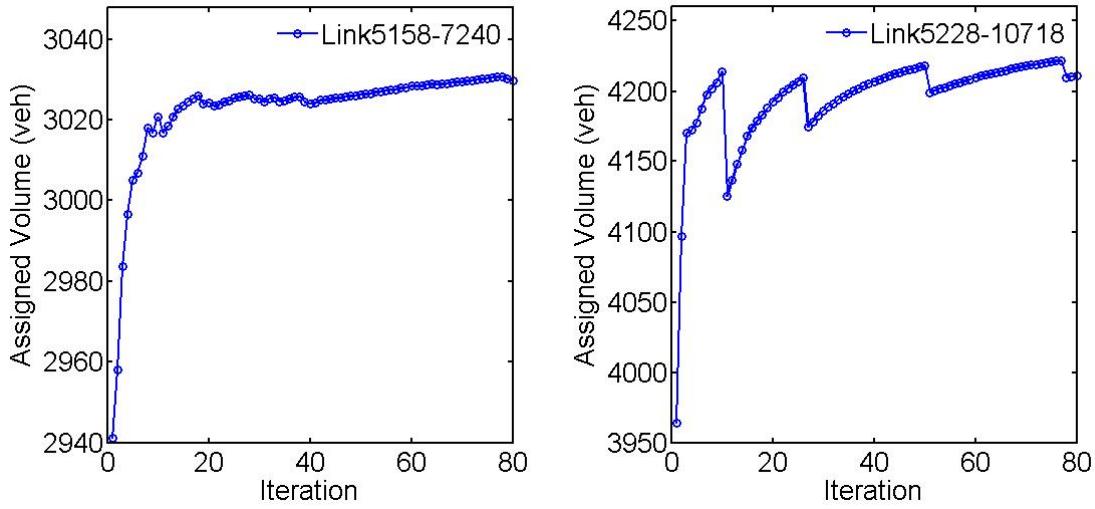

Figure 6.21 Assigned traffic volumes for links between Node 5158 and 7240, and 5228 and 10718.

In conclusion, the assignment with the newly developed model, coupled with MSA, reached convergence at network levels and close to convergence at the link level. At the link level, it is possible that small fluctuations exist (Ding *et al*. 2009).

6.5 Summary of Model Application in Assignment

The technical problems of applying the model in travel forecasting models, such as multi-approach volume coding and convergence issue, and solutions are described in this chapter. Qualitative tests of the model for a small hypothetical network shows that the developed model is better equipped to deal with delay estimation for an intersection by avoiding unnecessary crossings at an intersection. The quantitative test of the model for a large network shows that the developed model outperforms the current SERPM model in terms of MAPE of assigned traffic flows and actual counts for 3,544 links.

CHAPTER 7

CONCLUSIONS AND FUTURE WORK

7.1 Conclusions

This dissertation proposed a travel time estimation model for urban signal-controlled streets, which evinces the potential to improve the accuracy of traffic assignment in planning for a large scale network.

The model takes an analytical form, which is convenient to apply to a large scale network without significant efforts by modelers. The model separately considers the free-flow time and delay on a link. The parameters of the delay models are calibrated using microscopic simulation data. The signal timing plan in micro-simulation is optimized using TRANSYT-7F optimization software through simplification assumptions. The independent variables of a final travel time model are link length, free-flow speed, and traffic volumes from both competing movements. Compared to the traditional link-based or node-based models, such as the BPR, SERPM, HCM and Dowling method, this model has three main advantages.

First, the model considers the effect of signal timing plans, which is important to accurate estimation of intersection delays, for a variety of traffic volume combinations without actually requiring signal timing information as input. In contrast, existing travel time estimation methods require a signal timing plan to improve delay estimation, which limits their applications in modeling large-scale networks.

Second, the model describes the non-uniform spatial distribution of delay along a link. The model estimates the impacts of queues at different upstream locations of an intersection, allowing delays to be attributed to a subject link and upstream link. The

other models, such as the HCM, allocate all the intersection delay to the subject link without considering the possibility of queue extension to an upstream link. The HCM method overestimates the delay of a subject link when the link length is shorter than the queue, which is a common scenario under congested conditions or in a central business district (CBD). It also underestimates the delay for links when the queue at a downstream intersection extends to that link.

Third, the model shows promise of improving the accuracy of travel time prediction. The mean absolute percentage error (MAPE) of the model is 13% for a set of field data from Minnesota Department of Transportation (MDOT); this is close to the performance of uniform delay in the HCM 2000 method (11%). The HCM is currently the best analytical model in the existing literature, but it requires signal timing information as input for calculating delays. The developed model also outperformed the HCM 2000 method for a set of Miami-Dade County data that represent congested traffic conditions, with a MAPE of 29%, compared to 31% of the HCM 2000 method. The model performed better than the existing travel time estimation methods in planning, such as the BPR equation, conical equation, SERPM and Dowling model.

The advantages of the proposed models make them feasible for application to a large network without the burden of signal timing input, while improving the accuracy of travel time estimation. An assignment model integrating the developed travel time estimation method has been implemented in a South Florida planning model and has been shown to improve assignment results.

7.2 Limitations and Future Work

This dissertation has a number of limitations, which need to be addressed in future research.

First, the delay models are developed for isolated signal-controlled intersections. The coordination between multiple signals (signal progression) is not considered. The developed models need to incorporate progression factors when they are available. The developed delay models have been able to reproduce uniform delay of HCM, which makes them easy to be adjusted for future applications based on the concept of HCM.

Second, the simulated traffic volumes are up to 800 vphpl in this study. Further refinements of the models are being considered to address congested conditions.

Third, travel time models for unsignalized intersections need to be developed to properly consider delay for practical application. Applying a series of consistent models may improve the model accuracy.

Fourth, the application of the developed models needs to be further studied to explore all features that a model can provide. For instance, the implementation of the travel time model in SERPM only partially accounts for the spillback effect on immediate upstream link for the feeding through movement. It does not propagate the effect to upstream left-turn and right-turn feeding links.

Fifth and last, new modeling techniques continue to emerge, leading to next generation models, such as TRANSIMS. With newer techniques, travel time is generated for individual vehicles by microsimulation. However, signal timing plans for an intersection, especially for a future year, still need to be considered in an efficient way.

The idea of developing an analytical model in this dissertation may be extended to develop an analytical signal plan method for the next generation models.

REFERENCES

Aashtiani, H.Z., and Iravani, H. (1999). "Use of Intersection Delay Functions to Improve Reliability of Traffic Assignment Model." *The 14th Annual International EMME/2 Conference*, Chicago, Illinois.

Akçelik, R. (1981). "Traffic Signals: Capacity and Timing Analysis." *Australian Road Research Board*, Research Report ARR No. 123, Vermont South, Victoria, Australia.

Akçelik, R. (1991). "Travel Time Functions for Transport Planning Purposes: Davidson's Function, Its Time-Dependent Form and An Alternative Travel Time Function." *Australian Road Research,* Vol. 21, No.3, pp. 49–59. (Minor revisions: December 2000).

Allsop, R.E. (1974). "Some Possibilities of Using Traffic Control to Influence Trip Distribution and Route Choice." *Transportation and Traffic Theory – the Proceedings of the 6th International Symposium on Transportation and Traffic Theory*. Elsevier, Amsterdam, Netherlands, pp. 345–374.

Allsop, R.E. (1976). "Use of Traffic Signals to Influence the Amount and Routing of Traffic." *Proceedings of a Symposium: Getting the Most from our Transport Facilities—The Role of Traffic Engineering*, TRRL Supplementary Report SR231, Transport and Road Research Laboratory, Crowthorne, Berkshire, UK, pp. 154–166.

Allsop, R.E., and Charlesworth, J.A. (1977). "Traffic in a Signal-Controlled Road Network: An Example of Different Signal Timings Inducing Different Routings." *Traffic Engineering Control,* Vol. 18, No.5, pp. 262–264.

Bhat, C.R., Guo, J.Y., Srinivasan, S., and Sivakumar, A. (2004). "A Comprehensive Econometric Microsimulator for Daily Activity-Travel Patterns." *Transportation Research Record: Journal of the Transportation Research Board*, No. 1894, Transportation Research Board of the National Academies, Washington, D.C., pp. 57–66.

Bloomberg, L., and Dale, J. (2000). "A Comparison of the VISSIM and CORSIM Traffic Simulation Models." *Institute of Transportation Engineers Annual Meeting*. Nashville, TN.

Bonneson, J. A., Pratt, M.P., and Vandehey, M.A. (2008). *Predicting the Performance of Automobile Traffic on Urban Streets*." Technical report, NCHRP 3-79, prepared for National Cooperative Highway Research Program Transportation Research Board of The National Academies, Texas Transportation Institute Texas A&M University, College Station, Texas.

BPR (1964). *Traffic Assignment Manual*. U.S. Bureau of Public Roads, Washington, D.C.

Buckholz, J. W. and Courage, K.G. (2008). "Microscopic and Macroscopic Approaches to Delay Estimation with Oversaturated Conditions." *Transportation Research Record:*

Journal of the Transportation Research Board, No. 2071, Transportation Research Board of the National Academies, Washington, D.C., pp. 52–62.

Caliper (2002). *Travel Demand Modeling with TransCAD*. TransCAD Manual, Caliper Corp, Newton, MA.

Charlesworth, J.A. (1977). "The Calculation of Mutually Consistent Signal Settings and Traffic Assignment for a Signal Controlled Road Network." *Proceedings of the 7th International Symposium on Transportation and Traffic Theory*, Elsevier, Kyoto, Japan, pp. 545–569.

Chiou, S.-W. (1999). "Optimization of Area Traffic Control for Equilibrium Network Flows." *Transportation Science,* Vol. 33, No. 3, pp. 279–289.

Chiou, S.-W. (2003). "TRANSYT Derivatives for Area Traffic Control Optimization with Network Equilibrium Flows." *Transportation Research Part B*, Vol. 37, No. 3, pp. 263–290.

Cipriani, E., and Fusco, G. (2004). "Combined Signal Setting Design and Traffic Assignment Problem." *European Journal of Operational Research,* Vol. 155, No.3, pp. 569–583.

Cambridge Systematics Inc. (2008). *A Snapshot of Travel Modeling Activities*. Technical report, prepared for Federal Highway Administration, Cambridge, MA, available online at http://tmip.fhwa.dot.gov/resources/clearinghouse/docs/mpo/mpo_snapshot.pdf.

Corradino (2008). *Southeast Regional Planning Model 6.5: Model Data, Calibration, and Validation.* Technical report 1&2, Corradino Group, Miami, FL, online available at http://www.fsutmsonline.net/index.php?/model_pages/comments/2005_2030_serpm_65_created_on_10_10_2008/.

Davidson, K.B. (1966). "A Flow–Travel Time Relationship for Use in Transportation Planning." *Proceedings of the 3rd Australian Road Research Board Conference (Part 1)*, Australian Research Board, Melbourne, Victoria, Australia, pp. 183-194.

Davidson, K. B. (1978). "The Theoretical Basis of a Flow–Travel Time Relationship for Use in Transportation Planning." *Australian Road Research*, Vol. 8, No. 1, pp. 32-35; Discussion, pp. 45.

Davis, G. A., Xiong, H. (2007). *Access to Destination: Travel Time Estimation on Arterials*. Report MN/RC 2007-35, Published by Minnesota Department of Transportation, University of Minnesota, Minneapolis, MN.

Ding, Z. (2007). *A Static Traffic Assignment Model Combined with an Artificial Neural Network Delay Model*. Ph.D dissertation, Department of Civil and Environmental Engineering, Florida International University, Miami, FL, available online at http://digitalcommons.fiu.edu/cgi/viewcontent.cgi?article=1030&context=etd.

Ding, Z., Zhao, F. and Wu, Y. (2009). "An Artificial Neural Network Delay Model for Traffic Assignment Incorporating Intersection Delay Costs." *Transportation Research Record: Journal of the Transportation Research Board*, No. 2132, Transportation Research Board of the National Academies, Washington, D.C., pp. 25–32.

Demuth, H., Beale, M., and Hagan, M. (2006). *Neural Network Toolbox User's Guide*. The MathWorks, Inc., Natick, MA.

Dion, F., Rakha, H., and Kang, Y. (2004). "Comparison of Delay Estimates at Under-saturated and Oversaturated Pre-timed Signalized Intersections." *Transportation Research Part B,* Vol. 38, No. 2, pp. 99–122.

Dowling, R.G., Kittelson, W., Skabardonis, A., and Zegeer, J. (1997). *Techniques for Estimating Speed and Service Volumes for Planning Applications*. NCHRP Report 387, Transportation Research Board, National Research Council, Washington, D.C.

Dowling, R.G., Singh, R., and Cheng, W.W.K. (1998). "The Accuracy and Performance of Improved Speed-Flow Curves." *Transportation Research Record: Journal of the Transportation Research Board*, No. 1646, Transportation Research Board of the National Academies, Washington, D.C., pp. 9–17.

Dowling, R.G. and Skabardonis, A. (2006). "Urban Arterial Speed-Flow Equations for Travel Demand Models." Draft, Innovations in Travel Modeling, *Transportation Research Board Conference*, Austin, Texas.

Gartner, N. (1976). "Area Traffic Control and Network Equilibrium." *Proceedings of the International Symposium on Traffic Equilibrium Methods*, Universite de Montreal, Springer-Verlag, Berlin, Germany.

Gartner, N., and Al-Malik, M. (1996). "Combined Model for Signal Control and Route Choice in Urban Traffic Networks." *Transportation Research Record: Journal of the Transportation Research Board*, No. 1554, Transportation Research Board of the National Academies, Washington, D.C., pp. 27–35.

FDOT (1997). *Documentation and Procedural Updates to the Florida Standard Urban Transportation Model Structure*. Florida Department of Transportation, Tallahassee, FL.

FHWA and FTA (2007). *The Transportation Planning Process: Key Issues*. Technical report, FHWA-HEP-07-039, Washington, D.C., available online at http://www.planning.dot.gov/documents/briefingbook/bbook_07.pdf.

Frank, M., and Wolfe, P. (1956). "An Algorithm for Quadratic Programming." *Naval Research Logistics Quarterly,* Vol. 3, No. 1-2, pp. 95—110.

HCM (1994). *Highway Capacity Manual*. Transportation Research Board, National Research Council, Washington, D.C.

HCM (2000). *Highway Capacity Manual*. Transportation Research Board, National Research Council, Washington, D.C.

Heydecker, B.G. and Khoo, T.K. (1990). "The Equilibrium Network Design Problem." *Proceedings of AIRO'90 Conference on Models and Methods for Decision Support*, Sorrento, Florida, pp. 587–602.

Hornik, K., Stinchcombe, M., and White, H. (1989). "Multilayer Feedforward Networks Are Universal Approximators." *Neural Networks*, Vol. 2, No. 5, pp.359-366.

Horowitz, A. J. (1991). *Delay/Volume Relations for Travel Forecasting, Based on the 1985 Highway Capacity Manual*. Technical Report, FHWA-PD-92-015, FHWA, U.S. Department of Transportation, Milwaukee, WI, available online at https://pantherfile.uwm.edu/horowitz/www/SpeedVolume1985HCMReport.pdf.

Horowitz, A. J. (1992). "Implementing Travel Forecasting with Traffic Operational Strategies." *Transportation Research Record: Journal of the Transportation Research Board*, No. 1365, Transportation Research Board of the National Academies, Washington, D.C., pp. 54–61.

Horowitz, A.J. (1997). "Intersection Delay in Region-wide Traffic Assignment: Implications of the 1994 Update of the Highway Capacity Manual." *Transportation Research Record: Journal of the Transportation Research Board*, No. 1572, Transportation Research Board of the National Academies, Washington, D.C., pp. 1–8.

Hu, T.Y., Tong, C.C., Liao, T.Y., and Chen, L.W. (2008). "Simulation-Based Dynamic Traffic Assignment Model for Mixed Traffic Flows." *The 87th Transportation Research Board Annual Meeting*. CD-ROM 08-2096, Transportation Research Board of the National Academies, Washington, D.C.

Jeannotte, K., Chandra, A., Alexiadis, V., and Skabardonis, A. (2004a). *Traffic Analysis Toolbox Volume I: Traffic Analysis Tools Primer*. Technical report, FHWA-HRT-04-038;

Jeannotte, K., Chandra, A., Alexiadis, V., and Skabardonis, A. (2004b). *Traffic Analysis Toolbox Volume II: Decision Support Methodology for Selecting Traffic Analysis Tools*. Technical report, FHWA-HRT-04-039, Cambridge Systematics, Inc., Oakland, CA.

Jones, S.L., Sullivan, A.J., Cheekoti, N., Anderson, M.D., and Malave, D. (2004). *Traffic Simulation Software Comparison Study*, UTCA Report 02217, Birmingham, AL.

Kolday, T.G., Lewisz, R.M., and Torczonx, V. (2003). "Optimization by Direct Search: New Perspectives on Some Classical and Modern Methods." *Society for Industrial and Applied Mathematics*, Vol. 45, No. 3, pp. 385-482.

Lee, C., and Machemehl, R.B. (1999). "Local and Iterative Searches for the Combined Signal Control and Assignment Problem: Implementation and Numerical Examples." *Transportation Research Record: Journal of the Transportation Research Board*, No.

1683, Transportation Research Board of the National Academies, Washington, D.C., pp. 102–109.

Lee, C., and Machemehl, R.B. (2005). *Combined Traffic Signal Control and Traffic Assignment: Algorithms, Implementation and Numerical Results*. Technical report, DTRS95-G-0006, Southwest Region University Transportation Center, Texas A&M University System, College Station, TX.

Nagel, K., and Schreckenberg, M. (1992). "A Cellular Automaton Model for Freeway Traffic.". *J. Phys. I. France,* Vol. 2, No. 12, pp. 2221-2229.

Ortuzar, J.D., and Willumsen, L.G. (2004). *Modeling Transport*. 3rd Edition, John Wiley & Sons Ltd, Southern Gate, Chichester, England.

RDC, Inc. (1995). *Activity-based Modeling System for Travel Demand Forecasting*. Submitted to Metropolitan Washington Council of Governments, San Francisco, CA, available online at http://tmip.fhwa.dot.gov/resources/clearinghouse/docs/amos/amos.pdf.

SERPM (2008). *Southeast Regional Planning Model 6.5: Model Data, Calibration, and Validation.* Technical Report 1&2, Corradino Group, online available at http://www.fsutmsonline.net/index.php?/model_pages/comments/2005_2030_serpm_65_created_on_10_10_2008/.

Sheffi, Y. (1985). *Urban Transportation Networks*. Prentice-Hall, Englewood Cliffs, NJ.

SHRP2 (2010). Online at http://144.171.11.40/cmsfeed/comm_detail.asp?id=3662.

Skabardonis, A., and Dowling, R.G. (1997). "Improved Speed-Flow Relationships for Planning Applications." *Transportation Research Record: Journal of the Transportation Research Board*, No. 1572, Transportation Research Board of the National Academies, Washington, D.C., pp. 18–23.

Smith, M.J., Vuren, T. V. (1993). "Traffic Equilibrium with Responsive Traffic Control." *Transportation Science,* Vol. 17, No. 2, pp. 118–132.

Spiess, H. (1990). "Conical Volume-Delay Functions." *Transportation Science*, Vol. 24, No. 2, pp. 153-158.

TRB (2007). *Metropolitan Travel Forecasting: Current Practice and Future Direction*. Special Report 288, Transportation Research Board, Washington, D.C., available online at http://www.nap.edu/catalog/11981.html.

VHB (2006). *Results of FY2006 Travel Forecasting Research, Task 5: Review of Current Use of Activity-Based Modeling.* Metropolitan Washington Council of Governments, National Capital Region Transportation Planning Board, Washington, D.C.

Webster, F.V. (1958). “Traffic Signal Settings.” *Road Research Technical Paper*, No. 39, HMSO, London.

Weiner, E. (1997). *Urban Transportation Planning in the United states: an Historical Overview*. Technical report, DOT-T-93-02, Washington, D.C., available online at http://ntl.bts.gov/DOCS/UTP.html.

Wong, S.C. (1995). “Derivatives of the Performance Index for the Traffic Model from TRANSYT.” *Transportation Research B*, Vol. 29, No. 5, pp. 303–327.

Wong, S.C., Yang, C., and Lo, H.K (2001). “A Path-Based Traffic Assignment Algorithm Based on the Transyt Traffic Model.” *Transportation Research Part B*, Vol. 35, No.2, pp. 163-181.

Yang, H., and Yagar, S. (1995). “Traffic Assignment and Signal Control in Saturated Road Networks.” *Transportation Research A*, Vol. 29, No. 2, 125–139.

Yang, H. (1995). “Heuristic Algorithms for the Bilevel Origin–Destination Matrix Estimation Problem.” *Transportation Research Part B*, Vol. 29, No.4, 231–242.

Zhao, F., and Ding, Z. (2006). *Improving Highway Travel Time Estimation in FSUTMS by Considering Intersection Delays*. Technical report, BD015-15, prepared for Florida Department of Transportation, Lehman Center for Transportation Research, Florida International University, Miami, FL.

APPENDICES

APPENDIX A

Table A.1 Optimized signal plans for an intersection with subject volume of 200 vphpl and cross-street volume of 200 vphpl.

Method		*EW L* (s)	*EW Th* (s)	*NS L* (s)	*NS Th* (s)	Cycle (s)	Delay (min/veh)
TRANSYT	Control Delay	11	30	10	29	80	0.27
	Throughput	13	18	14	75	120	0.47
	Throughput/delay	11	30	10	29	80	0.27
	Throughput & Delay	13	18	14	75	120	0.47
	Queue Ratio	11	30	10	29	80	0.27
CORSIM	Control Delay	10	24	14	37	85	0.31
	Total Delay	10	24	14	37	85	0.31
	Stop Delay	10	24	14	37	85	0.31
	Queue Delay	10	24	14	37	85	0.31
	Throughput	65	16	21	18	120	0.62
	Percentage stop	11	94	11	9	125	1.61
	Average Speed	10	24	14	37	85	0.31

Table A.2 Optimized signal plans for an intersection with subject volume of 200 vphpl and cross-street volume of 750 vphpl.

Method		*EW L* (s)	*EW Th* (s)	*NS L* (s)	*NS Th* (s)	Cycle (s)	Delay (min/veh)
TRANSYT	Control Delay	11	16	13	50	90	0.31
	Throughput	10	15	15	80	120	0.39
	Throughput/delay	10	18	17	75	120	0.40
	Throughput & Delay	10	18	14	78	120	0.39
	Queue Ratio	11	16	13	50	90	0.31
CORSIM	Control Delay	12	18	14	76	120	0.39
	Total Delay	10	15	12	53	90	0.31
	Stop Delay	11	16	15	78	120	0.38
	Queue Delay	11	15	13	51	90	0.32
	Throughput	22	17	30	51	120	0.56
	Percentage stop	10	26	11	73	120	0.50
	Average Speed	11	13	13	53	90	0.31

Table A.3 Optimized signal plans for an intersection with subject volume of 200 vphpl and cross-street volume of 1,400 vphpl.

Method		*EW L* (s)	*EW Th* (s)	*NS L* (s)	*NS Th* (s)	Cycle (s)	Delay (min/veh)
TRANSYT	Control Delay	10	16	15	84	125	1.33
	Throughput	13	16	35	56	120	2.57
	Throughput/delay	10	16	15	84	125	1.33
	Throughput & Delay	13	16	35	56	120	2.57
	Queue Ratio	10	16	15	84	125	1.33
CORSIM	Control Delay	10	15	13	52	90	1.28
	Total Delay	10	15	13	52	90	1.28
	Stop Delay	11	17	14	68	110	0.92
	Queue Delay	10	15	13	52	90	1.28
	Throughput	10	18	24	68	120	1.42
	Percentage stop	28	77	11	9	125	7.91
	Average Speed	28	76	12	9	125	7.91

Table A.4 Optimized signal plans for an intersection with subject volume of 750 vphpl and cross-street volume of 200 vphpl.

Method		*EW L* (s)	*EW Th* (s)	*NS L* (s)	*NS Th* (s)	Cycle (s)	Delay (min/veh)
TRANSYT	Control Delay	15	48	11	16	90	0.36
	Throughput	18	77	12	18	125	0.39
	Throughput/delay	15	48	11	16	90	0.36
	Throughput & Delay	18	77	12	18	125	0.39
	Queue Ratio	15	48	11	16	90	0.36
CORSIM	Control Delay	12	52	10	11	85	0.31
	Total Delay	12	52	10	11	85	0.31
	Stop Delay	12	52	10	11	85	0.31
	Queue Delay	12	52	10	11	85	0.31
	Throughput	25	38	11	11	85	0.39
	Percentage stop	28	84	9	9	130	0.89
	Average Speed	12	52	10	11	85	0.31

Table A.5 Optimized signal plans for an intersection with subject volume of 750 vphpl and cross-street volume of 750 vphpl.

Method		*EW L* (s)	*EW Th* (s)	*NS L* (s)	*NS Th* (s)	Cycle (s)	Delay (min/veh)
TRANSYT	Control Delay	10	47	10	53	120	0.82
	Throughput	11	28	10	31	80	0.82
	Throughput/delay	10	47	13	50	120	0.71
	Throughput & Delay	11	30	10	29	80	0.75
	Queue Ratio	10	47	13	50	120	0.71
CORSIM	Control Delay	12	36	12	35	95	0.59
	Total Delay	12	36	12	35	95	0.59
	Stop Delay	12	36	12	35	95	0.59
	Queue Delay	12	36	12	35	95	0.59
	Throughput	12	43	13	42	110	0.69
	Percentage stop	28	84	9	9	130	3.48
	Average Speed	28	84	9	9	130	3.48

Table A.6 Optimized signal plans for an intersection with subject volume of 750 vphpl and cross-street volume of 1,400 vphpl.

Method		*EW L* (s)	*EW Th* (s)	*NS L* (s)	*NS Th* (s)	Cycle (s)	Delay (min/veh)
TRANSYT	Control Delay	10	29	13	68	120	2.40
	Throughput	13	49	30	28	120	3.95
	Throughput/delay	12	28	14	66	120	2.38
	Throughput & Delay	13	49	30	28	120	3.95
	Queue Ratio	12	34	10	34	90	2.72
CORSIM	Control Delay	28	84	9	9	130	5.59
	Total Delay	28	84	9	9	130	5.59
	Stop Delay	20	88	13	9	130	5.61
	Queue Delay	28	84	9	9	130	5.59
	Throughput	12	38	15	55	120	2.39
	Percentage stop	28	84	9	9	130	5.59
	Average Speed	28	84	9	9	130	5.59

Table A.7 Optimized signal plans for an intersection with subject volume of 1,400 vphpl and cross-street volume of 200 vphpl.

Method		*EW L* (s)	*EW Th* (s)	*NS L* (s)	*NS Th* (s)	Cycle (s)	Delay (min/veh)
TRANSYT	Control Delay	18	77	10	15	120	0.63
	Throughput	20	77	11	17	125	0.74
	Throughput/delay	18	77	10	15	120	0.63
	Throughput & Delay	20	77	11	17	125	0.74
	Queue Ratio	18	77	10	15	120	0.63
CORSIM	Control Delay	19	79	10	12	120	0.56
	Total Delay	19	79	10	12	120	0.56
	Stop Delay	12	61	10	12	95	0.92
	Queue Delay	19	77	10	14	120	0.60
	Throughput	19	76	10	15	120	0.53
	Percentage stop	14	18	16	72	120	6.51
	Average Speed	20	82	9	9	120	0.73

Table A.8 Optimized signal plans for an intersection with subject volume of 1,400 vphpl and cross-street volume of 750 vphpl.

Method		*EW L* (s)	*EW Th* (s)	*NS L* (s)	*NS Th* (s)	Cycle (s)	Delay (min/veh)
TRANSYT	Control Delay	10	51	13	46	120	2.36
	Throughput	22	26	27	45	120	4.13
	Throughput/delay	10	51	12	47	120	2.47
	Throughput & Delay	22	26	27	45	120	4.13
	Queue Ratio	10	51	13	46	120	2.36
CORSIM	Control Delay	22	83	11	9	125	2.61
	Total Delay	22	83	11	9	125	2.61
	Stop Delay	23	83	10	9	125	2.62
	Queue Delay	22	83	11	9	125	2.61
	Throughput	12	44	12	42	110	2.37
	Percentage stop	11	11	9	94	125	5.47
	Average Speed	14	16	17	73	120	4.94

Table A.9 Optimized signal plans for an intersection with subject volume of 1,400 vphpl and cross-street volume of 1,400 vphpl.

Method		*EW L* (s)	*EW Th* (s)	*NS L* (s)	*NS Th* (s)	Cycle (s)	Delay (min/veh)
TRANSYT	Control Delay	10	50	12	48	120	3.62
	Throughput	22	17	30	51	120	5.35
	Throughput/delay	10	50	12	48	120	3.62
	Throughput & Delay	22	17	30	51	120	5.35
	Queue Ratio	10	50	12	48	120	3.62
CORSIM	Control Delay	27	89	10	9	135	4.31
	Total Delay	27	89	10	9	135	4.31
	Stop Delay	27	89	10	9	135	4.31
	Queue Delay	27	89	10	9	135	4.31
	Throughput	12	49	12	47	120	3.54
	Percentage stop	10	90	11	9	120	4.72
	Average Speed	22	79	10	9	120	4.24

APPENDIX B

Table B.1 Testing random seeds for the scenario that both traffic volumes from subject direction and cross-street are 200 vphpl.

Seed	*EW L* (s)	*EW Th* (s)	*NS L* (s)	*NS Th* (s)	Cycle (s)	Control (s)	PI
1337	12	19	9	15	55	19.6	143.6
2973	12	14	19	15	60	25.0	112.8
5619	9	25	7	19	60	18.9	149.0
9431	7	20	11	17	55	18.6	151.3
7781	7	14	9	20	50	17.5	160.7
4573	7	15	7	11	40	15.9	177.2

Table B.2 Testing random seeds for the scenario that traffic volumes from subject direction and cross-street are 200 vphpl and 500 vphpl.

Seed	*EW L* (s)	*EW Th* (s)	*NS L* (s)	*NS Th* (s)	Cycle (s)	Control (s)	PI
1337	30	26	32	32	120	73.5	21.88
2973	30	30	30	30	120	132.0	12.06
5619	9	16	9	21	55	22.4	71.93
9431	7	13	12	23	55	20.7	77.99
7781	11	24	22	33	90	31.1	51.76
4573	6	10	10	19	45	19.7	81.59

Table B.3 Testing random seeds for the scenario that traffic volumes from subject direction and cross-street are 200 vphpl and 700 vphpl.

Seed	*EW L* (s)	*EW Th* (s)	*NS L* (s)	*NS Th* (s)	Cycle (s)	Control (s)	PI
1337	30	26	32	32	120	561.0	2.12
2973	7	34	19	45	105	36.6	34.41
5619	12	30	15	48	105	33.9	37.12
9431	7	15	16	32	70	26.1	48.13
7781	8	14	14	59	95	29.1	43.07
4573	7	13	11	34	65	22.5	55.74

Table B.4 Testing random seeds for the scenario that traffic volumes from subject direction and cross-street are 500 vphpl and 200 vphpl.

Seed	*EW L* (s)	*EW Th* (s)	*NS L* (s)	*NS Th* (s)	Cycle (s)	Control (s)	PI
1337	13	21	10	16	60	25.7	62.51
2973	30	33	29	28	120	61.1	26.31
5619	12	34	9	20	75	23.2	69.2
9431	35	30	10	15	90	38.2	42.05
7781	10	31	7	12	60	20.3	79.22
4573	8	19	7	11	45	19.1	84.0

Table B.5 Testing random seeds for the scenario that traffic volumes from subject direction and cross-street are 500 vphpl and 500 vphpl.

Seed	*EW L* (s)	*EW Th* (s)	*NS L* (s)	*NS Th* (s)	Cycle (s)	Control (s)	PI
1337	13	21	10	16	60	153.0	7.19
2973	30	30	30	30	120	167.0	6.61
5619	9	25	9	22	65	29.2	38.60
9431	8	44	23	55	130	58.2	18.50
7781	6	22	21	21	70	62.7	17.01
4573	10	20	7	18	55	37.1	30.38

Table B.6 Testing random seeds for the scenario that traffic volumes from subject direction and cross-street are 500 vphpl and 700 vphpl.

Seed	*EW L* (s)	*EW Th* (s)	*NS L* (s)	*NS Th* (s)	Cycle (s)	Control (s)	PI
1337	30	30	30	30	120	591.0	1.48
2973	30	30	30	30	120	591.0	1.48
5619	10	25	11	34	80	38.2	24.55
9431	7	22	7	24	60	62.0	14.47
7781	16	29	8	42	95	52.4	17.12
4573	22	25	8	60	115	242	3.54

Table B.7 Testing random seeds for the scenario that traffic volumes from subject direction and cross-street are 700 vphpl and 200 vphpl.

Seed	*EW L* (s)	*EW Th* (s)	*NS L* (s)	*NS Th* (s)	Cycle (s)	Control (s)	PI
1337	15	57	17	16	105	32.7	38.28
2973	14	41	9	16	80	25.2	49.73
5619	12	40	8	15	75	23.9	52.43
9431	59	51	11	19	140	68.6	18.07
7781	10	31	7	12	60	22.5	55.64
4573	8	48	8	26	90	44.9	26.92

Table B.8 Testing random seeds for the scenario that traffic volumes from subject direction and cross-street are 700 vphpl and 500 vphpl.

Seed	*EW L* (s)	*EW Th* (s)	*NS L* (s)	*NS Th* (s)	Cycle (s)	Control (s)	PI
1337	13	21	10	16	60	262.0	3.42
2973	30	33	29	28	120	488.0	1.79
5619	12	35	10	28	85	38.3	24.55
9431	15	38	10	27	90	41.0	22.9
7781	30	40	25	25	120	350.0	2.54
4573	16	37	10	27	90	42.1	22.26

Table B.9 Testing random seeds for the scenario that traffic volumes from subject direction and cross-street are 700 vphpl and 700 vphpl.

Seed	*EW L* (s)	*EW Th* (s)	*NS L* (s)	*NS Th* (s)	Cycle (s)	Control (s)	PI
1337	13	21	10	16	60	649.0	1.13
2973	30	30	30	30	120	890.0	0.80
5619	7	63	13	52	135	75.8	9.63
9431	7	42	17	39	105	65.4	11.47
7781	30	40	25	25	120	838.0	0.87
4573	17	42	8	38	105	75.1	10.15

APPENDIX C SCRIPT TO DEFINE TURN ATTRIBUTES

```
; Do not change filenames or add or remove FILEI/FILEO statements using an editor.
Use Cube/Application Manager.
RUN PGM=MATRIX
FILEI RECI = "{OUTDIR}\AMTURNTMP1.TXT"
FILEI LOOKUPI[1] = "{OUTDIR}\XY_{Year}{ALT}.DAT"

FILEO RECO[1] = "F:\TOD_MODEL_05302008\CUBE\AMMAT00K.DBF",
     FIELDS=INDEX, A, B, C, LTR, TVol
LOOKUP LOOKUPI=1,
      NAME=NodeXY,
        LOOKUP[1]=1, RESULT=2,
        LOOKUP[2]=1, RESULT=3,
      FAIL[3]=0

TurnMax=RECI.NUMRECORDS

Index=Index+1
A=RECI.NFIELD[1]
B=RECI.NFIELD[2]
C=RECI.NFIELD[3]
TVol=RECI.NFIELD[4]
LTR=0

AX=NodeXY(1,A)
AY=NodeXY(2,A)
BX=NodeXY(1,B)
BY=NodeXY(2,B)
CX=NodeXY(1,C)
CY=NodeXY(2,C)

;Move to coordinaor of A as origin
BX_1=BX-AX
BY_1=BY-AY
CX_1=CX-AX
CY_1=CY-AY
AB= sqrt(pow(BY_1,2)+pow(BX_1,2))
 if (BY_1>=0)
   alf_AB=arccos(BX_1/AB)
 else
   alf_AB=360-arccos(BX_1/AB)
 endif
;Move to coordinaor of B as origin
```

```
CX_2=CX-BX
CY_2=CY-BY
BC= sqrt(pow(CY_2,2)+pow(CX_2,2))
 if (CY_2>=0)
    alf_BC=arccos(CX_2/BC)
 else
    alf_BC=360-arccos(CX_2/BC)
 endif

;Calculate A'BC angle, A' is the image point of A about B
alf_ABC=alf_BC-alf_AB
if (alf_ABC<0) alf_ABC=360+alf_ABC

if ((alf_ABC>=0 & alf_ABC<45)|(alf_ABC>315 & alf_ABC<=360))
   LTR=2
elseif (alf_ABC>=45 & alf_ABC<180)
   LTR=1
elseif (alf_ABC>180 & alf_ABC<=315)
   LTR=3
else
   LTR=6
endif

write reco=1

if (index=TurnMax)
INDEX=999999, A=TurnMax, B=0, C=0, LTR=0, TVOL=0
write reco=1

endif

ENDRUN
```

APPENDIX D SCRIPT TO DEFINE CROSS-STREET VOLUME

```
;;<<PROCESS TEMPLATE>><<NETWORK>>;;
;{Title,note,12,"Create a New Attribute"}>>>
;{note1,note,10,"Input / Output Specification"}>>>
;Input  Highway Network File 1: {linki1,filename,"Enter Input Highway Network File Name",x,"{OUTDIR}\AMHWYTMP1.NET","Network File (*.net)|*.net"}
;Output Highway Network File:   {neto,filename,"Enter Output Highway Network File Name",x,"{OUTDIR}\APHWYTMP1.NET","Network File (*.net)|*.net"}
;New Attribute:{NEW_ATTR,editbox,"New Attribute",T,"NEWVAR"}
;;<<End Parameters>>;;

; Do not change filenames or add or remove FILEI/FILEO statements using an editor. Use Cube/Application Manager.
RUN PGM=NETWORK
FILEI LOOKUPI[2] = "{OUTDIR}\LINKI_{YEAR}{ALT}.DBF"
FILEI LOOKUPI[1] = "{OUTDIR}\AMTURNDEFI.DBF"

FILEI LINKI[1] = {LINKI1.Q}
FILEO NETO = {NETO.Q}

LOOKUP LOOKUPI=1,
     NAME=TTYPE,
       LOOKUP[1]=INDEX, RESULT=A,
       LOOKUP[2]=INDEX, RESULT=B,
       LOOKUP[3]=INDEX, RESULT=C,
       LOOKUP[4]=INDEX, RESULT=LTR,
       LOOKUP[5]=INDEX, RESULT=TVOL,
       FAIL[1]=0,FAIL[2]=0,FAIL[3]=0

LOOKUP LOOKUPI=2,
     NAME=LINKAB,
       LOOKUP[1]=INDEX, RESULT=A,
       LOOKUP[2]=INDEX, RESULT=B,
       LOOKUP[3]=INDEX, RESULT=NUM_LANES,
       LOOKUP[4]=INDEX, RESULT=DISTANCE,
       LOOKUP[5]=INDEX, RESULT=CAPACITY,
       FAIL[1]=0,FAIL[2]=0,FAIL[3]=0

PROCESS  PHASE = LINKMERGE

if (LI.1.FTC1=40 |li.1.FTC1=60)
LinkMax=LINKAB(1,999999)
TurnMax=TTYPE(1,999999)
```

```
LS1=0
THS1=0
RS1=0
ITER1=1
DOWN_SD=0
UP_NODE=0
UP_NODEN=0
LS1_C=0
THS1_C=0
RS1_C=0

;TURN VOLUME
_BNODE=LI.1.B
_BL=TTYPE(2,TURNMAX)
_BF=TTYPE(2,1)
_BINDEX=ROUND(TURNMAX*(_BNODE-_BF)/(_BL-_BF))

LOOP _K=1,1000
IF ((TTYPE(2,_BINDEX)>_BNODE)&(TTYPE(2,_BINDEX)-_BNODE>10))
   _BINDEX=_BINDEX-(TTYPE(2,_BINDEX)-_BNODE)
ELSEIF ((TTYPE(2,_BINDEX)<_BNODE)&(_BNODE-TTYPE(2,_BINDEX)>10))
   _BINDEX=_BINDEX-(TTYPE(2,_BINDEX)-_BNODE)
ELSE
BREAK
ENDIF
ENDLOOP

;;;;;;;FIRST LOOP for SUB Turn Lookup
IF (TTYPE(2,_BINDEX)<=_BNODE)

;TURN VOLUME
LOOP _N=_BINDEX, TURNMAX

;LEFT_SUB1
 IF (LI.1.A = TTYPE(1,_N) & LI.1.B = TTYPE(2,_N)& TTYPE(4,_N)=1 )
   LS1_A=TTYPE(1,_N)
   LS1_B=TTYPE(2,_N)
   LS1=1
    IF (LS1_C=0)
      LS1_C=TTYPE(3,_N)
      LEFTSUB1 = TTYPE(5,_N)
     ELSEIF (LS1_C>0 & TTYPE(5,_N)>LEFTSUB1)
      LS1_C=TTYPE(3,_N)
      LEFTSUB1 = TTYPE(5,_N)
     ELSE
```

```
    ENDIF
  ENDIF

;THROUGH_SUB1
  IF (LI.1.A = TTYPE(1,_N) & LI.1.B = TTYPE(2,_N)& TTYPE(4,_N)=2 )
    THS1_A=TTYPE(1,_N)
    THS1_B=TTYPE(2,_N)
    THS1=1
    IF (THS1_C=0)
      THS1_C=TTYPE(3,_N)
      THROUGHSUB1 = TTYPE(5,_N)
    ELSEIF (THS1_C>0 & TTYPE(5,_N)>THROUGHSUB1)
     THS1_C=TTYPE(3,_N)
     THROUGHSUB1 = TTYPE(5,_N)
    ELSE
    ENDIF
  ENDIF

;RIGHT_SUB1
  IF (LI.1.A = TTYPE(1,_N) & LI.1.B = TTYPE(2,_N)& TTYPE(4,_N)=3 )
    RS1_A=TTYPE(1,_N)
    RS1_B=TTYPE(2,_N)
    RS1=1
    IF (RS1_C=0)
      RS1_C=TTYPE(3,_N)
      RIGHTSUB1 = TTYPE(5,_N)
    ELSEIF (RS1_C>0 & TTYPE(5,_N)>RIGHTSUB1)
      RS1_C=TTYPE(3,_N)
      RIGHTSUB1 = TTYPE(5,_N)
    ELSE
    ENDIF
  ENDIF

;SUBVOL
   VOLSUB1=LEFTSUB1+THROUGHSUB1+RIGHTSUB1

;BREAK TO SAVE TIME
  IF (TTYPE(2,_N)>_BNODE)
  BREAK
  ENDIF
ENDLOOP

ENDIF
;;;;;;;FIRST LOOP for SUB Turn Lookup
;;;;;;;SECOND LOOP for SUB Turn Lookup
```

```
IF (TTYPE(2,_BINDEX)>=_BNODE)

;TURN VOLUME
TEMP=_BINDEX-1
LOOP _N=TEMP, 1,-1

;LEFT_SUB1
  IF (LI.1.A = TTYPE(1,_N) & LI.1.B = TTYPE(2,_N)& TTYPE(4,_N)=1 )
    LS1_A=TTYPE(1,_N)
    LS1_B=TTYPE(2,_N)
    LS1=1
     IF (LS1_C=0)
       LS1_C=TTYPE(3,_N)
       LEFTSUB1 = TTYPE(5,_N)
      ELSEIF (LS1_C>0 & TTYPE(5,_N)>LEFTSUB1)
       LS1_C=TTYPE(3,_N)
       LEFTSUB1 = TTYPE(5,_N)
      ELSE
      ENDIF
  ENDIF

;THROUGH_SUB1
  IF (LI.1.A = TTYPE(1,_N) & LI.1.B = TTYPE(2,_N)& TTYPE(4,_N)=2 )
    THS1_A=TTYPE(1,_N)
    THS1_B=TTYPE(2,_N)
    THS1=1
    IF (THS1_C=0)
       THS1_C=TTYPE(3,_N)
       THROUGHSUB1 = TTYPE(5,_N)
    ELSEIF (THS1_C>0 & TTYPE(5,_N)>THROUGHSUB1)
      THS1_C=TTYPE(3,_N)
      THROUGHSUB1 = TTYPE(5,_N)
    ELSE
    ENDIF
  ENDIF

;RIGHT_SUB1
  IF (LI.1.A = TTYPE(1,_N) & LI.1.B = TTYPE(2,_N)& TTYPE(4,_N)=3 )
    RS1_A=TTYPE(1,_N)
    RS1_B=TTYPE(2,_N)
    RS1=1
    IF (RS1_C=0)
       RS1_C=TTYPE(3,_N)
       RIGHTSUB1 = TTYPE(5,_N)
```

```
   ELSEIF (RS1_C>0 & TTYPE(5,_N)>RIGHTSUB1)
     RS1_C=TTYPE(3,_N)
     RIGHTSUB1 = TTYPE(5,_N)
   ELSE
   ENDIF
  ENDIF

;SUBVOL
   VOLSUB1=LEFTSUB1+THROUGHSUB1+RIGHTSUB1

  ;BREAK TO SAVE TIME
  IF (TTYPE(2,_N)<_BNODE)
  BREAK
  ENDIF
ENDLOOP
ENDIF
;;;;;;;SECOND LOOP for SUB Turn Lookup

;;;;;;;FIRST LOOP for OTHER TurnS Lookup
IF (TTYPE(2,_BINDEX)<=_BNODE)

;TURN VOLUME
LOOP _N=_BINDEX, TURNMAX
  IF (RS1=1)

;LEFT_CROSS1
   IF (LI.1.A = TTYPE(3,_N) & LI.1.B = TTYPE(2,_N)& RS1_C=TTYPE(1,_N))
     LEFTCROSS1 = TTYPE(5,_N)
   ENDIF

   ;THROUGH_CROSS1
   IF (LS1_C = TTYPE(3,_N) & LI.1.B = TTYPE(2,_N)& RS1_C=TTYPE(1,_N))
     THROUGHCROSS1 = TTYPE(5,_N)
   ENDIF

;RIGHT_CROSS1
   IF (THS1_C = TTYPE(3,_N) & LI.1.B = TTYPE(2,_N)& RS1_C=TTYPE(1,_N))
     RIGHTCROSS1 = TTYPE(5,_N)
   ENDIF

   VOLCROSS1=LEFTCROSS1+THROUGHCROSS1+RIGHTCROSS1
  ENDIF

  IF (LS1=1)
    ;LEFT_CROSS2
```

```
   IF (THS1_C = TTYPE(3,_N) & LI.1.B = TTYPE(2,_N)& LS1_C=TTYPE(1,_N))
    LEFTCROSS2 = TTYPE(5,_N)
   ENDIF

;THROUGH_CROSS2
   IF (RS1_C = TTYPE(3,_N) & LI.1.B = TTYPE(2,_N)& LS1_C=TTYPE(1,_N))
    THROUGHCROSS2 = TTYPE(5,_N)
   ENDIF

;RIGHT_CROSS2
   IF (LI.1.A = TTYPE(3,_N) & LI.1.B = TTYPE(2,_N)& LS1_C=TTYPE(1,_N))
    RIGHTCROSS2 = TTYPE(5,_N)
   ENDIF
   VOLCROSS2=LEFTCROSS2+THROUGHCROSS2+RIGHTCROSS2

 ENDIF

 IF (THS1=1)
;LEFT_SUB2
   IF (RS1_C = TTYPE(3,_N) & LI.1.B = TTYPE(2,_N)& THS1_C=TTYPE(1,_N))
    LEFTSUB2 = TTYPE(5,_N)
   ENDIF

;THROUGH_SUB2
   IF (LI.1.A = TTYPE(3,_N) & LI.1.B = TTYPE(2,_N)& THS1_C=TTYPE(1,_N))
    THROUGHSUB2 = TTYPE(5,_N)
   ENDIF

;RIGHT_SUB2
   IF (LS1_C = TTYPE(3,_N) & LI.1.B = TTYPE(2,_N)& THS1_C=TTYPE(1,_N))
    RIGHTSUB2 = TTYPE(5,_N)
   ENDIF
   VOLSUB2=LEFTSUB2+THROUGHSUB2+RIGHTSUB2

 ENDIF

;BREAK TO SAVE TIME
 IF (TTYPE(2,_N)>_BNODE)
 BREAK
 ENDIF
ENDLOOP

ENDIF
;;;;;;;FIRST LOOP for OTHER TurnS Lookup
;;;;;;;SECOND LOOP for OTHER TurnS Lookup
```

```
IF (TTYPE(2,_BINDEX)>=_BNODE)

;TURN VOLUME
TEMP=_BINDEX-1
LOOP _N=TEMP, 1,-1
 IF (RS1=1)
  ;LEFT_CROSS1
  IF (LI.1.A = TTYPE(3,_N) & LI.1.B = TTYPE(2,_N)& RS1_C=TTYPE(1,_N))
   LEFTCROSS1 = TTYPE(5,_N)
  ENDIF

 ;THROUGH_CROSS1
  IF (LS1_C = TTYPE(3,_N) & LI.1.B = TTYPE(2,_N)& RS1_C=TTYPE(1,_N))
   THROUGHCROSS1 = TTYPE(5,_N)
  ENDIF

;RIGHT_CROSS1
  IF (THS1_C = TTYPE(3,_N) & LI.1.B = TTYPE(2,_N)& RS1_C=TTYPE(1,_N))
   RIGHTCROSS1 = TTYPE(5,_N)
  ENDIF

  VOLCROSS1=LEFTCROSS1+THROUGHCROSS1+RIGHTCROSS1
 ENDIF

 IF (LS1=1)
;LEFT_CROSS2
  IF (THS1_C = TTYPE(3,_N) & LI.1.B = TTYPE(2,_N)& LS1_C=TTYPE(1,_N))
   LEFTCROSS2 = TTYPE(5,_N)
  ENDIF

;THROUGH_CROSS2
  IF (RS1_C = TTYPE(3,_N) & LI.1.B = TTYPE(2,_N)& LS1_C=TTYPE(1,_N))
   THROUGHCROSS2 = TTYPE(5,_N)
  ENDIF

;RIGHT_CROSS2
  IF (LI.1.A = TTYPE(3,_N) & LI.1.B = TTYPE(2,_N)& LS1_C=TTYPE(1,_N))
   RIGHTCROSS2 = TTYPE(5,_N)
  ENDIF
  VOLCROSS2=LEFTCROSS2+THROUGHCROSS2+RIGHTCROSS2

 ENDIF

 IF (THS1=1)
```

```
;LEFT_SUB2
   IF (RS1_C = TTYPE(3,_N) & LI.1.B = TTYPE(2,_N)& THS1_C=TTYPE(1,_N))
    LEFTSUB2 = TTYPE(5,_N)
   ENDIF

;THROUGH_SUB2
   IF (LI.1.A = TTYPE(3,_N) & LI.1.B = TTYPE(2,_N)& THS1_C=TTYPE(1,_N))
    THROUGHSUB2 = TTYPE(5,_N)
   ENDIF

;RIGHT_SUB2
   IF (LS1_C = TTYPE(3,_N) & LI.1.B = TTYPE(2,_N)& THS1_C=TTYPE(1,_N))
    RIGHTSUB2 = TTYPE(5,_N)
   ENDIF
   VOLSUB2=LEFTSUB2+THROUGHSUB2+RIGHTSUB2

 ENDIF

;BREAK TO SAVE TIME
 IF (TTYPE(2,_N)<_BNODE)
 BREAK
 ENDIF
ENDLOOP
ENDIF
;;;;;;;SECOND LOOP for OTHER TurnS Lookup

_BNODE=LI.1.A
_BF=TTYPE(2,1)
_BL=TTYPE(2,TURNMAX)
_BINDEX=ROUND(TURNMAX*(_BNODE-_BF)/(_BL-_BF))

LOOP _K=1,1000
IF ((TTYPE(2,_BINDEX)>_BNODE)&(TTYPE(2,_BINDEX)-_BNODE>10))
   _BINDEX=_BINDEX-(TTYPE(2,_BINDEX)-_BNODE)
ELSEIF ((TTYPE(2,_BINDEX)<_BNODE)&(_BNODE-TTYPE(2,_BINDEX)>10))
   _BINDEX=_BINDEX-(TTYPE(2,_BINDEX)-_BNODE)
ELSE
BREAK
ENDIF
ENDLOOP

;;;;;;;FIRST LOOP for UP NODE Lookup
IF (TTYPE(2,_BINDEX)<=_BNODE)
LOOP _N=_BINDEX, TURNMAX
;Upstream node
```

```
   IF (LI.1.A = TTYPE(2,_N) & LI.1.B = TTYPE(3,_N)& TTYPE(4,_N)=2 )
     IF (UP_NODE=0)
      UP_NODE=TTYPE(1,_N)
      UP_NODEN=TTYPE(5,_N)
     ELSEIF (UP_NODE>0 & TTYPE(5,_N)>UP_NODEN)
      UP_NODE=TTYPE(1,_N)
      UP_NODEN=TTYPE(5,_N)
     ENDIF
   ENDIF

  ;BREAK TO SAVE TIME
  IF (TTYPE(2,_N)>_BNODE)
  BREAK
  ENDIF
ENDLOOP

ENDIF
;;;;;;;FIRST LOOP for UP_NODE Lookup

;;;;;;;SECOND LOOP for UP NODE Lookup
IF (TTYPE(2,_BINDEX)>=_BNODE)
TEMP=_BINDEX-1
LOOP _N=TEMP, 1,-1
;Upstream node
   IF (LI.1.A = TTYPE(2,_N) & LI.1.B = TTYPE(3,_N)& TTYPE(4,_N)=2 )
     IF (UP_NODE=0)
      UP_NODE=TTYPE(1,_N)
      UP_NODEN=TTYPE(5,_N)
     ELSEIF (UP_NODE>0 & TTYPE(5,_N)>UP_NODEN)
      UP_NODE=TTYPE(1,_N)
      UP_NODEN=TTYPE(5,_N)
     ENDIF
   ENDIF

  ;BREAK TO SAVE TIME
  IF (TTYPE(2,_N)<_BNODE)
  BREAK
  ENDIF
ENDLOOP
ENDIF
;;;;;;;SECOND LOOP for UP NODE Lookup

; LANE NUMBER, CAPACITY AND UPTREAM LINK LENGTH
LOOP _M=1, 4
IF (_M=1)
```

```
  _ANODE=RS1_C
ELSEIF (_M=2)
  _ANODE=LS1_C
ELSEIF (_M=3)
  _ANODE=THS1_C
ELSEIF (_M=4)
  _ANODE=UP_NODE
ELSE
ENDIF

IF (_ANODE<>0)
_AF=LINKAB(1,1)
_AL=LINKAB(1,LINKMAX)
_AINDEX=ROUND(LINKMAX*(_ANODE-_AF)/(_AL-_AF))

LOOP _K=1,1000
IF ((LINKAB(1,_AINDEX)>_ANODE)&(LINKAB(1,_AINDEX)-_ANODE>10))
    _AINDEX=_AINDEX-(LINKAB(1,_AINDEX)-_ANODE)
ELSEIF ((LINKAB(1,_AINDEX)<_ANODE)&(_ANODE-LINKAB(1,_AINDEX)>10))
    _AINDEX=_AINDEX-(LINKAB(1,_AINDEX)-_ANODE)
ELSE
BREAK
ENDIF
ENDLOOP

;;;;;;;FIRST LOOP for LANE NUMBER AND CAPACITY Lookup
IF (LINKAB(1,_AINDEX)<=_ANODE)
LOOP _N=_AINDEX, LINKMAX
;NUMBER OF LANE AND CAPACITY
  IF (RS1_C = LINKAB(1,_N) & LI.1.B = LINKAB(2,_N))
    LNCROSS1=LINKAB(3,_N)
    CAPCROSS1=LINKAB(5,_N)


  ELSEIF (LS1_C = LINKAB(1,_N) & LI.1.B = LINKAB(2,_N))
    LNCROSS2=LINKAB(3,_N)
    CAPCROSS2=LINKAB(5,_N)


  ELSEIF (THS1_C = LINKAB(1,_N) & LI.1.B = LINKAB(2,_N))
    LNSUB2=LINKAB(3,_N)
    CAPSUB2=LINKAB(5,_N)

;upstream link length
  ELSEIF ( UP_NODE=LINKAB(1,_N) & LI.1.A = LINKAB(2,_N) )
```

```
   UP_LENGTH=LINKAB(4,_N)
  ENDIF

 IF (LINKAB(1,_N)>_ANODE)
 BREAK
 ENDIF
ENDLOOP
ENDIF
;;;;;;;FIRST LOOP for LANE NUMBER AND CAPACITY Lookup

;;;;;;;SECOND LOOP for LANE NUMBER AND CAPACITY Lookup
IF (LINKAB(1,_AINDEX)>=_ANODE)
TEMP=_AINDEX-1
LOOP _N=TEMP, 1,-1
; NUMBER OF LANE AND CAPACITY
  IF (RS1_C = LINKAB(1,_N) & LI.1.B = LINKAB(2,_N))
    LNCROSS1=LINKAB(3,_N)
    CAPCROSS1=LINKAB(5,_N)

  ELSEIF (LS1_C = LINKAB(1,_N) & LI.1.B = LINKAB(2,_N))
    LNCROSS2=LINKAB(3,_N)
    CAPCROSS2=LINKAB(5,_N)

  ELSEIF (THS1_C = LINKAB(1,_N) & LI.1.B = LINKAB(2,_N))
    LNSUB2=LINKAB(3,_N)
    CAPSUB2=LINKAB(5,_N)

;upstream link length
  ELSEIF ( UP_NODE=LINKAB(1,_N) & LI.1.A = LINKAB(2,_N) )
    UP_LENGTH=LINKAB(4,_N)
  ELSE
  ENDIF

IF (LINKAB(1,_N)<_ANODE)
BREAK
ENDIF
ENDLOOP
ENDIF
;;;;;;;SECOND LOOP for LANE NUMBER AND CAPACITY Lookup
ELSE
ENDIF
ENDLOOP

ELSE
ENDIF
```

```
ENDPROCESS

ENDRUN
```

APPENDIX E SCRIPT FOR METHOD OF SUCCESSIVE AVERAGE (MSA)

```
;;<<PROCESS TEMPLATE>><<NETWORK>>;;
;{Title,note,12,"Create a New Attribute"}>>>
;{note1,note,10,"Input / Output Specification"}>>>
;Input  Highway Network File 1: {linki1,filename,"Enter Input Highway Network File Name",x,"{OUTDIR}\AMPK-HLOAD_{ALT}{Year}.NET","Network File (*.net)|*.net"}
;Output Highway Network File:   {neto,filename,"Enter Output Highway Network File Name",x,"{OUTDIR}\APHWYTMP1.NET","Network File (*.net)|*.net"}
;New Attribute:{NEW_ATTR,editbox,"New Attribute",T,"NEWVAR"}
;;<<End Parameters>>;;

; Do not change filenames or add or remove FILEI/FILEO statements using an editor. Use Cube/Application Manager.
RUN PGM=NETWORK
FILEI LOOKUPI[2] = "{OUTDIR}\SPILL_DELAY.DBF"
FILEI LOOKUPI[1] = "{OUTDIR}\AMTURNTMP4.DBF"

FILEI LINKI[1] = {LINKI1.Q}
FILEO NETO = {NETO.Q}

LOOKUP LOOKUPI=1,
     NAME=TTYPE,
       LOOKUP[1]=INDEX, RESULT=A,
       LOOKUP[2]=INDEX, RESULT=B,
       LOOKUP[3]=INDEX, RESULT=C,
       LOOKUP[5]=INDEX, RESULT=TVOL,
       FAIL[1]=0,FAIL[2]=0,FAIL[3]=0

LOOKUP LOOKUPI=2,
     NAME=SD,
       LOOKUP[1]=INDEX, RESULT=A,
       LOOKUP[2]=INDEX, RESULT=B,
       LOOKUP[3]=INDEX, RESULT=DELAY,
     FAIL[1]=0,FAIL[2]=0,FAIL[3]=0

;read FILE = "E:\CUBEWORK\TURNNUMBER.PRN"

PROCESS  PHASE = LINKMERGE

if (li.1.FTC1=40 |li.1.FTC1=60)
ITER1=ITER1+1
```

```
TurnMax=TTYPE(1,999999)
SDMax=SD(1,999999)

_BNODE=LI.1.B
_BF=TTYPE(2,1)
_BL=TTYPE(2,TURNMAX)
_BINDEX=ROUND(TURNMAX*(_BNODE-_BF)/(_BL-_BF))

LOOP _K=1,1000
IF ((TTYPE(2,_BINDEX)>_BNODE)&(TTYPE(2,_BINDEX)-_BNODE>10))
   _BINDEX=_BINDEX-(TTYPE(2,_BINDEX)-_BNODE)
ELSEIF ((TTYPE(2,_BINDEX)<_BNODE)&(_BNODE-TTYPE(2,_BINDEX)>10))
   _BINDEX=_BINDEX-(TTYPE(2,_BINDEX)-_BNODE)
ELSE
BREAK
ENDIF

ENDLOOP

;;;;;;;FIRST LOOP for Turn Lookup
IF (TTYPE(2,_BINDEX)<=_BNODE)
;TURN VOLUME
LOOP _N=_BINDEX, TURNMAX

 ;LEFT_SUB1
 IF (LI.1.A = TTYPE(1,_N) & LI.1.B = TTYPE(2,_N)& LS1_C=TTYPE(3,_N) )
  LEFTSUB1 = TTYPE(4,_N)/ITER1+(1-1/ITER1)*LEFTSUB1
 ENDIF

 ;THROUGH_SUB1
 IF (LI.1.A = TTYPE(1,_N) & LI.1.B = TTYPE(2,_N)& THS1_C=TTYPE(3,_N) )
  THROUGHSUB1 = TTYPE(4,_N)/ITER1+(1-1/ITER1)*THROUGHSUB1
 ENDIF

 ;RIGHT_SUB1
 IF (LI.1.A = TTYPE(1,_N) & LI.1.B = TTYPE(2,_N)& RS1_C=TTYPE(3,_N) )
  RIGHTSUB1 = TTYPE(4,_N)/ITER1+(1-1/ITER1)*RIGHTSUB1
 ENDIF

 ;SUBVOL
  VOLSUB1=LEFTSUB1+THROUGHSUB1+RIGHTSUB1

 IF (RS1=1)
  ;LEFT_CROSS1
  IF (LI.1.A = TTYPE(3,_N) & LI.1.B = TTYPE(2,_N)& RS1_C=TTYPE(1,_N))
```

```
   LEFTCROSS1 = TTYPE(4,_N)/ITER1+(1-1/ITER1)*LEFTCROSS1
  ENDIF

  ;THROUGH_CROSS1
  IF (LS1_C = TTYPE(3,_N) & LI.1.B = TTYPE(2,_N)& RS1_C=TTYPE(1,_N))
   THROUGHCROSS1 = TTYPE(4,_N)/ITER1+(1-1/ITER1)*THROUGHCROSS1
  ENDIF

  ;RIGHT_CROSS1
  IF (THS1_C = TTYPE(3,_N) & LI.1.B = TTYPE(2,_N)& RS1_C=TTYPE(1,_N))
   RIGHTCROSS1 = TTYPE(4,_N)/ITER1+(1-1/ITER1)*RIGHTCROSS1
  ENDIF

  VOLCROSS1=LEFTCROSS1+THROUGHCROSS1+RIGHTCROSS1
 ENDIF

 IF (LS1=1)
  ;LEFT_CROSS2
  IF (THS1_C = TTYPE(3,_N) & LI.1.B = TTYPE(2,_N)& LS1_C=TTYPE(1,_N))
   LEFTCROSS2 = TTYPE(4,_N)/ITER1+(1-1/ITER1)*LEFTCROSS2
  ENDIF

 ;THROUGH_CROSS2
  IF (RS1_C = TTYPE(3,_N) & LI.1.B = TTYPE(2,_N)& LS1_C=TTYPE(1,_N))
   THROUGHCROSS2 = TTYPE(4,_N)/ITER1+(1-1/ITER1)*THROUGHCROSS2
  ENDIF

 ;RIGHT_CROSS2
  IF (LI.1.A = TTYPE(3,_N) & LI.1.B = TTYPE(2,_N)& LS1_C=TTYPE(1,_N))
   RIGHTCROSS2 = TTYPE(4,_N)/ITER1+(1-1/ITER1)*RIGHTCROSS2
  ENDIF
  VOLCROSS2=LEFTCROSS2+THROUGHCROSS2+RIGHTCROSS2

 ENDIF

 IF (THS1=1)
  ;LEFT_SUB2
  IF (RS1_C = TTYPE(3,_N) & LI.1.B = TTYPE(2,_N)& THS1_C=TTYPE(1,_N))
   LEFTSUB2 = TTYPE(4,_N)/ITER1+(1-1/ITER1)*LEFTSUB2
  ENDIF

  ;THROUGH_SUB2
  IF (LI.1.A = TTYPE(3,_N) & LI.1.B = TTYPE(2,_N)& THS1_C=TTYPE(1,_N))
   THROUGHSUB2 = TTYPE(4,_N)/ITER1+(1-1/ITER1)*THROUGHSUB2
  ENDIF
```

```
   ;RIGHT_SUB2
   IF (LS1_C = TTYPE(3,_N) & LI.1.B = TTYPE(2,_N)& THS1_C=TTYPE(1,_N))
    RIGHTSUB2 = TTYPE(4,_N)/ITER1+(1-1/ITER1)*RIGHTSUB2
   ENDIF
   VOLSUB2=LEFTSUB2+THROUGHSUB2+RIGHTSUB2

  ENDIF

IF (TTYPE(2,_N)>_BNODE)
BREAK
ENDIF
ENDLOOP

ENDIF
;;;;;;;FIRST LOOP for Turn Lookup

;;;;;;;SECOND LOOP for Turn Lookup
IF (TTYPE(2,_BINDEX)>=_BNODE)
;TURN VOLUME
TEMP=_BINDEX-1
LOOP _N=TEMP, 1,-1

   ;LEFT_SUB1
  IF (LI.1.A = TTYPE(1,_N) & LI.1.B = TTYPE(2,_N)& LS1_C=TTYPE(3,_N) )
   LEFTSUB1 = TTYPE(4,_N)/ITER1+(1-1/ITER1)*LEFTSUB1
  ENDIF

  ;THROUGH_SUB1
  IF (LI.1.A = TTYPE(1,_N) & LI.1.B = TTYPE(2,_N)& THS1_C=TTYPE(3,_N) )
   THROUGHSUB1 = TTYPE(4,_N)/ITER1+(1-1/ITER1)*THROUGHSUB1
  ENDIF

  ;RIGHT_SUB1
  IF (LI.1.A = TTYPE(1,_N) & LI.1.B = TTYPE(2,_N)& RS1_C=TTYPE(3,_N) )
   RIGHTSUB1 = TTYPE(4,_N)/ITER1+(1-1/ITER1)*RIGHTSUB1
  ENDIF

  ;SUBVOL
   VOLSUB1=LEFTSUB1+THROUGHSUB1+RIGHTSUB1

  IF (RS1=1)
   ;LEFT_CROSS1
   IF (LI.1.A = TTYPE(3,_N) & LI.1.B = TTYPE(2,_N)& RS1_C=TTYPE(1,_N))
    LEFTCROSS1 = TTYPE(4,_N)/ITER1+(1-1/ITER1)*LEFTCROSS1
   ENDIF
```

```
  ;THROUGH_CROSS1
  IF (LS1_C = TTYPE(3,_N) & LI.1.B = TTYPE(2,_N)& RS1_C=TTYPE(1,_N))
    THROUGHCROSS1 = TTYPE(4,_N)/ITER1+(1-1/ITER1)*THROUGHCROSS1
  ENDIF

  ;RIGHT_CROSS1
  IF (THS1_C = TTYPE(3,_N) & LI.1.B = TTYPE(2,_N)& RS1_C=TTYPE(1,_N))
    RIGHTCROSS1 = TTYPE(4,_N)/ITER1+(1-1/ITER1)*RIGHTCROSS1
  ENDIF

  VOLCROSS1=LEFTCROSS1+THROUGHCROSS1+RIGHTCROSS1
ENDIF

IF (LS1=1)
  ;LEFT_CROSS2
  IF (THS1_C = TTYPE(3,_N) & LI.1.B = TTYPE(2,_N)& LS1_C=TTYPE(1,_N))
    LEFTCROSS2 = TTYPE(4,_N)/ITER1+(1-1/ITER1)*LEFTCROSS2
  ENDIF

 ;THROUGH_CROSS2
  IF (RS1_C = TTYPE(3,_N) & LI.1.B = TTYPE(2,_N)& LS1_C=TTYPE(1,_N))
    THROUGHCROSS2 = TTYPE(4,_N)/ITER1+(1-1/ITER1)*THROUGHCROSS2
  ENDIF

 ;RIGHT_CROSS2
  IF (LI.1.A = TTYPE(3,_N) & LI.1.B = TTYPE(2,_N)& LS1_C=TTYPE(1,_N))
    RIGHTCROSS2 = TTYPE(4,_N)/ITER1+(1-1/ITER1)*RIGHTCROSS2
  ENDIF
  VOLCROSS2=LEFTCROSS2+THROUGHCROSS2+RIGHTCROSS2

ENDIF

IF (THS1=1)
  ;LEFT_SUB2
  IF (RS1_C = TTYPE(3,_N) & LI.1.B = TTYPE(2,_N)& THS1_C=TTYPE(1,_N))
    LEFTSUB2 = TTYPE(4,_N)/ITER1+(1-1/ITER1)*LEFTSUB2
  ENDIF

  ;THROUGH_SUB2
  IF (LI.1.A = TTYPE(3,_N) & LI.1.B = TTYPE(2,_N)& THS1_C=TTYPE(1,_N))
    THROUGHSUB2 = TTYPE(4,_N)/ITER1+(1-1/ITER1)*THROUGHSUB2
  ENDIF

  ;RIGHT_SUB2
  IF (LS1_C = TTYPE(3,_N) & LI.1.B = TTYPE(2,_N)& THS1_C=TTYPE(1,_N))
```

```
    RIGHTSUB2 = TTYPE(4,_N)/ITER1+(1-1/ITER1)*RIGHTSUB2
   ENDIF
   VOLSUB2=LEFTSUB2+THROUGHSUB2+RIGHTSUB2

  ENDIF

IF (TTYPE(2,_N)<_BNODE)
BREAK
ENDIF
ENDLOOP

ENDIF
;;;;;;;SECOND LOOP for Turn Lookup
_ANODE=LI.1.A
_AF=SD(1,1)
_AL=SD(1,SDMAX)
_AINDEX=ROUND(SDMAX*(_ANODE-_AF)/(_AL-_AF))

LOOP _K=1,1000
IF ((SD(1,_AINDEX)>_ANODE)&(SD(1,_AINDEX)-_ANODE>10))
   _AINDEX=_AINDEX-(SD(1,_AINDEX)-_ANODE)
ELSEIF ((SD(1,_AINDEX)<_ANODE)&(_ANODE-SD(1,_AINDEX)>10))
   _AINDEX=_AINDEX-(SD(1,_AINDEX)-_ANODE)
ELSE
BREAK
ENDIF
ENDLOOP


;;;;;;;FIRST LOOP for SPILLED DELAY Lookup
IF (SD(1,_AINDEX)<=_ANODE)
LOOP _N=_AINDEX, SDMAX
;SPILLED DELAY
  IF (LI.1.A = SD(1,_N) & LI.1.B = SD(2,_N))
   SP_DELAY=SD(3,_N)
  ENDIF

 IF (SD(1,_N)>_ANODE)
 BREAK
 ENDIF
ENDLOOP
ENDIF
;;;;;;;FIRST LOOP for SPILLED DELAY Lookup
```

```
;;;;;;;SECOND LOOP for SPILLED DELAY Lookup
IF (SD(1,_AINDEX)>=_ANODE)
TEMP=_AINDEX-1
LOOP _N=TEMP, 1,-1
 ;SPILLED DELAY
  IF (LI.1.A = SD(1,_N) & LI.1.B = SD(2,_N))
    SP_DELAY=SD(3,_N)
  ENDIF

IF (SD(1,_N)<_ANODE)
BREAK
ENDIF
ENDLOOP
ENDIF
;;;;;;;SECOND LOOP for SPILLED DELAY Lookup

;;;;;;; DOWN STREAM SPILLED DELAY
_ANODE=LI.1.B
_AF=SD(1,1)
_AL=SD(1,SDMAX)
_AINDEX=ROUND(SDMAX*(_ANODE-_AF)/(_AL-_AF))

LOOP _K=1,1000
IF ((SD(1,_AINDEX)>_ANODE)&(SD(1,_AINDEX)-_ANODE>10))
    _AINDEX=_AINDEX-(SD(1,_AINDEX)-_ANODE)
ELSEIF ((SD(1,_AINDEX)<_ANODE)&(_ANODE-SD(1,_AINDEX)>10))
    _AINDEX=_AINDEX-(SD(1,_AINDEX)-_ANODE)
ELSE
BREAK
ENDIF

ENDLOOP


;;;;;;;FIRST LOOP for DOWN STREAM SPILLED DELAY Lookup
IF (SD(1,_AINDEX)<=_ANODE)

LOOP _N=_AINDEX, SDMAX
;SPILLED DELAY

  IF (LI.1.B = SD(1,_N) & THS1_C = SD(2,_N)& VOLSUB1>0)
     DOWN_SD=SD(3,_N)
  ENDIF

 IF (SD(1,_N)>_ANODE)
```

```
 BREAK
 ENDIF
ENDLOOP
ENDIF
;;;;;;;FIRST LOOP for DOWN STREAM SPILLED DELAY Lookup

;;;;;;;SECOND LOOP for DOWN STREAM SPILLED DELAY Lookup
IF (SD(1,_AINDEX)>=_ANODE)
TEMP=_AINDEX-1
LOOP _N=TEMP, 1,-1
 ;SPILLED DELAY

  IF (LI.1.B = SD(1,_N) & THS1_C = SD(2,_N)& VOLSUB1>0)
     DOWN_SD=SD(3,_N)
  ENDIF

 IF (SD(1,_N)<_ANODE)
 BREAK
 ENDIF
ENDLOOP
;;;;;;;SECOND LOOP for DOWN STREAM SPILLED DELAY Lookup
ENDIF

ELSE
ENDIF

ENDPROCESS

ENDRUN
```

APPENDIX F SCRIPT FOR TRAFFIC ASSIGNMENT WITH THE DEVELOPED MODELS

```
; Do not change filenames or add or remove FILEI/FILEO statements using an editor. Use Cube/Application Manager.
RUN PGM=HIGHWAY PRNFILE="{OUTDIR}\ASHWY00H.PRN" MSG='Run AM Peak Period Hwy Assignment'
FILEO PRINTO[3] = "{OUTDIR}\DEBUG_TT.TXT"
FILEI NETI = "{OUTDIR}\APHWYTMP1.NET"
FILEI MATI[1] = "{OUTDIR}\HWYOD-AMPK_{ALT}{YEAR}.MAT"
FILEI LOOKUPI[1] = "{DATADIR}\TT2_Parameters.dbf"
FILEO PRINTO[2] = "{OUTDIR}\spill_delay.txt"
FILEO TURNVOLO[1] = "{OUTDIR}\AMPrdTVOL.BIN", format=bin
DISTRIBUTEINTRASTEP ProcessID='SERPM6ID',ProcessList=1-4
FILEO TURNVOLO[2] = "{OUTDIR}\AMPrdTVOL.TXT",
FORMAT=TXT,DEC=0
FILEO TURNPENO = "{OUTDIR}\AMPrdPnlty.DAT"
FILEI TURNPENI = "{OUTDIR}\TURNS_{Year}.PEN"
FILEO PRINTO[1] = "{OUTDIR}\AMPK-TOLLRPT.PRN"
FILEO NETO = "{OUTDIR}\AMPK-HLOAD_{ALT}{Year}.NET"
FILEO MATO[1] = "{OUTDIR}\SelLnkMatAM_{ALT}{Year}.MAT",
  MO=5-8, NAME=SelAM_DA,SelAM_SR2,SelAM_SR3P,SelAM_TRKS, dec=4*s

LOOKUP LOOKUPI=1,
    NAME=TTP,
      LOOKUP[1]=Parameter, RESULT=T1_V1,
      LOOKUP[2]=Parameter, RESULT=T1_V2,
      LOOKUP[3]=Parameter, RESULT=T1_V3,
      LOOKUP[4]=Parameter, RESULT=T1_V4,
      LOOKUP[5]=Parameter, RESULT=T2_V1,
      LOOKUP[6]=Parameter, RESULT=T2_V2,
      LOOKUP[7]=Parameter, RESULT=T2_V3,
      LOOKUP[8]=Parameter, RESULT=T2_V4,
      LOOKUP[9]=Parameter, RESULT=T3_V1,
      LOOKUP[10]=Parameter, RESULT=T3_V2,
      LOOKUP[11]=Parameter, RESULT=T3_V3,
      LOOKUP[12]=Parameter, RESULT=T3_V4,
      LOOKUP[13]=Parameter, RESULT=T4_V1,
      LOOKUP[14]=Parameter, RESULT=T4_V2,
      LOOKUP[15]=Parameter, RESULT=T4_V3,
      LOOKUP[16]=Parameter, RESULT=T4_V4,
      LOOKUP[17]=Parameter, RESULT=T5_V1,
      LOOKUP[18]=Parameter, RESULT=T5_V2,
```

```
        LOOKUP[19]=Parameter, RESULT=T5_V3,
        LOOKUP[20]=Parameter, RESULT=T5_V4,
        LOOKUP[21]=Parameter, RESULT=T6_V1,
        LOOKUP[22]=Parameter, RESULT=T6_V2,
        LOOKUP[23]=Parameter, RESULT=T6_V3,
        LOOKUP[24]=Parameter, RESULT=T6_V4,
        LOOKUP[25]=Parameter, RESULT=T7_V1,
        LOOKUP[26]=Parameter, RESULT=T7_V2,
        LOOKUP[27]=Parameter, RESULT=T7_V3,
        LOOKUP[28]=Parameter, RESULT=T7_V4,
        LOOKUP[29]=Parameter, RESULT=T8_V1,
        LOOKUP[30]=Parameter, RESULT=T8_V2,
        LOOKUP[31]=Parameter, RESULT=T8_V3,
        LOOKUP[32]=Parameter, RESULT=T8_V4,
        LOOKUP[33]=Parameter, RESULT=T9_V1,
        LOOKUP[34]=Parameter, RESULT=T9_V2,
        LOOKUP[35]=Parameter, RESULT=T9_V3,
        LOOKUP[36]=Parameter, RESULT=T9_V4,
        FAIL[1]=0,FAIL[2]=0,FAIL[3]=0

PAR ZONEMSG=100 COMBINE=EQUI MAXITERS=5 GAP={EPSILON2}
RAAD=0.00000 AAD=0.000000 RMSE=0.000000 ;

ARRAY TOLLREVENUE=99 TOLLVMT=99
ZONEMSG=100

; Look up deceleration rate based on approach speed
LOOKUP,
 INTERPOLATE=Y, LIST=Y, NAME=DECEL,
       LOOKUP[1]=1,RESULT=2,
R = '30 4',
   '70 6.2'

PROCESS PHASE=LINKREAD

; Basics-
  LW.FFTIME=LI.TIME
  T0=LI.TIME

;Period Model CTOLL Modification...
IF (('{TODMODEL}'=='YES')|('{TODMODEL}'=='Yes')|('{TODMODEL}'=='yes'))
   CTOLL={CTOLL}+({DevCtollPk})
 ELSE
   CTOLL={CTOLL}
ENDIF
```

```
IF (CTOLL<0) CTOLL=.01
IF (('{TODMODEL}'=='YES')|('{TODMODEL}'=='Yes')|('{TODMODEL}'=='yes'))
   LW.AMRCTOLL=LI.RCTOLL+({DevCtollPk})
 ELSE
   LW.AMRCTOLL=LI.RCTOLL
ENDIF
IF (LW.AMRCTOLL<0) LW.AMRCTOLL=0.01

;Calculate AM Peak period (3 Hour) roadway capacity; Note: LOSCCAP capacity is
;     LINK Hourly LOS-C capacity (LOSCCAP) derived from LOS-E Capacity and
UROADFAC
  IF(LI.HOT=1)
     C = {HOTCAPADJUST}*(LI.LOSCCAP)/LI.CONFACAMP ; CAPACITY FOR
HOT LANES ADJUSTED BY USING HOTCAPADJUST VALUE: ASR 04/21/2007
    ELSE
     C = (LI.LOSCCAP)/LI.CONFACAMP     ; 39.528% of traffic in AM peak period
occurs in the highest hour
  ENDIF

;Set EXCLUDE VOLUME GROUP for PATHLOAD
  IF (li.FTC2=83,84,86 & LI.HOT=0) ADDTOGROUP=1    ;HOV 2 & 3+ Facilites and
Non-HOT Lanes (FTC2=85->PM Only) => Exclude DA, Trucks Volume Grps
  IF (li.FTC2=82 & LI.HOT=0) ADDTOGROUP=3          ;HOV 3+ Facilites and Non-
HOT Lanes => Exclude HOV 2 persons Grps
  IF (li.FTC2=86 & LI.HOT=2) ADDTOGROUP=2          ;Dummy Entrance and Exit
from HOT facility (all trips are prevented)
  IF (LI.HOT=1) ADDTOGROUP=8                ;HOT Lane Facility
  IF (LI.FTC2=59,69) ADDTOGROUP=9                    ;Transit non-Highway opt
links(59,69)

;Reset/Modify ALPHA/LI.BPRCOEFFICIENT for freeways (SERPM602)so they
become same as surface streets during midday period--SKS(8/4/2006)
;Void that changes for SERPM65...
 IF (li.FTC2=11,12,81,82,91,92)                ;freeways
;serpm602 Changes--      LW.MBPRCOEFFICIENT=LI.BPRCOEFFICIENT+0.15
     LW.MBPRCOEFFICIENT=LI.BPRCOEFFICIENT+0.00
   else
     LW.MBPRCOEFFICIENT=LI.BPRCOEFFICIENT+0.00
 ENDIF

;Set LINKCLASS based on FTC2 Codes as follows:
    IF (LI.FTC2=11,12,21,41,51,52,59,61,69,71-75,81-86,91-94)    ; no toll
       LINKCLASS=1
      elseif (LI.FTC2=95)                        ;toll plaza
       LINKCLASS=2
```

```
      else
        LINKCLASS=9                          ;any missing valid FTC2-code links
     ENDIF


  if (lINKCLASS=2)                           ;toll plaza links
     LW.TOLLTIME=(LW.AMRCTOLL*LI.CARTOLL)*60
     T0=(LW.AMRCTOLL*LI.CARTOLL)*60      +      LI.SVCMINUTES      +
LI.SVCSECONDS/60
     if (iteration=0)
;
LW.ARRIVR=(V/LI.UROADFACTOR)*LI.CONFACAMP/LI.PLZALNSMAX  ;hourly
volume per toll lane ie. arrival rate in vehicles per hour
     LW.ARRIVR=V*LI.CONFACAMP/LI.PLZALNSMAX              ;hourly volume
per toll lane ie. arrival rate in vehicles per hour
     LW.SERVT=LI.SVCMINUTES+(LI.SVCSECONDS/60)           ;Plaza lane service
time in minutes per vehicle
      IF (LI.TOLLTYPE=1)
        LW.SERVR=(1/LW.SERVT)*60                         ;Plaza lane service rate in
vehicle per hour
       ELSE
        LW.SERVR=100
      ENDIF
     PRINT LIST='ARRIVR= ',LW.ARRIVR
     PRINT LIST='SERVT= ',LW.SERVT
     PRINT LIST='SERVR= ',LW.SERVR
;         if (LW.ARRIVR>=LW.SERVR) LW.ARRIVR=0.99*LW.SERVR      ;prevent
infinite or negative queue
     if  (LW.ARRIVR>=LW.SERVR)  LW.ARRIVR=0.95*LW.SERVR        ;prevent
infinite or negative queue
     endif
  endif

    if (li.TOLL_ACC>0)
     LINKCLASS=3                             ;Toll Plaza Acceleration link
     T0= T0 + (LI.FREEFLOWSPEED/{ACCELRATE})/60
    endif

    if (li.TOLL_DEC>0)
     LINKCLASS=4                             ;Toll Plaza Deceleration link
     T0 = T0 + (LI.FREEFLOWSPEED/DECEL(1,LI.FREEFLOWSPEED))/60
    endif
    if (li.toll>maxplzno) maxplzno=li.toll
    IF (LI.FTC2=59,69) LINKCLASS=5                   ;Transit non-Highway optional
links
```

```
;      IF (LI.ROUNDNODECLS=1) LINKCLASS=6                    ;JUNCTION DATA
PRESENT
   IF (LI.ROUNDNODECLS=1)                         ;JUNCTION DATA PRESENT
        LINKCLASS=6
        IF                                                                (LI.FTC2=11,12)
LW.MBPREXPONENT=LI.BPREXPONENT*1.00        ;*1.25
        IF (LI.FTC2=91) LW.MBPREXPONENT=LI.BPREXPONENT*1.00        ;*1.15
        IF                                                          (LI.FTC2=71,72,75)
LW.MBPREXPONENT=LI.BPREXPONENT*1.00   ;*1.25
        IF (LI.FTC2=93) LW.MBPREXPONENT=LI.BPREXPONENT*1.00        ;*1.50
    ENDIF

;Turning Volume  Node list:
   ;TURNS N=7708,10238,16110,19046,24772,23433
TURNS N=1-99999


;;;;;;;;;;;;;;;;;;;;;;;;;;;;;;;;;;;;;;;;;;;;;;;;;;;;;;;;;;;;;;;;;;;;;;;;;;;;;;;;;;;;
; developed model module
IF (LI.FTC1=40 | LI.FTC1=60)

;Set LINKCLASS based on FTC2 Codes as follows:

LW.UP_LENGTH=LI.UP_LENGTH
LW.DOWN_SD=LI.DOWN_SD
LW.POSTSPD=LI.POSTSPD
;progression factor
LW.DF=LI.DF
;define work variable from link base AND NORMALIZED TO PER LANE BASIS
lw.lnsub1=li.NUM_LANES
lw.lnsub2=li.lnsub2
LW.LNCROSS1=LI.LNCROSS1
LW.LNCROSS2=LI.LNCROSS2
lw.CAPsub1=LI.CAPACITY
lw.CAPsub2=li.CAPsub2
LW.CAPCROSS1=LI.CAPCROSS1
LW.CAPCROSS2=LI.CAPCROSS2

IF (LW.LNSUB1<>0)
LW.VOLSUB1=LI.VOLSUB1/LW.LNSUB1
LW.CAPSUB1=LW.CAPSUB1/LW.LNSUB1
LW.LEFTSUB1=LI.LEFTSUB1/LW.LNSUB1
LW.THROUGHSUB1=LI.THROUGHSUB1/LW.LNSUB1
LW.RIGHTSUB1=LI.RIGHTSUB1/LW.LNSUB1
```

```
ELSE
LW.CAPSUB1=0
LW.VOLSUB1=0
LW.LEFTSUB1=0
LW.THROUGHSUB1=0
LW.RIGHTSUB1=0
ENDIF

IF (LW.LNSUB2<>0)
LW.VOLSUB2=LI.VOLSUB2/LW.LNSUB2
LW.CAPSUB2=LW.CAPSUB2/LW.LNSUB2
LW.LEFTSUB2=LI.LEFTSUB2/LW.LNSUB2
LW.THROUGHSUB2=LI.THROUGHSUB2/LW.LNSUB2
LW.RIGHTSUB2=LI.RIGHTSUB2/LW.LNSUB2
ELSE
LW.CAPSUB2=0
LW.VOLSUB2=0
LW.LEFTSUB2=0
LW.THROUGHSUB2=0
LW.RIGHTSUB2=0
ENDIF

IF (LW.LNCROSS1<>0)
LW.VOLCROSS1=LI.VOLCROSS1/LW.LNCROSS1
LW.CAPCROSS1=LW.CAPCROSS1/LW.LNCROSS1
LW.LEFTCROSS1=LI.LEFTCROSS1/LW.LNCROSS1
LW.THROUGHCROSS1=LI.THROUGHCROSS1/LW.LNCROSS1
LW.RIGHTCROSS1=LI.RIGHTCROSS1/LW.LNCROSS1
ELSE
LW.CAPCROSS1=0
LW.VOLCROSS1=0
LW.LEFTCROSS1=0
LW.THROUGHCROSS1=0
LW.RIGHTCROSS1=0
ENDIF

IF (LW.LNCROSS2<>0)
LW.VOLCROSS2=LI.VOLCROSS2/LW.LNCROSS2
LW.CAPCROSS2=LW.CAPCROSS2/LW.LNCROSS2
LW.LEFTCROSS2=LI.LEFTCROSS2/LW.LNCROSS2
LW.THROUGHCROSS2=LI.THROUGHCROSS2/LW.LNCROSS2
LW.RIGHTCROSS2=LI.RIGHTCROSS2/LW.LNCROSS2
ELSE
LW.CAPCROSS2=0
LW.VOLCROSS2=0
```

```
LW.LEFTCROSS2=0
LW.THROUGHCROSS2=0
LW.RIGHTCROSS2=0
ENDIF

;define SUBJECT volume
 LW.VOLSUB=LW.VOLSUB1
 LW.LEFTSUB=LW.LEFTSUB1
 LW.RIGHTSUB=LW.RIGHTSUB1
 LW.LNSUB=LW.LNSUB1
 LW.CAPSUB=LW.CAPSUB1
;DEFINE MAXIMUM CROSS VOLUME
 IF (LW.VOLCROSS1>LW.VOLCROSS2)
  LW.VOLCROSS=Lw.VOLCROSS1
  LW.LEFTcross=Lw.leftcross1
  LW.RIGHTcross=Lw.RIGHTcross1
  LW.LNCROSS=lw.LNCROSS1
  LW.CAPCROSS=LW.CAPCROSS1
 ELSE
  LW.VOLCROSS=Lw.VOLCROSS2
  LW.leftcross=Lw.leftcross2
  LW.RIGHTcross=Lw.RIGHTcross2
  LW.LNCROSS=lw.LNCROSS2
  LW.CAPCROSS=LW.CAPCROSS2
 ENDIF


;adjusted virtual volume
   IF (LW.VOLCROSS<200 & LW.VOLCROSS>0)
     LW.VOLCROSS=200
   ENDIF
   IF (LW.VOLsub<200 & LW.VOLsub>0)
     LW.VOLsub=200
   ENDIF


;SET LINKCLASS,IF ANY VOLUMES ARE 0,THE EQUATION IS DIFFERENT
 ; BOTH SUBJECT AND CROSS VOLUME IS NON-ZERO
 IF ((LW.LNCROSS<>0)& (LW.VOLCROSS<>0)&(LW.VOLSUB<>0))
   LINKCLASS=7
 ELSE
   LINKCLASS=1
 ENDIF
 LW.LCLASS=LINKCLASS
```

```
;SET SPEED
;speed=li.speed

;IF (LINKCLASS=1)
IF (lw.lclass=7)
;define left-turn, RIGHT-turn ratio for both approach
 LW.LeftSUBp=Lw.LEFTSUB/Lw.volSUB
 LW.RIGHTSUBp=Lw.RIGHTSUB/Lw.volSUB

 LW.leftcrossp=Lw.leftcross/Lw.VOLCROSS
 LW.RIGHTcrossp=Lw.RIGHTcross/Lw.VOLCROSS

 ;LW.LeftSUBmaxp=Lw.LEFTSUBmax/Lw.volSUBmax
 ;LW.RIGHTSUBmaxp=Lw.RIGHTSUBmax/Lw.volSUBmax

 LW.SUBS=LW.CAPSUB*(1-0.15*LW.RIGHTSUBP)/(1+0.05*LW.LEFTSUBP)
 ;LW.SUBMAXS=LW.LNSUBMAX*1800*(1-
0.15*LW.RIGHTSUBMAXP)/(1+0.05*LW.LEFTSUBMAXP)
 LW.CROSSS=LW.CAPCROSS*(1-
0.15*LW.RIGHTCROSSP)/(1+0.05*LW.LEFTCROSSP)

  IF ((LW.LNSUB<=3) & (LW.LNCROSS<=3)&(LW.VOLSUB <=500) &
(LW.VOLCROSS <=500))
   LW.A1=TTP(1+4*(3*(LW.LNSUB-1)+(LW.LNCROSS-1)),1)
   LW.A3=TTP(1+4*(3*(LW.LNSUB-1)+(LW.LNCROSS-1)),3)
   LW.A4=TTP(1+4*(3*(LW.LNSUB-1)+(LW.LNCROSS-1)),4)
   LW.A5=TTP(1+4*(3*(LW.LNSUB-1)+(LW.LNCROSS-1)),5)
   LW.A6=TTP(1+4*(3*(LW.LNSUB-1)+(LW.LNCROSS-1)),6)
   LW.A9=TTP(1+4*(3*(LW.LNSUB-1)+(LW.LNCROSS-1)),9)
 ELSEIF ((LW.LNSUB<=3) & (LW.LNCROSS<=3)&(LW.VOLSUB <=500) &
(LW.VOLCROSS >500))
   LW.A1=TTP(2+4*(3*(LW.LNSUB-1)+(LW.LNCROSS-1)),1)
   LW.A3=TTP(2+4*(3*(LW.LNSUB-1)+(LW.LNCROSS-1)),3)
   LW.A4=TTP(2+4*(3*(LW.LNSUB-1)+(LW.LNCROSS-1)),4)
   LW.A5=TTP(2+4*(3*(LW.LNSUB-1)+(LW.LNCROSS-1)),5)
   LW.A6=TTP(2+4*(3*(LW.LNSUB-1)+(LW.LNCROSS-1)),6)
   LW.A9=TTP(2+4*(3*(LW.LNSUB-1)+(LW.LNCROSS-1)),9)
 ELSEIF ((LW.LNSUB<=3) & (LW.LNCROSS<=3)&(LW.VOLSUB >500)&
(LW.VOLCROSS <=500))
   LW.A1=TTP(3+4*(3*(LW.LNSUB-1)+(LW.LNCROSS-1)),1)
   LW.A3=TTP(3+4*(3*(LW.LNSUB-1)+(LW.LNCROSS-1)),3)
   LW.A4=TTP(3+4*(3*(LW.LNSUB-1)+(LW.LNCROSS-1)),4)
   LW.A5=TTP(3+4*(3*(LW.LNSUB-1)+(LW.LNCROSS-1)),5)
   LW.A6=TTP(3+4*(3*(LW.LNSUB-1)+(LW.LNCROSS-1)),6)
   LW.A9=TTP(3+4*(3*(LW.LNSUB-1)+(LW.LNCROSS-1)),9)
```

```
  ELSEIF ((LW.LNSUB<=3) & (LW.LNCROSS<=3))
   LW.A1=TTP(4+4*(3*(LW.LNSUB-1)+(LW.LNCROSS-1)),1)
   LW.A3=TTP(4+4*(3*(LW.LNSUB-1)+(LW.LNCROSS-1)),3)
   LW.A4=TTP(4+4*(3*(LW.LNSUB-1)+(LW.LNCROSS-1)),4)
   LW.A5=TTP(4+4*(3*(LW.LNSUB-1)+(LW.LNCROSS-1)),5)
   LW.A6=TTP(4+4*(3*(LW.LNSUB-1)+(LW.LNCROSS-1)),6)
   LW.A9=TTP(4+4*(3*(LW.LNSUB-1)+(LW.LNCROSS-1)),9)

  ELSEIF ((LW.VOLSUB <=500) & (LW.VOLCROSS <=500))
   LW.A1=TTP(1,1)
   LW.A3=TTP(1,3)
   LW.A4=TTP(1,4)
   LW.A5=TTP(1,5)
   LW.A6=TTP(1,6)
   LW.A9=TTP(1,9)
  ELSEIF ((LW.VOLSUB <=500) & (LW.VOLCROSS >500))
   LW.A1=TTP(2,1)
   LW.A3=TTP(2,3)
   LW.A4=TTP(2,4)
   LW.A5=TTP(2,5)
   LW.A6=TTP(2,6)
   LW.A9=TTP(2,9)
  ELSEIF ((LW.VOLSUB >500) & (LW.VOLCROSS <=500))
   LW.A1=TTP(3,1)
   LW.A3=TTP(3,3)
   LW.A4=TTP(3,4)
   LW.A5=TTP(3,5)
   LW.A6=TTP(3,6)
   LW.A9=TTP(3,9)
  ELSE
   LW.A1=TTP(4,1)
   LW.A3=TTP(4,3)
   LW.A4=TTP(4,4)
   LW.A5=TTP(4,5)
   LW.A6=TTP(4,6)
   LW.A9=TTP(4,9)

  ENDIF
ENDIF

ENDIF
;;;;;;;;;;;;;;;;;;;;;;;;;;;;;;;;;;;;;;;;;;;;;;;;;;;;;;;;;;;;;;;;;;;;;;;;;;;;;;;;;;;;


ENDPHASE
```

```
;===============================================================
;=== ILOOP (ASSIGNMENT) PHASE ===
;===============================================================
PHASE=ILOOP
  MW[1]=MI.1.AMPK_DA            ;Table 1
  MW[2]=MI.1.AMPK_SR2           ;Table 2
  MW[3]=MI.1.AMPK_SR3P          ;Table 3
  MW[4]=MI.1.AMPK_TRKS          ;Table 4 - Trucks in PCE


;With Select Link Loadings....
  PATHLOAD PATH=COST, VOL[1]=MW[1], PENI=1-2, EXCLUDEGROUP=1,2,9,
MW[5]=MI.1.AMPK_DA, SELECTLINK=(L={SELLINK})   ;Without HOV
  PATHLOAD PATH=COST, VOL[2]=MW[2], PENI=1-2, EXCLUDEGROUP=2,3,9,
MW[6]=MI.1.AMPK_SR2, SELECTLINK=(L={SELLINK})   ;With HOV2 -Note Here,
Trucks are NOT alowed on HOV lanes
  PATHLOAD PATH=TIME, VOL[3]=MW[3], PENI=1-2, EXCLUDEGROUP=2,9,
MW[7]=MI.1.AMPK_SR3P, SELECTLINK=(L={SELLINK})   ;With HOV3+ -Note
Here, Trucks are NOT alowed on HOV lanes
  PATHLOAD PATH=TIME, VOL[4]=MW[4], PENI=1-2,
EXCLUDEGROUP=1,2,9,8,MW[8]=MI.1.AMPK_TRKS,
SELECTLINK=(L={SELLINK})  ;Without HOV - Truck Trips
;Select Link Analysis on Purpose1
  PATH=COST,VOL[5]=MW[5], PENI=1-2, EXCLUDEGROUP=1,2,9
;Select Link Analysis on Purpose2
  PATH=COST,VOL[6]=MW[6], PENI=1-2, EXCLUDEGROUP=2,3,9
;Select Link Analysis on Purpose3
  PATH=TIME,VOL[7]=MW[7], PENI=1-2, EXCLUDEGROUP=2,9
;Select Link Analysis on Purpose4
  PATH=TIME,VOL[8]=MW[8], PENI=1-2, EXCLUDEGROUP=1,2,9,8

;       PATHLOAD PATH=TIME, VOL[2]=MW[2], VOL[3]=MW[3], PENI=1,
EXCLUDEGROUP=9    ;With HOV -Note Here, Trucks are alowed on HOV lanes
    ; Add this to above PATHLOAD for a PATH file:
    ;       PATHO=1, name='AM Peak Period Assignment',allj=f,includecosts=f

ENDPHASE

;===============================================================
;=== ADJUST PHASE (WITH REPORTING)===
;===============================================================
PHASE=ADJUST
; Define volume to be used for V/C calculation -- this includes the truck PCE.
 FUNCTION   V=VOL[1] + VOL[2] + vol[3] + vol[4]
```

```
;Revise Volume for Freeway Ramp Merge Volumes
; FUNCTION   V=MIN(3600,(VOL[1] + VOL[2] + vol[3])*LW.FWYRMPMRGFAC)
;      FUNCTION                V=MIN(LW.MINVOL,(VOL[1]      +      VOL[2]      +
vol[3])*LW.FWYRMPMRGFAC)

 if (time>0) LW.CGSTSPEED=(LI.DISTANCE/TIME)*60
; if (LW.ARRIVR>=LW.SERVR) LW.ARRIVR=0.99*LW.SERVR                ; prevent
infinite or negative queue
 if (LW.ARRIVR>=LW.SERVR) LW.ARRIVR=0.95*LW.SERVR                ; prevent
infinite or negative queue
 if (li.cartoll>0 | li.tolltype>0)
;   LW.ARRIVR=(V/LI.UROADFACTOR)*LI.CONFACAMP/LI.PLZALNSMAX      ;
hourly volume per toll lane ie. arrival rate in vehicles per hour
  LW.ARRIVR=V*LI.CONFACAMP/LI.PLZALNSMAX       ; hourly volume per toll
lane ie. arrival rate in vehicles per hour
  LW.SERVT=LI.SVCMINUTES+(LI.SVCSECONDS/60)                    ; Plaza lane
service time in minutes per vehicle
  IF (LI.TOLLTYPE=1)
       LW.SERVR=(1/LW.SERVT)*60                          ; Plaza lane service rate in
vehicle per hour

;            if (LW.ARRIVR>=LW.SERVR) LW.ARRIVR=0.99*LW.SERVR    ; prevent
infinite or negative queue
       if  (LW.ARRIVR>=LW.SERVR)  LW.ARRIVR=0.95*LW.SERVR      ;  prevent
infinite or negative queue
  ELSE
       LW.SERVR=100
       LW.ARRIVR=1
  ENDIF
print list="****",LI.PLAZADESC,"****"
PRINT LIST='ARRIVR= ',LW.ARRIVR
PRINT LIST='SERVT= ',LW.SERVT
PRINT LIST='SERVR= ',LW.SERVR
PRINT LIST='TOLLTIME= ',TIME
endif
if (lw.servr-lw.arrivr=0.0) lw.servr=lw.servr+0.01

;Update Time and Cost for PATHLOAD
;---TIME is TIME plus regular toll time and toll equivalent time
;---COST is Time plus HOT toll time equivalent
;Capture HOT toll time equivalent
IF(LI.HOT=1)
 LW.VCVAL=V/C ; V/C CALCULATION
```

```
; IF (LW.VCVAL=0)                    ;REMOVED IN LOGIT TOLL APPLICATION BY
SV
  ; LW.HOTTOLL={MINHOTTOLL}          ; HOT TOLL VALUE MIN AT $0.13
  ;ELSEIF (LW.VCVAL<=1.0)
  ;                                  LW.HOTTOLL=                ({MAXHOTTOLL}-
{MINHOTTOLL})*LW.VCVAL+{MINHOTTOLL} ; CALCULATE THE HOT TOLL
Rate REMOVED BY SV
LW.HOTTOLL                =                {MINHOTTOLL}+({MAXHOTTOLL}-
{MINHOTTOLL})/(1+EXP(6-9*LW.VCVAL)) ; LOGIT EQN APPLIED BY SV
060707
 ;ELSE
  ;LW.HOTTOLL={MAXHOTTOLL} ; HOT TOLL VALUE MAXED AT $0.25
 ;ENDIF
ELSE
  LW.HOTTOLL=0
ENDIF

;Define EACH LINKCLASS TC and COST Funs
; Link Class 1 - Non Regular Toll (it may be a HOT link)
 ;FUNCTION                  TC[1]                                                =
LI.TIME*(1+LW.MBPRCOEFFICIENT*(MIN(V/C,{VCMAX}))^LI.BPREXPONENT)
 ;FUNCTION                                  COST[1]                             =
LI.TIME*(1+LW.MBPRCOEFFICIENT*(MIN(V/C,{VCMAX}))^LI.BPREXPONENT
)+LI.DISTANCE*(LW.HOTTOLL)*60*LW.AMRCTOLL
 if (LI.FTC1=40 | LI.FTC1=60)
  Index_TD=Index_TD+1
 IF (LW.LCLASS=7)
  LW.T1_SD                                                                      =
(LW.volSUB/LW.SUBs)*(LW.A3+LW.A4*POW((LW.VOLCROSS/LW.crosss),LW.A
5)/POW((LW.VolSUB/LW.SUBs),LW.A6))*(EXP(-
LW.A9*DISTANCE*LW.SUBs/LW.volSUB)-EXP(-
LW.A9*(DISTANCE+LW.UP_LENGTH)*LW.SUBs/LW.volSUB))/60
  LW.T_SD=LW.T1_SD
  LW.T1_TT=DISTANCE/LW.POSTSPD*60                                               +
((LW.A1*DISTANCE+(LW.volSUB/LW.SUBs)*(LW.A3+LW.A4*POW((LW.VOLCR
OSS/LW.crosss),LW.A5)/POW((LW.VolSUB/LW.SUBs),LW.A6))*(1-EXP(-
LW.A9*DISTANCE*LW.SUBs/LW.volSUB)))/60)

 ELSE
   LW.T2_SD = 0
   LW.T_SD=LW.T2_SD

LW.T1_TT=LI.TIME*(1+LW.MBPRCOEFFICIENT*(MIN(V/C,{VCMAX}))^LI.BPR
EXPONENT)
 endif
```

```
 PRINT LIST=Index_TD(6.0),A(6.0), B(6.0), ' ', LW.T_SD(8.3), printo=2
 PRINT LIST=A(6.0), B(6.0), LW.T1_TT(16.4),
LW.LCLASS(5.0),LW.SUBS(8.0),lw.crosss(8.0),lw.postspd(4.0),distance(5.2),LW.VOL
SUB(8.0),LW.volcross(8.0),LW.LNSUB(3.0),LW.LNCROSS(3.0),LW.VOLSUB1(8.0),
LW.VOLSUB2(8.0),LW.VOLCROSS1(8.0),LW.VOLCROSS2(8.0),LW.UP_LENGTH(
8.3),LW.DOWN_SD(16.3),LW.A1(10.4),LW.A3(10.4),LW.A4(10.4),LW.A5(10.4),LW.
A6(10.4),LW.A9(10.4),printo=3

ELSE

ENDIF

 FUNCTION TC[1] =
LI.TIME*(1+LW.MBPRCOEFFICIENT*(MIN(V/C,{VCMAX}))^LI.BPREXPONENT)
 FUNCTION COST[1] =
LI.TIME*(1+LW.MBPRCOEFFICIENT*(MIN(V/C,{VCMAX}))^LI.BPREXPONENT
)+LI.DISTANCE*(LW.HOTTOLL)*60*LW.AMRCTOLL

; Link Class 2 - Regular Tollplaza Link (Never HOT link)
 FUNCTION TC[2]=MIN(5,(1/(2.0*(LW.SERVR-LW.ARRIVR)))*60) +
LW.AMRCTOLL*LI.CARTOLL*60 ; congested time for toll links
 FUNCTION COST[2]=MIN(5,(1/(2.0*(LW.SERVR-LW.ARRIVR)))*60) +
LW.AMRCTOLL*LI.CARTOLL*60 ; congested time for toll links
; Link Class 3 - Regular Toll Accln Link (Never HOT link)
 FUNCTION
TC[3]=LI.TIME*(1+LW.MBPRCOEFFICIENT*(MIN(V/C,{VCMAX}))^LI.BPREXP
ONENT) + (LW.CGSTSPEED/{ACCELRATE})/60; congested time toll acceleration
links
 FUNCTION
COST[3]=LI.TIME*(1+LW.MBPRCOEFFICIENT*(MIN(V/C,{VCMAX}))^LI.BPRE
XPONENT) + (LW.CGSTSPEED/{ACCELRATE})/60; congested time toll acceleration
links
; Link Class 4 - Regular Toll Decln Link (Never HOT link)
 FUNCTION
TC[4]=LI.TIME*(1+LW.MBPRCOEFFICIENT*(MIN(V/C,{VCMAX}))^LI.BPREXP
ONENT) + (LW.CGSTSPEED/DECEL(1,LW.CGSTSPEED))/60; congested time toll
deceleration links
 FUNCTION
COST[4]=LI.TIME*(1+LW.MBPRCOEFFICIENT*(MIN(V/C,{VCMAX}))^LI.BPRE
XPONENT) + (LW.CGSTSPEED/DECEL(1,LW.CGSTSPEED))/60; congested time toll
deceleration links
; Link Class 5 - Transit Optional Link (Never USED)
```

```
 FUNCTION   TC[5]=LI.TIME                                    ;congested time
transit-only optional links
 FUNCTION COST[5]=LI.TIME                                    ;congested time
transit-only optional links
;Link Class 6 -Links with junction data
 FUNCTION
TC[6]=(LI.TIME+LI.AM_LnkJctDelay)*(1+LW.MBPRCOEFFICIENT*(MIN(V/C,{V
CMAX}))^LW.MBPREXPONENT) ;congested time for Freeway/Ramp Junction
Approaches
 FUNCTION
COST[6]=(LI.TIME+LI.AM_LnkJctDelay)*(1+LW.MBPRCOEFFICIENT*(MIN(V/C,{
VCMAX}))^LW.MBPREXPONENT) ;congested time for Freeway/Ramp Junction
Approaches
 ;FUNCTION
TC[6]=(LI.TIME)*(1+LW.MBPRCOEFFICIENT*(MIN(V/C,{VCMAX}))^LW.MBPR
EXPONENT) ;congested time for Freeway/Ramp Junction Approaches
 ;FUNCTION
COST[6]=(LI.TIME)*(1+LW.MBPRCOEFFICIENT*(MIN(V/C,{VCMAX}))^LW.MB
PREXPONENT) ;congested time for Freeway/Ramp Junction Approaches

 FUNCTION TC[7] = DISTANCE/LW.POSTSPD*60 +
((LW.A1*DISTANCE+(LW.volSUB/LW.SUBs)*(LW.A3+LW.A4*POW((LW.VOLCR
OSS/LW.crosss),LW.A5)/POW((LW.VolSUB/LW.SUBs),LW.A6))*(1-EXP(-
LW.A9*DISTANCE*LW.SUBs/LW.volSUB)))/60)
 FUNCTION COST[7] = DISTANCE/LW.POSTSPD*60 +
((LW.A1*DISTANCE+(LW.volSUB/LW.SUBs)*(LW.A3+LW.A4*POW((LW.VOLCR
OSS/LW.crosss),LW.A5)/POW((LW.VolSUB/LW.SUBs),LW.A6))*(1-EXP(-
LW.A9*DISTANCE*LW.SUBs/LW.volSUB)))/60)+LI.DISTANCE*(LW.HOTTOLL)*
60*LW.AMRCTOLL
 ; FUNCTION TC[7] = DISTANCE/LW.POSTSPD*60 +
LW.DF*(LW.DOWN_SD+(LW.A1*DISTANCE+(LW.volSUB/LW.SUBs)*(LW.A3+L
W.A4*POW((LW.VOLCROSS_lth/LW.crosss),LW.A5)/POW((LW.VolSUB/LW.SUBs
),LW.A6))*(1-EXP(-LW.A9*DISTANCE*LW.SUBs/LW.volSUB)))/60)
 ; FUNCTION COST[7] = DISTANCE/LW.POSTSPD*60 +
LW.DF*(LW.DOWN_SD+(LW.A1*DISTANCE+(LW.volSUB/LW.SUBs)*(LW.A3+L
W.A4*POW((LW.VOLCROSS_lth/LW.crosss),LW.A5)/POW((LW.VolSUB/LW.SUBs
),LW.A6))*(1-EXP(-
LW.A9*DISTANCE*LW.SUBs/LW.volSUB)))/60)+LI.DISTANCE*(LW.HOTTOLL)*
60*LW.AMRCTOLL

;Link Class 9 - Missing FTC2 code links, Unlikely to Happen - Just a EXTRA Check
 FUNCTION   TC[9]=LI.TIME*1.20                               ;any missing
valid FTC2-code links
 FUNCTION COST[9]=LI.TIME*1.20
```

```
ENDPHASE

; Converge phase is new for Cube 4.0.
PHASE=CONVERGE
  IF (ITERATION < 6) BREAK; Do not even test for Iterations 2-5
  IF (GAP[ITERATION]<GAPCUTOFF & GAP[ITERATION-1]<GAPCUTOFF &
GAP[ITERATION-2]<GAPCUTOFF)
    BALANCE = 1
  ENDIF

ENDPHASE

ENDRUN
```

VITA

CHENXI LU

March, 1972	Born, Hequ, Shanxi, P.R. China
1989 - 1993	B.S. in Physics Fudan University, Shanghai, P.R.China
1993 – 1996	Research Assistant Institute of Applied Physics and Computational Mathematics Beijing, P.R. China
1996 – 1999	M.S. in Physics China Academy of Engineering Physics in Beijing Beijing, P.R. China
2000 – 2005	Ph.D. in Physics Florida International University Miami, Florida, USA
2006 – present	Doctoral Candidate, Civil Engineering, Teaching/Research Assistant/Dissertation Year Fellowship Florida International University Miami, Florida, USA

PUBLICATIONS

1. Chenxi Lu (2010). "A Travel Time Estimation for Planning Models Considering Signalized Intersections." ITE's 2010 Daniel B. Fambro Student Paper Award, accepted by *ITE Journal*.
2. Chenxi Lu, Shanshan Yang, and Fang Zhao (2010). "An Operational Method for Identifying Special Need Populations in a Future Hurricane." To be submitted to *ASCE Journal of Natural Hazards Review*.
3. Chenxi Lu, Fang Zhao, and Mohammed Hadi (2010). "A Travel Time Estimation Method for Planning Models Considering Signalized Intersections." Accepted by *the 10th International Conference of Chinese Transportation Professionals (ICCTP)*, ASCE, August 4-8, Beijing, China.
4. Chenxi Lu, Shanshan Yang, Fang Zhao, Richard Reel, and Doug O'Hara (2010). "Seasonal Factor Assignment Based on the Similarity of Hourly Traffic Patterns and Influential Variables." Submitted to *ASCE Journal of Transportation Engineering* (SCI; Impact Factor: 0.383).
5. Chenxi Lu, Fang Zhao and Mohammed Hadi (2010). "An Analytical Travel Time Estimation Method for Planning Models." *The 89th Transportation Research*

6. Shanshan Yang, Chenxi Lu, Fang Zhao and Richard Reel (2009). "Alternative Traffic Seasonal Factor Estimation for Urban Roads in Florida." *Transportation Research Record: Journal of the Transportation Research Board*, *No. 2121*, Transportation Research Board of the National Academies, Washington, D.C., pp 74-80 (SCI; Impact Factor: 0.206).
7. Hongbo Chi, Chenxi Lu and Fang Zhao (2009). "An Intensity, Chromaticity, and Lane Based Method for Vehicle Detection from Satellite Images." *Transportation Research Record: Journal of the Transportation Research Board*, *No. 2105*, Transportation Research Board of the National Academies, Washington, D.C., pp 109-117 (SCI; Impact Factor: 0.206).
8. Fang Zhao, Keqiang Xing, Shanshan Yang, Chenxi Lu, and Soon Chung (2009). *Hurricane Evacuation Planning for Disadvantaged Populations*, Final Report prepared for the Office of Research, Demonstration, and Innovation, Federal Transit Administration, U.S. Department of Transportation, Washington, D.C. (Technical Report).
9. Chenxi Lu , Fang Zhao and Shanshan Yang (2008). "Exploitation of Hourly Traffic Patterns for Modeling Seasonal Factors." *The 10th International Conference on Application of Advanced Technologies in Transportation*, Athens, Greece (Conference Proceeding).
10. Fang Zhao, Shanshan Yang, and Chenxi Lu (2008). *Alternatives for Estimating Seasonal Factors on Rural and Urban Roads in Florida (Phase II),* Final Report prepared for the Research Center, Florida Department of Transportation, Tallahassee, Florida (Technical Report).
11. Chenxi Lu, Jiandi Zhang, R. Jin, Hongwei Qu, J. He, D. Mandrus, Ku-Ding Tsuei, Chuan-Tze Tzeng, Li-Cheng Lin, and E. W. Plummer (2004). "Imperfection-Driven Phase Transition at 120 K in $Cd_2Re_2O_7$." *Phys. Rev. B*, 70, 092506 (SCI; Impact Factor: 3.172 ; Citation: 4).
12. S.-C. Wang, H.-B. Yang, A.K.P. Sekharan, S. Souma, H. Matsui, T. Sato, T. Takahashi, Chenxi Lu, Jiandi Zhang, R. Jin, D. Mandrus, and E.W. Plummer, Z. Wang, H. Ding (2004). "Fermi Surface Topology of $Ca_{1.5}Sr_{0.5}RuO_4$ Determined by Angle-Resolved Photoelectron Spectroscopy." *Phys. Rev. Lett*., 93, 177007 (SCI; Impact Factor: 6.944 ; Citation: 19).
13. Lei Cai, Hongwei Qu, Chenxi Lu, S. Ducharme, P.A. Dowben and Jiandi Zhang (2004). "Surface structure of ultrathin copolymer films of ferroelectric vinylidene fluoride (70%) with trifluoroethylene (30%) on graphite." *Phys. Rev. B*, 70, 155411 (SCI; Impact Factor: 3.172 ; Citation: 17).
14. Chenxi Lu, Werner U. Boeglin (2000). *Intrinsic Time Resolution and Position resolution of Neutron Detector for E93-026*. Progress report, Jefferson Lab, Newport News, VA, USA (Technical Report).